

STRUCTURAL, ELECTRONIC, AND MAGNETIC PROPERTIES OF
SMMCON ($M + N \leq 3$) MICROCLUSTERS:
DENSITY FUNCTIONAL THEORY CALCULATIONS

A THESIS SUBMITTED TO
THE GRADUATE SCHOOL OF NATURAL AND APPLIED SCIENCES
OF
MIDDLE EAST TECHNICAL UNIVERSITY

BY

NAZAN KARA

IN PARTIAL FULFILLMENT OF THE REQUIREMENTS
FOR
THE DEGREE OF MASTER OF SCIENCE
IN
PHYSICS

SEPTEMBER 2013

Approval of the thesis:

**STRUCTURAL, ELECTRONIC, AND MAGNETIC PROPERTIES OF
SMMCON ($M + N \leq 3$) MICROCLUSTERS:
DENSITY FUNCTIONAL THEORY CALCULATIONS**

submitted by **NAZAN KARA** in partial fulfillment of the requirements for the degree of **Master of Science in Physics Department, Middle East Technical University** by,

Prof. Dr. Canan Özgen
Dean, Graduate School of **Natural and Applied Sciences** _____

Prof. Dr. Mehmet T. Zeyrek
Head of Department, **Physics** _____

Prof. Dr. Şakir Erkoç
Supervisor, **Department of Physics, METU** _____

Assoc. Prof. Dr. Hüseyin Oymak
Co-supervisor, **Elec.and Electronics Eng Dept., Atılım University** _____

Examining Committee Members:

Prof. Dr. Ümit Kızıloğlu
Department of Physics, METU _____

Prof. Dr. Şakir Erkoç
Department of Physics, METU _____

Prof. Dr. Enver Bulur
Department of Physics, METU _____

Assoc. Prof. Dr. Hüseyin Oymak
Elec.and Electronics Eng Dept., Atılım University _____

Assoc. Prof. Dr. Hande Toffoli
Department of Physics, METU _____

Date: _____

I hereby declare that all information in this document has been obtained and presented in accordance with academic rules and ethical conduct. I also declare that, as required by these rules and conduct, I have fully cited and referenced all material and results that are not original to this work.

Name, Last Name: NAZAN KARA

Signature :

ABSTRACT

STRUCTURAL, ELECTRONIC, AND MAGNETIC PROPERTIES OF SMMCON ($M + N \leq 3$) MICROCLUSTERS: DENSITY FUNCTIONAL THEORY CALCULATIONS

Kara, Nazan

M.S., Department of Physics

Supervisor : Prof. Dr. Şakir Erkoç

Co-Supervisor : Assoc. Prof. Dr. Hüseyin Oymak

September 2013, 81 pages

Performing density functional theory calculations with many possible exchange correlational energy functionals, the most stable structures, symmetries, electronic, and magnetic properties of Sm_MCo_N ($M + N \leq 3$) microclusters have been studied in a systematic and statistical manner. Starting from the atoms of cobalt and samarium, dimers and trimers have been investigated in their ground states. The optimum geometries, binding energies, vibrational properties, possible dissociation channels, local magnetic moments and their enhancements with the growing size of the microclusters under study have been obtained. The calculations have been performed by using 13 DFT methods in the scope of present study.

Keywords: Density Functional Theory (DFT), Transition Metal Clusters, Rare Earth Elements, Cobalt, Samarium

ÖZ

SMMCON ($M + N \leq 3$) MİKROTOPAKLARININ YAPISAL, ELEKTRONİK VE MANYETİK ÖZELLİKLERİ: YOĞUNLUK FONKSİYONELİ TEORİSİ HESAPLARI

Kara, Nazan

Yüksek Lisans, Fizik Bölümü

Tez Yöneticisi : Prof. Dr. Şakir Erkoç

Ortak Tez Yöneticisi : Doç. Dr. Hüseyin Oymak

Eylül 2013 , 81 sayfa

Sm_MCo_N ($M + N \leq 3$) mikrotopaklarının en kararlı yapısı, simetrisi, elektronik ve manyetik özellikleri muhtemel birçok yerdeğiştirme-korelasyon enerji fonksiyonelleri ile yoğunluk fonksiyonel teorisi (YFT) hesapları kullanılarak sistematik ve istatistiksel olarak çalışılmıştır. Kobalt ve Samaryum atomlarından başlayarak, ikili ve üçlü yapıları sıfır enerji seviyesinde çalışılmıştır. Çalışılan bu topakların optimum geometrileri, bağ enerjileri, titreşim özellikleri, mümkün ayrışma kanalları, yerel manyetik momentleri ve bu momentlerin topağın yapısı ile ilgili değişimleri elde edilmiştir. Bu çalışma kapsamında, hesaplar 13 YFT metodu kullanılarak gerçekleştirilmiştir.

Anahtar Kelimeler: Yoğunluk Fonksiyoneli Teoremi (YFT), Geçiş Metali Topakları, Nadir Toprak Elementleri, Kobalt, Samaryum

To my family...

ACKNOWLEDGMENTS

In this thesis my special thanks go to Prof. Şakir Erkoç and Assoc. Prof. Hüseyin Oymak, whom I venerate as my masters, nor did I ever regret it from the first day I got to know them. I would like to thank Yasin Ahmet Mutlu, for technical support. My colleagues in Çankaya University never give up to show interest and reinforcement, appreciate to work with them.

I really do not know a way to thank Vedat Tanrıverdi, everything will be harder without his aid and moral support.

And special thanks to my family, Inci, Ilhan and Ozan Kara. I am grateful for their invaluable support, motivation and love. I feel so lucky to have such a great family.

My hearties Beste Korutlu, Gülten Karaoglan, and Bahadır Bebek, I always feel your encouragement and love. There may be distance, but I know you are not so far. It will be the worst to forget our lovely cat Çıtır, since this thesis is the last one of his hat-trick.

TABLE OF CONTENTS

| | |
|---|------|
| ABSTRACT | v |
| ÖZ | vi |
| ACKNOWLEDGMENTS | viii |
| TABLE OF CONTENTS | ix |
| LIST OF TABLES | xi |
| LIST OF FIGURES | xvi |
| LIST OF ABBREVIATIONS | xvii |
| CHAPTERS | |
| 1 INTRODUCTION | 1 |
| 1.1 Sm-Co Systems | 1 |
| 1.2 Transition Metals | 2 |
| 1.3 Rare Earth Elements (Lanthanides) | 2 |
| 2 DENSITY FUNCTIONAL THEORY | 5 |
| 2.1 Theoretical Background | 5 |
| 2.2 Hartree–Fock Method | 6 |
| 2.3 Electron Density | 7 |
| 2.4 The Hohenberg–Kohn Theorem | 8 |
| 2.5 The Kohn–Sham Method | 9 |

| | | |
|-------|--|----|
| 2.6 | Exchange-Correlation Functionals | 11 |
| 3 | RESULTS AND DISCUSSION | 15 |
| 3.1 | Co and Sm Atoms | 16 |
| 3.1.1 | Calculations of Co Atoms | 16 |
| 3.1.2 | Calculations of Sm Atoms | 25 |
| 3.2 | Dimers | 32 |
| 3.2.1 | SmCo Dimer Calculations | 32 |
| 3.2.2 | Co ₂ Dimer Calculations | 40 |
| 3.2.3 | Sm ₂ Dimer Calculations | 43 |
| 3.2.4 | SCF Calculations | 45 |
| 3.3 | Trimers | 49 |
| 3.3.1 | Co ₃ Trimer Calculations | 49 |
| 3.3.2 | Sm ₃ Trimer Calculations | 55 |
| 3.3.3 | SmCo ₂ Trimer Calculations | 58 |
| 3.3.4 | Sm ₂ Co Trimer Calculations | 62 |
| 4 | CONCLUSION | 77 |
| | REFERENCES | 79 |

LIST OF TABLES

TABLES

| | |
|--|----|
| Table 3.1 Total energies, E_m , in Hartrees, for a Co atom for different multiplicities, $m(2S + 1)$. The starred ones show the lowest energy. | 18 |
| Table 3.2 Similar to Table 3.1 for Co^{1+} | 19 |
| Table 3.3 Similar to Table 3.1 for Co^{2+} | 20 |
| Table 3.4 Similar to Table 3.1 for Co^{3+} | 21 |
| Table 3.5 Similar to Table 3.1 for Co^{1-} | 22 |
| Table 3.6 The first ionization energy IE_1 of Co atom for the process $IE_1 + \text{Co} \rightarrow \text{Co}^{1+} + e^-$, calculated as $IE_1 = E_5(\text{Co}^{1+}) - E_4(\text{Co})$. The experimental value is 7.881 eV [43]. Δ in the second column gives the error between the experimental and the calculated results; the last column is for the corresponding percentage error. | 24 |
| Table 3.7 The second ionization energy IE_2 of Co atom for the process $IE_2 + \text{Co}^{1+} \rightarrow \text{Co}^{2+} + e^-$, calculated as $IE_2 = E_4(\text{Co}^{2+}) - E_5(\text{Co}^{1+})$. The experimental value is 17.080 eV [43]. Δ in the second column gives the error between the experimental and the calculated results; the last column is for the corresponding percentage error. | 25 |
| Table 3.8 The third ionization energy IE_3 of Co atom for the process $IE_3 + \text{Co}^{2+} \rightarrow \text{Co}^{3+} + e^-$, calculated as $IE_3 = E_5(\text{Co}^{3+}) - E_4(\text{Co}^{2+})$. The experimental value is 33.497 eV [43]. Δ in the second column gives the error between the experimental and the calculated results; the last column is for the corresponding percentage error. | 26 |

| | | |
|------------|--|----|
| Table 3.9 | The electron affinity EA of Co atom for the process $\text{Co} + e^- \rightarrow \text{Co}^{1-}$, calculated as $EA = E_4(\text{Co}) - E_3(\text{Co}^{1-})$. The experimental value is 0.662 eV [43]. Δ in the second column gives the error between the experimental and the calculated results; the last column is for the corresponding percentage error. | 27 |
| Table 3.10 | Total energies, E_m , in Hartrees, for a Sm atom for different multiplicities, m ($2S + 1$). The starred ones show the lowest energy. ‘nc’ indicates a ‘not completed’ calculation due to a non-convergent- or confused-SCF process. | 28 |
| Table 3.11 | Similar to Table 3.1 for Sm^{1+} | 29 |
| Table 3.12 | Similar to Table 3.1 for Sm^{2+} | 30 |
| Table 3.13 | Similar to Table 3.1 for Sm^{3+} | 31 |
| Table 3.14 | Similar to Table 3.1 for Sm^{1-} | 33 |
| Table 3.15 | The first ionization energy IE_1 of Sm atom for the process $IE_1 + \text{Sm} \rightarrow \text{Sm}^{1+} + e^-$, calculated as $IE_1 = E_8(\text{Sm}^{1+}) - E_7(\text{Sm})$. The experimental value is 5.643 eV [43]. Δ in the second column gives the error between the experimental and the calculated results; the last column is for the corresponding percentage error. | 34 |
| Table 3.16 | The second ionization energy IE_2 of Sm atom for the process $IE_2 + \text{Sm}^{1+} \rightarrow \text{Sm}^{2+} + e^-$, calculated as $IE_2 = E_7(\text{Sm}^{2+}) - E_8(\text{Sm}^{1+})$. The experimental value is 11.090 eV [43]. Δ in the second column gives the error between the experimental and the calculated results; the last column is for the corresponding percentage error. | 35 |
| Table 3.17 | The third ionization energy IE_3 of Sm atom for the process $IE_3 + \text{Sm}^{2+} \rightarrow \text{Sm}^{3+} + e^-$, calculated as $IE_3 = E_6(\text{Sm}^{3+}) - E_7(\text{Sm}^{2+})$. The experimental value is 23.423 eV [43]. Δ in the second column gives the error between the experimental and the calculated results; the last column is for the corresponding percentage error. | 36 |
| Table 3.18 | The electron affinity EA of Sm atom for the process $\text{Sm} + e^- \rightarrow \text{Sm}^{1-}$, calculated as $EA = E_8(\text{Sm}) - E_7(\text{Sm}^{1-})$. The experimental value is 0.518 eV [43]. Δ in the second column gives the error between the experimental and the calculated results; the last column is for the corresponding percentage error. | 37 |

| | |
|--|----|
| Table 3.19 Total energies, E_m , in Hartrees, for SmCo dimer for different multiplicities, $m (2S + 1)$. The starred ones show the lowest energy. | 38 |
| Table 3.20 Spectroscopic constants of the SmCo dimer calculated for the multiplicity, $m (2S + 1)$, at which the total energy is minimum. Binding energy D_e is in eV, equilibrium interatomic separation r_e is in Å, and the fundamental frequency ω_e is in cm^{-1} . Also given are the calculated excess charge $q(\text{Sm})$ on the Sm atom (in units of electron charge $ e $) and the dipole moment μ (in Debyes). Note that for the excess charge on the Co atom, we have $q(\text{Co}) = -q(\text{Sm})$ | 39 |
| Table 3.21 HOMO and LUMO energies (in Hartrees), and HOMO-LUMO gap (E_g) energies (in eV) of the SmCo dimer, calculated for the multiplicity, $m (2S + 1)$, at which the total energy is minimum. | 40 |
| Table 3.22 Results for Co_2 from previous works in literature. | 40 |
| Table 3.23 Total energies, E_m , in Hartrees, for Co_2 dimer for different multiplicities, $m (2S + 1)$. The starred ones show the lowest energy. | 42 |
| Table 3.24 Spectroscopic constants of the Co_2 dimer calculated for the multiplicity, $m (2S + 1)$, at which the total energy is minimum. For notation used, see Table 3.20. 43 | 43 |
| Table 3.25 HOMO and LUMO energies (in Hartrees), and HOMO-LUMO gap (E_g) energies (in eV) of the Co_2 dimer, calculated for the multiplicity, $m (2S + 1)$, at which the total energy is minimum. | 44 |
| Table 3.26 Total energies, E_m , in Hartrees, for a Sm_2 dimer for different multiplicities, $m (2S + 1)$. The starred ones show the lowest energy. ‘nc’ indicates a ‘not completed’ calculation due to a non-convergent- or confused-SCF process. | 45 |
| Table 3.27 Spectroscopic constants of the Sm_2 dimer calculated for the multiplicity, $m (2S + 1)$, at which the total energy is minimum. For notation used, see Table 3.20. 46 | 46 |
| Table 3.28 HOMO and LUMO energies (in Hartrees), and HOMO-LUMO gap (E_g) energies (in eV) of the Sm_2 dimer, calculated for the multiplicity, $m (2S + 1)$, at which the total energy is minimum. | 47 |

| | |
|---|----|
| Table 3.29 Total energies, E_m , in Hartrees, for Co_3 trimer for different multiplicities, $m (2S + 1)$ | 51 |
| Table 3.30 Bond lengths R_{12} and R_{23} (Å), bond angle θ_{123} (deg), and vibrational frequencies ω_n (cm^{-1}) of Co_3 trimer. For the notation used, see Fig. 3.9. | 52 |
| Table 3.31 Calculated excess charge (in units of electron charge) on atoms and dipole moments (in Debye) of Co_3 trimer. | 54 |
| Table 3.32 HOMO and LUMO energies (in Hartrees), and HOMO-LUMO gap (E_g) energies (in eV) of the Co_3 trimer, calculated for the multiplicity, $m (2S + 1)$, at which the total energy is minimum. | 55 |
| Table 3.33 Total energies, E_m , in Hartrees, for Sm_3 trimer for different multiplicities, $m (2S + 1)$. The starred ones show the lowest energy. ‘nc’ indicates a ‘not completed’ calculation due to a non-convergent- or confused-SCF process. | 56 |
| Table 3.34 Bond lengths R_{12} and R_{23} (Å), bond angle θ_{123} (deg), and vibrational frequencies ω_n (cm^{-1}) of Sm_3 trimer. For the notation used, see Fig. 3.9. | 57 |
| Table 3.35 Calculated excess charge (in units of electron charge) on atoms and dipole moments (in Debye) of Sm_3 trimer. | 58 |
| Table 3.36 HOMO and LUMO energies (in Hartrees), and HOMO-LUMO gap (E_g) energies (in eV) of the Sm_3 trimer, calculated for the multiplicity, $m (2S + 1)$, at which the total energy is minimum. | 59 |
| Table 3.37 Total energies, E_m , in Hartrees, for SmCo_2 trimer for different multiplicities, $m (2S + 1)$ | 60 |
| Table 3.38 Bond lengths R_{12} and R_{23} (Å), bond angle θ_{123} (deg), and vibrational frequencies ω_n (cm^{-1}) of SmCo_2 trimer. For the notation used, see Fig. 3.9. | 61 |
| Table 3.39 Calculated excess charge (in units of electron charge) on atoms and dipole moments (in Debye) of SmCo_2 trimer. | 62 |

| | |
|---|----|
| Table 3.40 HOMO and LUMO energies (in Hartrees), and HOMO-LUMO gap (E_g) energies (in eV) of the SmCo_2 trimer, calculated for the multiplicity, $m (2S + 1)$, at which the total energy is minimum. | 63 |
| Table 3.41 Total energies, E_m , in Hartrees, for Sm_2Co trimer for different multiplicities, $m (2S + 1)$ | 64 |
| Table 3.42 Bond lengths R_{12} and R_{23} (\AA), bond angle θ_{123} (deg), and vibrational frequencies ω_n (cm^{-1}) of Sm_2Co trimer. For the notation used, see Fig. 3.9. | 65 |
| Table 3.43 Calculated excess charge (in units of electron charge) on atoms and dipole moments (in Debye) of Sm_2Co trimer. | 66 |
| Table 3.44 HOMO and LUMO energies (in Hartrees), and HOMO-LUMO gap (E_g) energies (in eV) of the Sm_2Co trimer, calculated for the multiplicity, $m (2S + 1)$, at which the total energy is minimum. | 76 |

LIST OF FIGURES

FIGURES

| | |
|---|----|
| Figure 3.1 Nominal Lennard-Jones curves, describing the nature of the interaction between Sm and Co atoms, for the 12 methods in Tables or in which the total energy values are minimum for the multiplicity $m = 10$ | 67 |
| Figure 3.2 Nominal Lennard-Jones curves, describing the nature of the interaction between Sm and Co atoms, for the 12 methods in Tables or in which the total energy values are minimum for the multiplicity $m = 10$ (Cont). | 68 |
| Figure 3.3 Nominal Lennard-Jones curves for Co ₂ dimer with respect to DFT methods for $m = 7$ | 69 |
| Figure 3.4 Nominal Lennard-Jones curves for Co ₂ dimer with respect to DFT methods for $m = 7$.(Cont.) | 70 |
| Figure 3.5 Nominal Lennard-Jones curves for Co ₂ dimer with respect to DFT methods for $m = 7$ | 71 |
| Figure 3.6 Nominal Lennard-Jones curves for Co ₂ dimer with respect to DFT methods for $m = 7$.(Cont.) | 72 |
| Figure 3.7 Nominal Lennard-Jones curves for Sm ₂ dimer with respect to DFT methods. | 73 |
| Figure 3.8 Nominal Lennard-Jones curves for Sm ₂ dimer with respect to DFT methods.(Cont.) | 74 |
| Figure 3.9 Trimer Angle | 75 |

LIST OF ABBREVIATIONS

| | |
|-----------|---|
| DFT | Density Functional Theory |
| SCF | Self Consistent Field |
| ECP | Effective Core Potential (pseudopotential) |
| $X\alpha$ | A local density method, α is a parameter |
| GGA | Generalized Gradient Approximation |
| LDA | Local Density Approximation |
| LSDA | Local Spin Density Approximation |
| XC | Exchange–Correlation |
| HF | Hartree–Fock |
| RHF | Restricted Hartree–Fock |
| HFS | Hartree–Fock–Slater |
| HFB | Hartree–Fock–Becke |
| LYP | Lee–Yang–Parr |
| PBE | Perdew–Burke–Ernzerhof |
| PW | Perdew–Wang |
| mPW | Modified Perdew–Wang |

CHAPTER 1

INTRODUCTION

In industry and technology, the applications of transition metal (TM)–rare earth (RE) alloys, offer a significant amount of research opportunities, since they have remarkably high magnetocrystalline anisotropy which causes a large coercivity [1]. For the scope of the present study samarium (Sm)–cobalt (Co) alloys have been chosen. In order to try, for the first time to the best of our knowledge, to give an insight into the building blocks of the Sm-Co system, we investigate its smallest microclusters, namely Sm, Co, Sm₂, Co₂, SmCo, Sm₃, Co₃, Sm₂Co, and SmCo₂.

1.1 Sm-Co Systems

In the literature, some binary alloys of Sm and Co are available in different phases. These are SmCo₂, SmCo₃, SmCo₅, Sm₂Co₇, Sm₂Co₁₇, Sm₃Co, Sm₅Co₂, Sm₅Co₁₉, and Sm₉Co₄ which have been investigated by many researchers from several fields [1, 2]. Especially, SmCo₅ and Sm₂Co₁₇ are of great importance, since they are known to belong to the strongest permanent magnet class. In the room temperature, their magnetocrystalline anisotropy constant is of the order of 10^7 J/m³ [3–6]. The Curie temperature of these alloys are very high that give them an advantage over other magnets in the same category for high temperature applications. In addition, coercivities of these magnets are very high, which means that they cannot be demagnetized easily [7].

Because of these high magnetocrystalline anisotropy, coercivity, and high Curie temperature, Sm-Co alloys have an important place in many applications; examples are high-performance permanent magnets [4, 8], high-density data storage media [5, 8], high performance thin films

[5, 7], and high-resolution nuclear magnetic resonance spectroscopy [9].

The scope of the present study comprises the ground state investigations of Cobalt and Samarium atoms, their dimers (Co_2 , Sm_2 , and SmCo), and trimers (Co_3 , Sm_3 , SmCo_2 , and Sm_2Co). These investigations will also contain some spectroscopic and electronic properties of the atoms and their compounds.

1.2 Transition Metals

Transition metals have unfilled d-subshells or easily give rise in ions with incomplete d-subshells. They have relatively small atomic radii, so that they have strong atomic bonds. On this account, TMs have high densities and high melting and boiling points. Since the electrons in d-subshells are loosely bounded, they exhibit high electrical and heat conductivity and malleability. Another valuable property of TMs is that they show a wide range of oxidation state because their valence electrons are usually distributed more than one subshell. The compounds of TMs are mostly paramagnetic because of their incompletely filled d-subshells [10–12].

Another important point about TMs is their orbital energies. It is known that the energy of the 4s orbital is lower than that of the 3d orbitals. Thus, it might be expected that when forming a compound TM will lose its electron from its more energetic 3d-subshell. But this is not true because electrons are first lost from its 4s-subshell [12]. Therefore, the electron configuration of Co^{2+} ion is $[\text{Ar}] 3d^7$ instead of $[\text{Ar}] 3d^5 4s^2$. The reason of this situation can be explained by the stability of the orbitals that 3d-subshells are more stable than 4s-subshells in TM ions [10].

1.3 Rare Earth Elements (Lanthanides)

Rare earth elements are the series of elements which have atomic numbers 57 through 71. Except lutetium (a d-block element with atomic number 71), RE elements are f-block elements, in other words, their 4f-orbitals are gradually filled. The history of these elements do not date back so long, until their analysis with the help of x-ray spectra in 1907, they could not be grouped or placed in the periodic table correctly [13]. Rare earth elements also known as

inner transition metals, although they differ from TMs in various features. For example, REs are more reactive than TMs; they do not form multiple bonds like TMs, etc. [10, 11, 13, 14].

Compounds of the RE elements are generally ionic and most of them are strongly paramagnetic. They have high melting and boiling points in accordance with TMs. They are relatively soft metals and their hardness increases with increasing atomic number. The coordination number of REs are high, generally 8 or 9 [13].

Rare earth elements are located in 5d-block of the periodic table and their electron configuration is generally written as $[\text{Xe}]6s^24f^n5d^0$. Lanthanum, cerium, gadolinium, and lutetium have exceptional electron configurations of the form $[\text{Xe}]6s^24f^n5d^1$. The energy spacing of the 5d- and 4f-orbitals are very close, so that for some configurations electron enters into the 5d-orbital instead of staying at the expected 4f-orbital. For instance, gadolinium has $[\text{Xe}]6s^24f^75d^1$ because it gains extra stability from the half-filled subshell 5d. Another similarity between REs and TMs is about forming the positive ions. Electrons are lost first from 6s and 5d, instead from 4f. As a result, all the 3+ ions have the configuration $[\text{Xe}]4f^n$ [10, 11, 13].

Rare earths have many scientific and industrial uses. For instance, their compounds are utilized as catalysts in the production of petroleum and some synthetic products. They are essential in lamps, lasers, magnets, phosphors, motion picture projectors, and x-ray intensifying screens [13]. As a result, it is not surprising at all that there have been innumerable many researches carried out nowadays trying to explore the chemical and physical properties of REs, and their possible industrial applications. The present study is such a small example to this end.

CHAPTER 2

DENSITY FUNCTIONAL THEORY

Density functional theory (DFT) brought a fresh breath to physics and chemistry in 60s. Number of studies about the field increased rapidly at 80s and now reach to a huge number [15]. The new approach that brings DFT such popularity is its basis on electron density instead of wave function. In other words, DFT provides an alternative computational method to examine many body systems such as atoms, molecules or larger systems, for which it is impossible to obtain exact solution of the Schrödinger equation.

2.1 Theoretical Background

Many information about any molecular system can be obtained from the solution of time-independent non-relativistic wave function, $\psi(x_1^{\vec{r}}, \dots, x_N^{\vec{r}})$. To obtain the wave function, time-independent Schrödinger equation has to be solved.

$$\hat{H}\Psi_e = E_e\Psi_e \quad (2.1)$$

In computational physics, we focus on atoms, molecules, and solids, on their structural and cohesive properties, and on how they interact with each other. For an M -nuclei and N -electrons system the Hamiltonian is given by,

$$\hat{H} = -\frac{1}{2} \sum_{i=1}^N (\nabla_i^2) - \frac{1}{M_{\mathbf{A}}} \sum_{A=1}^M (\nabla_A^2) - \sum_{i=1}^N \sum_{A=1}^M \frac{Z_A}{r_{i\mathbf{A}}} + \sum_{A=1}^M \sum_{A<B}^M \frac{Z_A Z_B}{R_{\mathbf{AB}}} + \sum_{i=1}^N \sum_{i<j}^N \frac{1}{r_{ij}}, \quad (2.2)$$

where r_{iA} is the distance between electrons and the nuclei, R_{AB} indicates distance between each nuclei, and r_{ij} is distance between each electrons. The first term indicates total kinetic

energy of electrons and the second term indicates kinetic energy of the nuclei. Next three are the potential energy terms, based on the Coulombic interactions. First potential term due to interaction among nuclei and electrons, second one due to nucleus–nucleus interaction and the last one electron–electron interaction [16–18].

It is well known that the electrons are very tiny particles with respect to nuclei. As an approximation we can assume that the nuclei move much more slowly than electron. Now, only related terms are the kinetic energy term of electrons with electron–electron and electron–nuclei interaction of the potential terms. The effect of all nuclei can be written as an external potential exerted on i th electron:

$$V_{ext}(\vec{r}) = - \sum_i \frac{Z_i}{|\vec{r} - \vec{r}_i|}. \quad (2.3)$$

At least the Hamiltonian of the N -electron system reduces to;

$$\hat{H} = -\frac{1}{2} \sum_{i=1}^N (\nabla_i^2) + \sum_{i=1}^N V_{ext}(\vec{r}_i) + \sum_{i=1}^N \sum_{j>i}^N \frac{1}{r_{ij}}. \quad (2.4)$$

As the solution of Schrödinger equation for many particle system, we obtain a many body wave functions;

$$\Psi = \Psi(\mathbf{r}_1, \mathbf{r}_2, \dots, \mathbf{r}_N). \quad (2.5)$$

It is not possible to solve Schrödinger equation exactly for many body systems because the eigen function depends on $3N$ position coordinates. We need to use some approximation methods to overcome the problem and attain the solution. One of the simplest examples of these approaches is Hartree Fock method.

2.2 Hartree–Fock Method

The assumption is that the wavefunctions of the electrons are written as a product of N orthonormal spin orbitals $\psi_i(\vec{x}_i)$, as if they do not interact with each other. Each spin orbital is assumed to be a combination of spatial orbital $\phi_i(\vec{r})$ and a spin function $\sigma(\mathbf{s})$. Since we deal with fermions, there are only two types of spin function, spin up $\alpha(\mathbf{s})$ or spin down $\beta(\mathbf{s})$.

The Hartree product which is the simplest application to a many-body wave function can be written as,

$$\Psi = \psi_1(\vec{r}_1) \psi_2(\vec{r}_2) \cdots \psi_N(\vec{r}_N). \quad (2.6)$$

The Hartree product does not satisfy some properties of a fermionic wave function, i.e. the antisymmetry principle. If the product written as Slater determinant, single electron wave functions can be stated to obtain N-electron wavefunction satisfying the antisymmetry principle [19–21]. For N electrons, the Slater determinant is

$$\psi(\vec{x}_1, \vec{x}_2, \dots, \vec{x}_N) = \frac{1}{\sqrt{N!}} \begin{vmatrix} \psi_1(\vec{x}_1) & \psi_2(\vec{x}_1) & \cdots & \psi_N(\vec{x}_1) \\ \psi_1(\vec{x}_2) & \psi_2(\vec{x}_2) & \cdots & \psi_N(\vec{x}_2) \\ \vdots & \vdots & & \vdots \\ \psi_1(\vec{x}_N) & \psi_2(\vec{x}_N) & \cdots & \psi_N(\vec{x}_N) \end{vmatrix}. \quad (2.7)$$

Another advantage of the Slater determinant is satisfying the Pauli exclusion principle. If the single electron wave functions of two or more electrons are same, it vanishes. This result is in accordance with the claim of exclusion principle that the two electrons can not be located to same orbital with the same spin. As a solution of the Schrödinger equation, Slater determinant includes exchange term however Hartree Fock method does not describe electron interaction, so correlation term. It is well known that electrons are interacting, so HF method does not fulfill the solution of the Schrödinger equation, on the other hand DFT calculations are similar to the HF calculations in some ways [15].

2.3 Electron Density

As stated above, exact solution of the Schrödinger equation is hard to achieve. The electron density is an important quantity for a given state, since it provides an alternative solution method instead of wave function. The electron density for an electronic system, can be defined as the number of electrons in the infinitesimal volume element $d\vec{r}$ and denoted by $\rho(\vec{r})$. In terms of the wave function, the electron density is,

$$\rho(\vec{r}) = N \int \dots \int |\psi(\vec{x}_1, \vec{x}_2, \dots, \vec{x}_N)|^2 ds_1 d\vec{x}_2 \dots d\vec{x}_N. \quad (2.8)$$

By the definition, integration over all space of electron density gives the total number of electrons.

$$\int \rho(\vec{r}) d\vec{r} = N. \quad (2.9)$$

The many body wave functions has $3N$ spatial coordinates, whereas by using electron density it can be decreased to only three variables. If all the energy terms can be written in terms of electron density, there is no need to use wave functions.

2.4 The Hohenberg–Kohn Theorem

The DFT lays the foundations especially by the theorem of the Hohenberg and Kohn published in 1964 [22]. As mentioned before, to obtain the observables of any system, we need to solve Schrödinger equation. For an N -electron system, the external potential $V_{ext}(\vec{r})$ determines the hamiltonian, given by Eqn. 2.4, by this means determine all the electronic properties of a system with N electrons.

Hohenberg and Kohn brought a new approach that the external potential $V_{ext}(\vec{r})$ could be determined by the electron density. The first Hohenberg-Kohn theorem provides a simple proof to show that the external potential $V_{ext}(\vec{r})$ is uniquely determined by $\rho(\vec{r})$ [22]. Since external potential fixes the Hamiltonian, the full many particle system can be expressed as a functional of electron density $\rho(\vec{r})$ [17].

The total energy is expressed with respect to electron density,

$$E[\rho] = T[\rho] + V_{ne}[\rho] + V_{ee}[\rho] = \int \rho(\mathbf{r}) v(\mathbf{r}) d\mathbf{r} + F_{HK}[\rho], \quad (2.10)$$

with Hohenberg–Kohn functional,

$$F_{HK}[\rho] = T[\rho] + V_{ee}[\rho], \quad (2.11)$$

which includes $T[\rho]$, the kinetic energy of the real system and $V_{ee}[\rho]$ is the potential energy of the electron–electron interactions. The functional for the electron–electron interaction is given as

$$V_{ee}[\rho] = J[\rho] + \text{nonclassical term}, \quad (2.12)$$

where $J[\rho]$ is the well known classical Coulombic electrostatic interactions between the electrons,

$$J[\rho] = \frac{1}{2} \int \int \frac{\rho(\mathbf{r}) \rho(\mathbf{r}')}{|\mathbf{r} - \mathbf{r}'|} d\mathbf{r} d\mathbf{r}', \quad (2.13)$$

and the nonclassical term includes all self interaction correction effects, exchange and Coulomb correlation. It is not surprising that $F_{HK}[\rho]$ is the major problem in DFT, which consists of completely or partly unknown $T[\rho]$ and $V_{ee}[\rho]$ functionals.

The second theorem of the Hohenberg–Kohn is about to provide an electron density that minimizing the total energy $E[\rho]$. It is well known that only ground state electron density satisfies the ground state energy. This theorem specifies that to obtain ground state energy, true ground state electron density has to be searched by variational principle,

$$E_0 \leq E[\tilde{\rho}] = T[\tilde{\rho}] + V_{ne}[\tilde{\rho}] + V_{ee}[\tilde{\rho}]. \quad (2.14)$$

For any trial density $\tilde{\rho}(\vec{r})$, there are necessary boundary conditions which has to be satisfied, such as

$$\tilde{\rho}(\vec{r}) \geq 0, \quad (2.15)$$

and

$$\int \tilde{\rho}(\vec{r}) d\vec{r}_1 = N. \quad (2.16)$$

The proof of the second Hohenberg–Kohn theorem is obtained by using the variational principle to form ground state wave function [23] and can be found in various sources about the theorem.

2.5 The Kohn–Sham Method

After Hohenberg–Kohn theorem, another massive and the most powerful brick was put on the wall by Kohn–Sham in 1965 [24]. The Kohn–Sham method suggests a way to obtain kinetic energy in terms of electron density. We start with variational principle one more time, $E[\rho]$ and the ground state density need to satisfy the equation;

$$\delta \left(E[\rho] - \mu \left[\int \rho(\vec{r}) d\vec{r} - N \right] \right) = 0, \quad (2.17)$$

where μ is the Langrange multiplier related to obtain density for acquiring the correct number of electrons N . μ associated with the chemical potential and following equation is obtained by differentiation of functional,

$$\mu = \frac{\delta E[\rho]}{\delta \rho(\vec{r})} = V_{ext}(\vec{r}) + \frac{\delta F_{HK}[\rho(\vec{r})]}{\delta \rho(\vec{r})}. \quad (2.18)$$

If the exact form of $F_{HK}[\rho(\vec{r})]$ can be obtained, ground state electron density is also acquired by Eqn. 2.17. The main point here is to determine $F_{HK}[\rho(\vec{r})]$ which is equal to $T[\rho(\vec{r})]$, for

non-interacting electrons, but T is also unknown. The kinetic energy term is written for an N -electron non-interacting reference system as following

$$T = \sum_i^N n_i \langle \psi_i | -\frac{1}{2} \nabla_i^2 | \psi_i \rangle, \quad (2.19)$$

where ψ_i are spin orbitals and n_i are the corresponding occupation numbers. All physically accepted densities of the non-interacting N -electron system can be expressed as

$$\rho(\mathbf{r}) = \sum_i^\infty n_i \sum_s |\psi_i(\mathbf{r}, s)|^2 \quad (2.20)$$

The valuable part of this theorem is the simplification of these equations by assuming $n_i = 1$ for N orbitals and $n_i = 0$ for the remaining. The equations reduce to

$$T_s = \sum_i^N \langle \psi_i | -\frac{1}{2} \nabla_i^2 | \psi_i \rangle \quad (2.21)$$

and

$$\rho(\mathbf{r}) = \sum_i^N \sum_s |\psi_i(\mathbf{r}, s)|^2 \quad (2.22)$$

The following Hamiltonian of N -noninteracting electrons is obtained

$$\hat{H}_S = -\frac{1}{2} \sum_{i=1}^N \nabla_i^2 + \sum_{i=1}^N V_S(\vec{r}_i) \quad (2.23)$$

without electron–electron repulsion terms and with exact ground state density ρ .

The exact determinantal wave function of the system is

$$\Psi_s = \frac{1}{\sqrt{N!}} |\psi_1 \psi_2 \dots \psi_N|, \quad (2.24)$$

where ψ_i reflects the N lowest eigenstates of the one electron Hamiltonian h_s ;

$$h_s \psi_i = \left[-\frac{1}{2} \nabla^2 + V_s(\mathbf{r}_i) \right] \psi_i = \varepsilon_i \psi_i. \quad (2.25)$$

Now, the kinetic energy functional turns to

$$T_s[\rho] = \sum_i^N \langle \Psi_s | -\frac{1}{2} \nabla_i^2 | \Psi_s \rangle. \quad (2.26)$$

For isolating kinetic energy term, we write $F[\rho]$ again as,

$$F[\rho] = T_s[\rho] + J[\rho] + E_{xc}[\rho] \quad (2.27)$$

where

$$E_{xc}[\rho] = T[\rho] - T_s[\rho] + V_{ee}[\rho] - J[\rho]. \quad (2.28)$$

The $E_{xc}[\rho]$ is known as exchange-correlation energy and in definition it originates by the difference between $T[\rho]$ and $T_s[\rho]$ and the non-classical part of the potential energy of electron-electron interaction.

Now, let us turn to Euler equation again, that becomes

$$\mu = v_{\text{eff}}(\mathbf{r}) + \frac{\delta T_s[\rho]}{\delta \rho(\mathbf{r})}, \quad (2.29)$$

where the effective potential is,

$$v_{\text{eff}}(\mathbf{r}) = v(\mathbf{r}) + \frac{\delta J[\rho]}{\delta \rho(\mathbf{r})} + \frac{\delta E_{xc}[\rho]}{\delta \rho(\mathbf{r})} = v(\mathbf{r}) + \int \frac{\rho(\mathbf{r}')}{|\mathbf{r} - \mathbf{r}'|} d\mathbf{r}' + v_{xc}(\mathbf{r}), \quad (2.30)$$

where the exchange–correlation potential define as,

$$v_{xc}(\mathbf{r}) = \frac{\delta E_{xc}[\rho]}{\delta \rho(\mathbf{r})}. \quad (2.31)$$

We still try to obtain the explicit form of $T_s[\rho]$. We can rewrite Eqn. 2.25 by replacing V_s with V_{eff} given in Eqn. 2.30;

$$\left[-\frac{1}{2}\nabla^2 + v_{\text{eff}}(\mathbf{r})\right]\psi_i = \epsilon_i \psi_i \quad (2.32)$$

and the following expression can be obtained for electron density given by Eqn.2.22.

The procedure begins with a trial density, than V_{eff} is obtained by Eqn.2.30, and then one finds a new electron density by using Eqn.2.22 and Eqn.2.32. The total energy can be computed as,

$$E = \sum_i^N \epsilon_i - \frac{1}{2} \int \int \frac{\rho(\mathbf{r}) \rho(\mathbf{r}')}{|\mathbf{r} - \mathbf{r}'|} d\mathbf{r} d\mathbf{r}' + E_{xc}[\rho] - \int v_{xc}(\mathbf{r}) \rho(\mathbf{r}) d\mathbf{r}, \quad (2.33)$$

where

$$\sum_i^N \epsilon_i = \sum_i^N \langle \psi_i | -\frac{1}{2}\nabla^2 + v_{\text{eff}}(\mathbf{r}) | \psi_i \rangle = T_s[\rho] + \int v_{\text{eff}}(\mathbf{r}) \rho(\mathbf{r}) d\mathbf{r}. \quad (2.34)$$

2.6 Exchange-Correlation Functionals

There are dozens of functionals developed and used, particularly for calculations with isolated molecules. Some of the widely used exchange functionals are Becke's 1988 functional **B** [25],

Perdew and Wang's 1991 functional **PW91** [26], and Perdew, Burke and Ernzerhof's 1996 functional **PBE** [27] which are also the components of the functionals that used in previous study. Similarly, correlation functional of Lee, Yang, and Parr **LYP** [28], Perdew and Wang's gradient-corrected correlation functional **PW91** [26, 27], and Perdew, Burke, and Ernzerhof's correlation function **PBE** [27] constitute the functionals of used methods. The combinations of these functionals and similar ones are used to form methods for DFT calculations.

It is necessary to specify what functional was used in any particular calculation because different functionals will give somewhat different results for any particular configuration of atoms. In the scope of previous study 13 DFT methods have been used and only one of them, HFB is an only exchange functional, the remaining 12 are hybrid functionals. HFB is named by Hartree-Fock-Becke, important for the study since it will reflect the contribution of the correlational effects by distinction from other methods.

Hybrid Functionals

The hybrid functionals includes both exchange-correlation affect, with the exact exchange from Hartree-Fock theory and changing proportion of exchange and correlation effects from other sources. The explanations about these methods can be listed as follows.

- **B1LYP**: It is one parameter hybrid density functional that was designed by Becke in 1996 [29]. The form of the functional is

$$E_{XC} = E_{XC}^{DFT} + a_0(E_X^{HF} - E_X^{DFT}), \quad (2.35)$$

where a_0 takes a value in the range of 0.16-0.28 and changes according to the chosen correlation functional [30].

- **B3P86**: An example of hybrid functional with three parameters. The following equation was developed;

$$E_{XC} = E_{XC}^{LSDA} + a_0(E_X^{HF} - E_X^{LSDA}) + a_x \Delta E_X^{B88} + a_c \Delta E_C^{P86}, \quad (2.36)$$

where a_0 , a_x , and a_c are the parameters were determined by fitting to the G1 database which is a set of thermochemical data and obtained as 0.20, 0.72, and 0.81 a.u. respectively [29, 31].

- B3LYP: It is also a three parameters hybrid functional which uses Eqn.2.36 with the LYP correlation functional in stead of the P86 functional [25,28].
- B3PW91: This method also uses Eqn.2.36 with the PW91 correlation functional [32].
The following three methods are the revisions of Becke's 1997 functional τ dependent gradient-corrected correlation functional, defined as part of this one parameter hybrid functional [33].
- B98: The revision of Becke's B97 functional in 1998 [34].
- B971: The revision of B97 by Handy, Tozer, and co-workers in 1998 [35].
- B972: Another modification of B97 by Wilson, Bradley, and Tozer in 2001 [36].
- PBE1PBE: The PBE functional is a modification of PW91 correlation functional, which can satisfy only significantly energetic conditions, unlike PW91 which is for all exact conditions [30]. The one parameter combination of functionals form this method and the parameter is not empirical [27]. PBE1PBE method gives appropriate results for electronic, magnetic, and vibrational properties of molecules in comparison to other functionals with extensive parametrization [37].
- mPW1PW91: It includes the modification of PW exchange functional by Adamo and Barone [38]. Similar to PBE1PBE, it also gives satisfactory results by combining one parameter approach.
- O3LYP: Similar to B3LYP, O3LYP also a three-parameter functional and the parameters were defined by Cohen and Handy [39].
Half and half functionals use a combination that includes equal ratio of DFT and exact exchange energies.
- BHandH: The related equation of the functional is,

$$0.5E_X^{HF} + 0.5E_X^{LSDA} + E_C^{LYP}. \quad (2.37)$$

- BHandHLYP: Similarly, the equation of the funtional is as follows,

$$0.5E_X^{HF} + 0.5E_X^{LSDA} + 0.5\Delta E_X^{Becke88} + E_C^{LYP}. \quad (2.38)$$

- HFB: As mentioned before, the method named from Hartre–Fock–Becke and does not include correlational functional. Namely, it is Becke’s 1988 functional that also contains the Slater exchange with the gradient of the density [25]. It was chosen to determine the affect of correlation in comparison to other methods.

CHAPTER 3

RESULTS AND DISCUSSION

The calculation part of the present study consists of three main sets. The first of these sets includes calculations of minimum energy values with corresponding multiplicity values of cobalt and samarium atoms and their ions. Out of curiosity, we also wondered if the DFT methods we used are successful in spotting the correct multiplicity values for Co and Sm elements and their cations and anions. To this end, we have carried out some further atomic calculations for Co^{1+} , Co^{2+} , Co^{3+} , Co^{1-} , Sm^{1+} , Sm^{2+} , Sm^{3+} , and Sm^{1-} . The second set includes calculations of SmCo , Sm_2 , and Co_2 dimers in the same way and single-point (sp) self-consistent field calculations (SCF) were performed. The third set includes Co_3 , Sm_3 , SmCo_2 , and Sm_2Co trimers calculations. All parts have been carried out by 13 DFT methods to control their usefulness and convenience. In the scope of this study 38.000 calculations have been achieved.

At the beginning, it will be essential to point out that the present study is based on a pre-study that has been covered the calculations about samarium (Sm) and cobalt (Co) elements and SmCo by using 21 DFT methods [5]. The idea of the previous study was the determination of the well-behaved and useful methods; which give appropriate results for Co and Sm atoms and SmCo dimer, so that they might also work properly for the higher order alloys of these atoms. As a conclusion, it was claimed that the only exchange functionals and the standalone functionals cannot fulfill the sufficient performance although hybrid functionals usually show great success [5]. According to this conclusion, 13 hybrid functionals have been chosen and calculations were performed by them in the scope of present study. The common purpose of both studies is forming preknowledge for investigation of higher order Sm–Co alloys.

In this chapter of the study, calculated spectroscopic constants (binding energy D_e , equilib-

rium interatomic separation r_e , and fundamental frequency w_e) of the dimers and trimers, the minimum energy configurations of the trimers (bond lengths and bond angle, as well as their fundamental frequencies w_n) are reported. For all the microclusters considered, the possible dissociation channels and the corresponding dissociation energies, the calculated HOMO (highest occupied molecular orbital), LUMO (lowest unoccupied molecular orbital), and HOMO–LUMO gap energies are presented. The calculated dipole moments and excess charges on the atoms of the trimers are also given.

The structure of higher order clusters of transition metals are generally investigated experimentally by photoelectron spectroscopy or chemical probe experiments [40,41]. Due to these familiar methodologies it is possible to find information in the literature about higher order clusters, unfortunately this is not the case for smaller ones. This is why small clusters of transition metals still have not been well identified. At this point of view, it is clear that the theoretical studies come into prominence.

The present work exhibits the results of density functional theory calculations within the effective core potential (ECP) level, for small Sm-Co clusters up to trimers. The DFT calculations were carried out by using the GAUSSIAN 03 package [42]. For this study, the basis Cep-121G has been preferred and used for all calculations. Alternatively, UGBS and SDD would be used as basis, however much more works and effort will be needed for SDD, and UGBS has not been attempted.

3.1 Co and Sm Atoms

3.1.1 Calculations of Co Atoms

Co atom has 27 electrons and the electron configuration of the Co atom is $[Ar]3d^74s^2$. There are three unpaired electrons in the 3d orbital, so its expected multiplicity is four (by the formula $2S+1$). For the sake of thoroughness we searched self consistent energies for all possible values of the multiplicity, from 2 to 18. These results are demonstrated in the Table 3.1. The first step is to control the methods which give the expected multiplicity value, can be controlled by corresponding total energy if it is minimum or not. Only nine of the methods give multiplicity value four for the minimum total energy. These methods are B1LYP, B3LYP, B3P86, B971, B98, BHandHLYP, HFB, O3LYP, and PBE1PBE. For other four methods,

the minimum energy values noted for $m = 2$. These are B3PW91, B972, BHandH, and MPW1PW91.

For values of m between 6 and 18, energies calculated using all methods increase monotonically with m . The difference between E_{10} and E_{12} is remarkably greater than the others, because there are nine electrons in the outer shells of the Co atom, except than the nearest noble gas (Ar) configuration. To obtain E_{12} , the electron from close shell configuration has to be excited that needs much more energy than the other outer-shell electrons.

At the end of the discussion about Co atom, we should claim that the functionals, B3PW91, B972, BHandH, and MPW1PW91 are the controversial functionals, and the remaining nine functionals (with minimum E_4 value) can be marked as the suitable functionals. The evaluation of the results continues by ions of Co atom. The expected electron configurations and the corresponding multiplicity values for Co are as the following: Co^{1+} : $[\text{Ar}] 3d^7 4s^1$, $m = 5$; Co^{2+} : $[\text{Ar}] 3d^7$, $m = 4$; Co^{3+} : $[\text{Ar}] 3d^6$, $m = 5$; and Co^{1-} : $[\text{Ar}] 3d^8 4s^1$, $m = 3$. Tables 3.2–3.5 tabulate the total energies for the all possible multiplicities, of course, in accord with the number of electrons used by GAUSSION03.

As is seen from Table 3.2, only B3PW91, BHandH, BHandHLYP, HFB, and MPW1PW91 have ended up with the correct multiplicity value $m = 5$ for Co^{1+} . All the others have spotted the $m = 3$ energies as their minima, which is logically unexplainable. Fortunately, the energy differences ΔE_{5-3} between E_5 and E_3 values for the cases in which $m = 5$ is not spotted as the minimum are always so small, at most 0.026 Hartrees for B3P86. What we want to say is that the incorrect results are not as bad as they look, for GAUSSIAN package have originally been designated for the ground-states of elements and/or molecules, not for excited states.

Now comes the interesting, and equally surprising part of the story. If we look at the corresponding situations for Co^{2+} , Co^{3+} , Co^{1-} from Tables 3.3, 3.4, and 3.5, respectively, all the 13 DFT methods have flawlessly resulted in the correct multiplicity values for the minimum energies: $m = 4$ for Co^{2+} and $m = 5$ for Co^{3+} . A quick glance at Tables 3.3–3.5 reveals that there exists always a definite pattern in energy values from the smallest to highest multiplicity values: they have only one minimum and that minimum is the correct one; put in another way, there is no fluctuation in energy values as we have witnessed previously in Co and Co^{1+} tables.

Table3.1: Total energies, E_m , in Hartrees, for a Co atom for different multiplicities, m ($2S + 1$). The starred ones show the lowest energy.

| method | $-E_2$ | $-E_4$ | $-E_6$ | $-E_8$ | $-E_{10}$ | $-E_{12}$ | $-E_{14}$ | $-E_{16}$ | $-E_{18}$ |
|-----------|-----------|-----------|----------|----------|-----------|-----------|-----------|-----------|-----------|
| B1LYP | 145.0030 | 145.0132* | 144.9096 | 144.6152 | 144.1686 | 141.1180 | 137.6516 | 133.8410 | 128.4115 |
| B3LYP | 145.1134 | 145.1244* | 145.0147 | 144.7172 | 144.2683 | 141.2179 | 137.7551 | 133.9518 | 128.5384 |
| B3P86 | 145.4932 | 145.5072* | 145.3901 | 145.1187 | 144.6658 | 141.6178 | 138.1715 | 134.3714 | 129.0535 |
| B3PW91 | 145.1410* | 145.1409 | 145.0533 | 144.7809 | 144.3313 | 141.2912 | 137.8531 | 134.0831 | 128.7404 |
| B971 | 145.0425 | 145.0665* | 144.9369 | 144.6505 | 144.1864 | 141.1359 | 137.6889 | 133.9122 | 128.5915 |
| B972 | 145.2484* | 145.2443 | 145.1342 | 144.8514 | 144.3931 | 141.3251 | 137.8715 | 134.0965 | 128.7823 |
| B98 | 145.0828 | 145.1068* | 144.9791 | 144.6943 | 144.2310 | 141.1827 | 137.7371 | 133.9606 | 128.6327 |
| BHandH | 144.5442* | 144.5432 | 144.4701 | 144.2183 | 143.7920 | 140.7446 | 137.2904 | 133.4822 | 128.1243 |
| BHandHLYP | 144.9438 | 144.9525* | 144.8712 | 144.5948 | 144.1651 | 141.1081 | 137.6382 | 133.8326 | 128.4049 |
| HFB | 144.4087 | 144.4330* | 144.3401 | 144.0880 | 143.6643 | 140.6998 | 137.3359 | 133.6450 | 128.4204 |
| MPW1PW91 | 145.1156* | 145.1153 | 145.0339 | 144.7652 | 144.3189 | 141.2794 | 137.8426 | 134.0733 | 128.7404 |
| O3LYP | 145.2852 | 145.2965* | 145.1795 | 144.8936 | 144.4298 | 141.3670 | 137.9078 | 134.1159 | 128.7118 |
| PBE1PBE | 145.0443 | 145.0576* | 144.9612 | 144.6939 | 144.2493 | 141.2115 | 137.7772 | 133.9877 | 128.6859 |

Table 3.2: Similar to Table 3.1 for Co¹⁺.

| method | $-E_1$ | $-E_3$ | $-E_5$ | $-E_7$ | $-E_9$ | $-E_{11}$ | $-E_{13}$ | $-E_{15}$ | $-E_{17}$ |
|-----------|----------|-----------|-----------|----------|----------|-----------|-----------|-----------|-----------|
| B1LYP | 144.6309 | 144.7330* | 144.7254 | 144.3903 | 143.8654 | 141.0078 | 137.5239 | 133.7030 | 128.2480 |
| B3LYP | 144.7357 | 144.8366* | 144.8251 | 144.4862 | 143.9586 | 141.1015 | 137.6209 | 133.8068 | 128.3670 |
| B3P86 | 145.0950 | 145.2020* | 145.1756 | 144.8520 | 144.3288 | 141.4806 | 138.0156 | 134.2264 | 128.8496 |
| B3PW91 | 144.7628 | 144.8562 | 144.8603* | 144.5306 | 144.0137 | 141.1724 | 137.7159 | 133.9341 | 128.5570 |
| B971 | 144.6836 | 144.7771* | 144.7533 | 144.4095 | 143.8756 | 141.0241 | 137.5580 | 133.7694 | 128.4146 |
| B972 | 144.8879 | 144.9765* | 144.9534 | 144.6109 | 144.0834 | 141.2164 | 137.7440 | 133.9532 | 128.6032 |
| B98 | 144.7220 | 144.8167* | 144.7940 | 144.4511 | 143.9182 | 141.0699 | 137.6052 | 133.8166 | 128.4544 |
| BHandH | 144.1818 | 144.2751 | 144.2882* | 143.9789 | 143.4876 | 140.6388 | 137.1676 | 133.3591 | 127.9389 |
| BHandHLYP | 144.5790 | 144.6837 | 144.6865* | 144.3682 | 143.8598 | 141.0012 | 137.5145 | 133.6890 | 128.2421 |
| HFB | nc | 144.1503 | 144.1599* | 143.8538 | 143.3651 | 140.5865 | 137.2044 | 133.5020 | 128.2544 |
| MPW1PW91 | 144.7388 | 144.8343 | 144.8410* | 144.5018 | 144.0013 | 141.1615 | 137.7060 | 133.9252 | 128.5578 |
| O3LYP | 144.9195 | 145.0203* | 144.9950 | 144.6518 | 144.1212 | 141.2563 | 137.7779 | 133.9701 | 128.5365 |
| PBE1PBE | 144.6674 | 144.7781* | 144.7698 | 144.4317 | 143.9332 | 141.0938 | 137.6408 | 133.8644 | 128.4812 |

Table 3.3: Similar to Table 3.1 for Co^{2+} .

| method | $-E_2$ | $-E_4$ | $-E_6$ | $-E_8$ | $-E_{10}$ | $-E_{12}$ | $-E_{14}$ | $-E_{16}$ |
|-----------|----------|-----------|----------|----------|-----------|-----------|-----------|-----------|
| B1LYP | 144.0025 | 144.1012* | 143.8917 | 143.2966 | 140.3619 | 137.1811 | 133.2990 | 127.7709 |
| B3LYP | 144.0961 | 144.1934* | 143.9819 | 143.3833 | 140.4488 | 137.2708 | 133.3960 | 127.8827 |
| B3P86 | 144.4369 | 144.5283* | 144.3250 | 143.7273 | 140.7995 | 137.6365 | 133.7860 | 128.3357 |
| B3PW91 | 144.0985 | 144.2335* | 144.0226 | 143.4320 | 140.5117 | 137.3560 | 133.5134 | 128.0629 |
| B971 | 144.0931 | 144.1441* | 143.9126 | 143.3035 | 140.3726 | 137.2025 | 133.3534 | 127.9268 |
| B972 | 144.2206 | 144.3514* | 144.1155 | 143.5123 | 140.5649 | 137.3883 | 133.5415 | 128.1143 |
| B98 | 144.0944 | 144.1817* | 143.9515 | 143.3435 | 140.4154 | 137.2484 | 133.4000 | 127.9652 |
| BHandH | 143.5393 | 143.6758* | 143.4830 | 142.9189 | 139.9914 | 136.8304 | 132.9800 | 127.5053 |
| BHandHLYP | 143.9684 | 144.0730* | 143.8689 | 143.2893 | 140.3532 | 137.1729 | 133.2909 | 127.7835 |
| HFB | 143.4839 | 143.5405* | 143.3614 | 142.8011 | 139.9462 | 136.8601 | 133.0982 | 127.8006 |
| MPW1PW91 | 144.0802 | 144.2174* | 144.0072 | 143.4203 | 140.5014 | 137.3470 | 133.5054 | 128.0644 |
| O3LYP | 144.3133 | 144.3761* | 144.1536 | 143.5500 | 140.6057 | 137.4247 | 133.5611 | 128.0690 |
| PBE1PBE | 144.0374 | 144.1474* | 143.9388 | 143.3542 | 140.4358 | 137.2832 | 133.4460 | 128.0120 |

Table 3.4: Similar to Table 3.1 for Co^{3+} .

| method | $-E_1$ | $-E_3$ | $-E_5$ | $-E_7$ | $-E_9$ | $-E_{11}$ | $-E_{13}$ | $-E_{15}$ |
|-----------|----------|----------|-----------|----------|----------|-----------|-----------|-----------|
| B1LYP | 142.6897 | 142.7386 | 142.8568* | 142.4395 | 139.4134 | 136.1416 | 132.6207 | 127.0347 |
| B3LYP | 142.7738 | 142.8217 | 142.9391* | 142.5198 | 139.4935 | 136.2242 | 132.7097 | 127.1389 |
| B3P86 | 143.0897 | 143.1550 | 143.2689* | 142.8406 | 139.8184 | 136.5620 | 133.0711 | 127.5606 |
| B3PW91 | 142.7392 | 142.8567 | 142.9857* | 142.5648 | 139.5507 | 136.3022 | 132.8182 | 127.3079 |
| B971 | 142.7540 | 142.7928 | 142.8946* | 142.4480 | 139.4234 | 136.1598 | 132.6649 | 127.1799 |
| B972 | 142.8627 | 142.9739 | 143.1074* | 142.6581 | 139.6162 | 136.3452 | 132.8524 | 127.3671 |
| B98 | 142.7878 | 142.8709 | 142.9294* | 142.4851 | 139.4629 | 136.2022 | 132.7094 | 127.2170 |
| BHandH | 142.2000 | 142.3201 | 142.4599* | 142.0645 | 139.0436 | 135.7571 | 132.3076 | 126.7558 |
| BHandHLYP | 142.6652 | 142.7181 | 142.8447* | 142.4316 | 139.4038 | 136.1317 | 132.6141 | 127.0300 |
| HFB | 142.1570 | 142.2544 | 142.3317* | 141.9495 | 139.0034 | 135.8270 | 132.4180 | 127.0405 |
| MPW1PW91 | 142.7235 | 142.8429 | 142.9728* | 142.5541 | 139.5416 | 136.2943 | 132.8113 | 127.3112 |
| O3LYP | 142.9329 | 142.9954 | 143.1266* | 142.6936 | 139.6558 | 136.3815 | 132.8737 | 127.3057 |
| PBE1PBE | 142.7108 | 142.7724 | 142.9059* | 142.4904 | 139.4785 | 136.2329 | 132.7534 | 127.2599 |

Table 3.5: Similar to Table 3.1 for Co^{1-} .

| method | $-E_1$ | $-E_3$ | $-E_5$ | $-E_7$ | $-E_9$ | $-E_{11}$ | $-E_{13}$ | $-E_{15}$ | $-E_{17}$ | $-E_{19}$ |
|-----------|----------|-----------|----------|----------|----------|-----------|-----------|-----------|-----------|-----------|
| B1LYP | 144.9423 | 145.0402* | 144.9957 | 144.9027 | 144.6523 | 144.0943 | 141.0478 | 137.5836 | 133.7823 | 128.3710 |
| B3LYP | 145.0607 | 145.1574* | 145.1069 | 145.0134 | 144.7602 | 144.1999 | 141.1535 | 137.6915 | 133.9002 | 128.5046 |
| B3P86 | 145.4532 | 145.5551* | 145.4981 | 145.4140 | 145.1759 | 144.6187 | 141.5726 | 138.1272 | 134.3731 | 129.0425 |
| B3PW91 | 145.0784 | 145.1817* | 145.1287 | 145.0572 | 144.8167 | 144.2656 | 141.2339 | 137.7944 | 134.0427 | 128.7107 |
| B971 | 144.9922 | 145.0841* | 145.0355 | 144.9325 | 144.6804 | 144.1125 | 141.0694 | 137.6249 | 133.8681 | 128.5563 |
| B972 | 145.1903 | 145.2888* | 145.2333 | 145.1278 | 144.8772 | 144.3165 | 141.2585 | 137.8119 | 134.0425 | 128.7422 |
| B98 | 145.0344 | 145.1252* | 145.0776 | 144.9763 | 144.7231 | 144.1585 | 141.1167 | 137.6728 | 133.9172 | 128.5986 |
| BHandH | 144.4746 | 144.5723* | 144.5477 | 144.4624 | 144.2410 | 143.7137 | 140.6711 | 137.2260 | 133.4518 | 128.0274 |
| BHandHLYP | 144.8727 | 144.9738* | 144.9514 | 144.8648 | 144.6323 | 144.0873 | 141.0369 | 137.5700 | 133.7694 | 128.3609 |
| HFB | nc | 128.3609* | 144.3957 | 144.3318 | 144.1109 | 143.5932 | 140.6305 | 137.2773 | nc | 128.3808 |
| MPW1PW91 | 145.0513 | 145.1533* | 145.1126 | 145.0369 | 144.7993 | 144.2518 | 141.2169 | 137.7833 | 134.0326 | 128.7100 |
| O3LYP | 145.2221 | 145.3188* | 145.2627 | 145.1738 | 144.9189 | 144.3545 | 141.2983 | 137.8493 | 134.0686 | 128.6750 |
| PBE1PBE | 144.9759 | 145.0820* | 145.0415 | 144.9635 | 144.7275 | 144.1818 | 141.1480 | 137.7253 | 133.9711 | 128.6551 |

After the calculation of the anions and cations of Co atom, what naturally comes is the performances of the DFT methods in the prediction of the first, second, and third ionization energies and the (first) electron affinity of Co atom. In Table 3.6 are shown the calculated first ionization energies of Co for the process $\text{Co} \rightarrow \text{Co}^{1+} + e^-$. The experimental value is 7.881 eV [43]. The calculations were performed following the recipe $IE_1 = E_5(\text{Co}^{1+}) - E_5(\text{Co})$. (Similar calculations were performed for the other Co ions and for Sm ions.) First of all, the errors produced by the methods are not so large, usually acceptably reasonable. The biggest errors for IE_1 are seen for B3P86 and then for BHandH methods. The smallest ones are for B972, PBE1PBE, and B1LYP, which are all nearly zero. B3LYP needs more attention at this point because researchers usually believe that it is the best one among the other DFT methods. As we see from Table 3.6, its first ionization energy prediction is only about 3 percent; so that B3LYP deserves its fame. (In Tables 3.7 and 3.8 we see that the predictions of B3LYP are nearly zero and around 1 percent for the second and third ionization energies; solidifying further its glory.) We can speak well also of PBE1PBE and B1LYP methods. The former is also distinguished among the researchers for its prominent performances. As we notice from Tables 3.7—3.9, PBE1PBE have produced better results than expected for all kinds of ions of Co we considered in this work: the errors for all ionization energies and the electron affinity of Co are all nearly zero. If its results happen to be in this accuracy also for Sm, we would choose PBE1PBE method as the best and most appropriate method in studying all Sm-Co type clusters. As we will see shortly, this is not the case, unfortunately.

In Table 3.7 we show the results for the second ionization energies, for which the experimental value is 17.080 eV [43]. Here all the methods lead to very small errors; among them B1LYP, B3LYP, B3PW91, MPW1PW91, and PBE1PBE (as we mentioned above) have produced IE_2 with nearly zero errors. It is interesting to note also that HFB method, which does not include electron correlation energy in its formulation, have given somehow unexpectedly a result with about 1 percent error. The fact here that O3LYP method has generated a similar 1-percent error is also noticeable.

Some similar words can be said about the third ionization energy given in Table 3.8. The experimental value of IE_3 is 33.497 eV [43]. The results in this table are the best ones compared to the first and second ionization energies, for the errors here are so small: except B3P86, all are about 1 percent. BHandHLYP and PBE1PBE methods resulted in the best

Table3.6: The first ionization energy IE_1 of Co atom for the process $IE_1 + \text{Co} \rightarrow \text{Co}^{1+} + e^-$, calculated as $IE_1 = E_5(\text{Co}^{1+}) - E_4(\text{Co})$. The experimental value is 7.881 eV [43]. Δ in the second column gives the error between the experimental and the calculated results; the last column is for the corresponding percentage error.

| method | IE_1 (eV) | Δ (eV) | % error |
|-----------|-------------|---------------|---------|
| B1LYP | 7.831 | 0.050 | 0 |
| B3LYP | 8.147 | 0.266 | 3 |
| B3P86 | 9.023 | 1.142 | 14 |
| B3PW91 | 7.636 | 0.245 | 3 |
| B971 | 8.522 | 0.641 | 8 |
| B972 | 7.916 | 0.035 | 0 |
| B98 | 8.512 | 0.631 | 8 |
| BHandH | 6.939 | 0.942 | 11 |
| BHandHLYP | 7.236 | 1.645 | 8 |
| HFB | 7.433 | 0.448 | 5 |
| MPW1PW91 | 7.464 | 0.417 | 5 |
| O3LYP | 8.206 | 0.325 | 4 |
| PBE1PBE | 7.833 | 0.048 | 0 |

values.

Finally about Co atom is its electron affinity EA values for each method, which are listed in Table 3.9. The process to define EA is $\text{Co} + e^- \rightarrow \text{Co}^{1-}$ and the calculation were carried out according to the formula $EA = E_4(\text{Co}) - E_3(\text{Co}^{1-})$. (A similar calculation was done for the electron affinity of Sm element.) The experimental value EA of Co is 0.662 eV [43]. As we said previously, the best result has been produced by PBE1PBE nearly flawlessly. The other satisfactory results were from O3LYP, B1LYP, and BHandHLYP. All the other methods generated outcomes with much bigger errors. These are all expected. Notice that the three experimental ionization energies of Co are all on the order of 10. But its experimental electron affinity is on the order of only 1. In another words, ionization energies are roughly 10 times bigger than electron affinity value. The conclusion we may therefore draw vaguely is that it is very unlikely that we could reach an EA value as accurate as IE_i values for Co. As we shall witness below, the situation for the electron affinity of Sm is much worse than that for Co. Be prepared to see an error about 700 percent which was produced by PBE1PBE! What we want to say here that the zero error generated by PBE1PBE method is probably only an incident, so that should not be taken into account seriously.

Table3.7: The second ionization energy IE_2 of Co atom for the process $IE_2 + \text{Co}^{1+} \rightarrow \text{Co}^{2+} + e^-$, calculated as $IE_2 = E_4(\text{Co}^{2+}) - E_5(\text{Co}^{1+})$. The experimental value is 17.080 eV [43]. Δ in the second column gives the error between the experimental and the calculated results; the last column is for the corresponding percentage error.

| method | IE_2 (eV) | Δ (eV) | % error |
|-----------|-------------|---------------|---------|
| B1LYP | 16.987 | 0.093 | 0 |
| B3LYP | 17.190 | 0.110 | 0 |
| B3P86 | 17.613 | 0.533 | 3 |
| B3PW91 | 17.055 | 0.025 | 0 |
| B971 | 16.579 | 0.501 | 2 |
| B972 | 16.380 | 0.700 | 4 |
| B98 | 16.661 | 0.419 | 2 |
| BHandH | 16.666 | 0.414 | 2 |
| BHandHLYP | 16.694 | 0.386 | 2 |
| HFB | 16.854 | 0.226 | 1 |
| MPW1PW91 | 16.970 | 0.110 | 0 |
| O3LYP | 16.839 | 0.241 | 1 |
| PBE1PBE | 16.936 | 0.144 | 0 |

3.1.2 Calculations of Sm Atoms

The discussion continues with 62-electrons Sm atom. The ground state electron configuration of Samarium is $[Xe]4f^66s^2$. It has 6 unpaired electrons in the 4f shell that causes expected multiplicity of 7. In accordance with Co atom, Sm also investigated in terms of self-consistent energy values and among all possible multiplicity values from 1 to 17 are indicated in the Table 3.10. It can be easily recognized, all methods give the minimum energy for multiplicity value 7.

Even when CEP-121G basis is used some of the calculations do not complete substantially since Sm is a large atom. Although there are some non-convergent results, all 13 functionals indicate perfect consistence to accept lowest energy as E_7 . B3P86, BHandH, and HFB produce the non-convergent results but they may not be so problematic since these non-convergent results do not belong to minimum energy column, they are E_3 , E_1 , and E_9 , respectively.

Another interesting result arises while energy values are put in order. Other than a few exceptions, the general inclination is destroyed by E_9 . Corresponding multiplicity to E_9 can be obtained by unpaired eight electrons in the outer shells, needs to transfer one of the paired 6s

Table3.8: The third ionization energy IE_3 of Co atom for the process $IE_3 + \text{Co}^{2+} \rightarrow \text{Co}^{3+} + e^-$, calculated as $IE_3 = E_5(\text{Co}^{3+}) - E_4(\text{Co}^{2+})$. The experimental value is 33.497 eV [43]. Δ in the second column gives the error between the experimental and the calculated results; the last column is for the corresponding percentage error.

| method | IE_3 (eV) | Δ (eV) | % error |
|-----------|-------------|---------------|---------|
| B1LYP | 33.861 | 0.364 | 1 |
| B3LYP | 34.130 | 0.633 | 1 |
| B3P86 | 34.272 | 0.775 | 2 |
| B3PW91 | 33.953 | 0.456 | 1 |
| B971 | 34.000 | 0.503 | 1 |
| B972 | 33.850 | 0.353 | 1 |
| B98 | 34.076 | 0.579 | 1 |
| BHandH | 33.085 | 0.412 | 1 |
| BHandHLYP | 33.425 | 0.072 | 0 |
| HFB | 32.892 | 0.605 | 1 |
| MPW1PW91 | 33.867 | 0.370 | 1 |
| O3LYP | 34.002 | 0.505 | 1 |
| PBE1PBE | 33.783 | 0.286 | 0 |

electron to unoccupied 4f energy level. The O3LYP method turn out the E_9 value with a great difference, means that it excepts this situation with a little possibility however others do not allocate this condition.

The energy difference between the E_9 and E_{11} values are remarkably greater than the others. Since the possibility of obtaining E_{11} is due to excitation of an electron from Xe noble gas configuration, it needs more energy than needed for smaller multiplicity values.

A discussion can be carried out about the total energy values of Sm cations and anion, similar to the evaluation of Co ions. The results of energy calculations for every possible multiplicity values have been indicated to the Tables 3.11—3.18. The expected electron configurations of these ions and their corresponding multiplicity values can be given as Sm^{1+} : $[\text{Xe}] 6s^1 4f^6$, $m = 8$; Sm^{2+} : $[\text{Xe}] 4f^6$, $m = 7$; Sm^{3+} : $[\text{Xe}] 4f^5$, $m = 6$; and Sm^{1-} : $[\text{Xe}] 6s^2 4f^7$, $m = 8$.

If we start from Sm^{1+} ion whose energies are given in Table 3.11, most of the methods complete the calculations with expected multiplicity values, only B98 and O3LYP fail, they give $m = 6$. As mentioned above, it is known that for rare earth elements, the given electrons to form a cation, lost from the 6s-subshell instead of 4f. To obtained $m = 6$ case for minimum energy, Sm has to lost its electron from 4f, so we can claim that B98 and O3LYP gives the wrong multiplicity values. Other 11 methods can be described as successful since they give

Table3.9: The electron affinity EA of Co atom for the process $\text{Co} + e^- \rightarrow \text{Co}^{1-}$, calculated as $EA = E_4(\text{Co}) - E_3(\text{Co}^{1-})$. The experimental value is 0.662 eV [43]. Δ in the second column gives the error between the experimental and the calculated results; the last column is for the corresponding percentage error.

| method | EA (eV) | Δ (eV) | % error |
|-----------|-----------|---------------|---------|
| B1LYP | 0.735 | 0.073 | 11 |
| B3LYP | 0.896 | 0.234 | 35 |
| B3P86 | 1.303 | 0.641 | 96 |
| B3PW91 | 1.111 | 0.449 | 67 |
| B971 | 0.478 | 0.184 | 27 |
| B972 | 1.212 | 0.550 | 83 |
| B98 | 0.502 | 0.160 | 24 |
| BHandH | 0.792 | 0.130 | 19 |
| BHandHLYP | 0.579 | 0.083 | 12 |
| HFB | -0.021 | 0.683 | 103 |
| MPW1PW91 | 1.034 | 0.372 | 56 |
| O3LYP | 0.606 | 0.056 | 8 |
| PBE1PBE | 0.664 | 0.002 | 0 |

expected multiplicity 8. If we scan the energy values closely, the pattern can be observed for most of the methods, which have only one minimum corresponding to $m = 8$, except B1LYP, B3PW91, and HFB. The E_2 and E_4 energies break down the pattern for latter methods by interchanging the sequence from smaller to greater.

The cases for Sm^{2+} and Sm^{3+} ions seem more succesful, that all the methods give the minimum energy at expected multiplicity values 7 and 6 respectively. This situation is also surprising as well as that mentioned for Co^{2+} and Co^{3+} ions. According to Table 3.12, the sequences of the energies also appear more smooth. Only B972 and HFB ruin the pattern, however the differences of these energy values are very small, numerically 0.0526 Hartrees for B972 and 0.0181 for HFB, so it is not so disturbing. A similar situation occurs for Table 3.13 and the related methods are B1LYP, B3P86, and BHandHLYP.

Unfortunately, Sm^{1-} ions results which are tabulated in Table 3.14 are not so regular as previous two tables. The methods B3P86, B3PW91, MPW1PW91, and PBE1PBE fail to give minimum total energy at expected multiplicity value 8. They conclude the calculations with $m = 6$ which is inadmissible, because it means one of the valence electrons paired with imported electron; strictly banned situation according to Hund's Rule. In addition, even for other methods, which are successful to present correct multiplicity value, any pattern has not

Table 3.10: Total energies, E_m , in Hartrees, for a Sn atom for different multiplicities, m ($2S + 1$). The starred ones show the lowest energy. ‘nc’ indicates a ‘not completed’ calculation due to a non-convergent- or confused-SCF process.

| method | $-E_1$ | $-E_3$ | $-E_5$ | $-E_7$ | $-E_9$ | $-E_{11}$ | $-E_{13}$ | $-E_{15}$ | $-E_{17}$ |
|-----------|---------|---------|---------|----------|---------|-----------|-----------|-----------|-----------|
| BLLYP | 80.9767 | 81.1066 | 81.1206 | 81.2383* | 81.1420 | 80.4743 | 79.8524 | 79.2364 | 77.9589 |
| B3LYP | 79.5032 | 81.1449 | 81.3103 | 81.4139* | 81.3185 | 80.6690 | 80.0493 | 79.4370 | 78.1700 |
| B3P86 | 81.4817 | nc | 81.6812 | 81.7856* | 81.7021 | 81.0606 | 80.4737 | 79.8724 | 78.6599 |
| B3PW91 | 81.1579 | 81.1520 | 81.3673 | 81.4599* | 81.3867 | 80.7493 | 80.1630 | 79.5667 | 78.3541 |
| B971 | 81.1207 | 81.0281 | 81.2394 | 81.3568* | 81.2664 | 80.6228 | 80.0243 | 79.4236 | 78.2404 |
| B972 | 81.1733 | 81.0886 | 81.3451 | 81.4633* | 81.3542 | 80.7323 | 80.1307 | 79.5299 | 78.3487 |
| B98 | 81.1252 | 81.0567 | 81.2724 | 81.3809* | 81.2887 | 80.6471 | 80.0514 | 79.4506 | 78.2610 |
| BHandH | nc | 80.2748 | 80.3698 | 80.5407* | 80.4614 | 79.8222 | 79.1646 | 78.5562 | 77.2856 |
| BHandHLYP | 80.4282 | 80.5762 | 80.7436 | 80.8219* | 80.7413 | 80.0052 | 79.4284 | 78.7822 | 77.4875 |
| HFB | 80.9420 | 81.0298 | 81.1741 | 81.2689* | nc | 80.4295 | 80.0775 | 79.5262 | 78.4046 |
| MPW1PW91 | 81.0418 | 81.0819 | 81.2709 | 81.3640* | 81.2813 | 80.6570 | 80.0509 | 79.4643 | 78.2611 |
| O3LYP | 81.2874 | 81.2518 | 81.4755 | 81.6235* | 70.0165 | 80.9413 | 80.3365 | 79.7183 | 78.4574 |
| PBE1PBE | 80.9665 | 80.9867 | 81.2189 | 81.3171* | 81.2317 | 80.5978 | 79.9987 | 79.4168 | 78.2160 |

Table 3.11: Similar to Table 3.1 for Sm^{1+} .

| method | $-E_2$ | $-E_4$ | $-E_6$ | $-E_8$ | $-E_{10}$ | $-E_{12}$ | $-E_{14}$ | $-E_{16}$ |
|-----------|---------|---------|----------|----------|-----------|-----------|-----------|-----------|
| BILYP | 80.9345 | 80.9266 | 81.0393 | 81.0523* | 80.3532 | 79.7173 | 79.0405 | 77.7428 |
| B3LYP | 81.0664 | 81.1164 | 81.2172 | 81.2223* | 80.5507 | 79.9082 | 79.2406 | 77.9445 |
| B3P86 | 81.3845 | 81.4061 | 81.5555 | 81.5766* | 80.9243 | 80.2596 | 79.6505 | 78.4080 |
| B3PW91 | 81.1034 | 81.0408 | 81.2698 | 81.2811* | 80.6298 | 80.0033 | 79.3645 | 78.1229 |
| B971 | 80.9380 | 80.9985 | 81.1506 | 81.1622* | 80.5110 | 79.8768 | 79.2303 | 78.0169 |
| B972 | 80.9782 | 81.0819 | 81.2575 | 81.2677* | 80.6219 | 79.9831 | 79.3371 | 78.1287 |
| B98 | 80.9622 | 81.0166 | 81.1822* | 81.1797 | 80.5323 | 79.9001 | 79.2544 | 78.0357 |
| BHandH | 79.5234 | 80.1900 | 80.3497 | 80.3579* | 79.6705 | 78.9724 | 78.3643 | 77.1125 |
| BHandHLYP | 80.5141 | 80.5540 | 80.6272 | 80.6425* | 79.9430 | 79.2351 | 78.5901 | 77.3156 |
| HFB | 80.8805 | 80.8296 | 81.0967 | 81.1054* | 80.5280 | 79.9432 | 79.3485 | 78.1877 |
| MPW1PW91 | 81.0109 | 81.0531 | 81.1736 | 81.1781* | 80.4937 | 79.8656 | 79.2531 | 78.0323 |
| O3LYP | 81.2048 | 81.2790 | 81.4425* | 81.4382 | 80.8288 | 80.1878 | 79.5290 | 78.2338 |
| PBE1PBE | 80.9330 | 80.9933 | 81.1157 | 81.1347* | 80.4424 | 79.8177 | 79.1855 | 77.9885 |

Table 3.12: Similar to Table 3.1 for Sm^{2+} .

| method | $-E_1$ | $-E_3$ | $-E_5$ | $-E_7$ | $-E_9$ | $-E_{11}$ | $-E_{13}$ | $-E_{15}$ |
|-----------|---------|---------|---------|----------|---------|-----------|-----------|-----------|
| B1LYP | 80.4084 | 80.5279 | 80.5575 | 80.6446* | 79.9602 | 79.2934 | 78.6073 | 77.2723 |
| B3LYP | nc | 80.6627 | 80.7046 | 80.8096* | 80.1439 | 79.4771 | 78.7927 | 77.4668 |
| B3P86 | 80.8529 | 80.9828 | 81.0204 | 81.1446* | 80.5034 | 79.8432 | 79.1739 | 77.8978 |
| B3PW91 | 80.5596 | 80.7140 | 80.7413 | 80.8783* | 80.2282 | 79.5723 | 78.9084 | 77.6346 |
| B971 | 80.5273 | 80.4747 | 80.5794 | 80.7703* | 80.1207 | 79.4580 | 78.7866 | 77.5374 |
| B972 | 80.5913 | 80.6383 | 80.7035 | 80.8687* | 80.2384 | 79.5697 | 78.8974 | 77.6488 |
| B98 | 80.3501 | 80.5583 | 80.6273 | 80.7872* | 80.1407 | 79.4798 | 78.8089 | 77.5533 |
| BHandH | 79.5597 | 79.6932 | 79.7373 | 79.9643* | 79.2419 | 78.5913 | 77.9073 | 76.6369 |
| BHandHLYP | 79.3709 | 79.9919 | 80.1646 | 80.2360* | 79.4902 | 78.8314 | 78.1577 | 76.8416 |
| HFB | 80.3863 | 80.3682 | 80.4113 | 80.7079* | 80.1343 | 79.5182 | 78.8959 | 77.7111 |
| MPW1PW91 | 80.4544 | 80.5916 | 80.6432 | 80.7769* | 80.1221 | 79.4688 | 78.8085 | 77.5449 |
| O3LYP | 80.7038 | 80.8385 | 80.8858 | 81.0331* | 80.4287 | 79.7636 | 79.0781 | 77.7570 |
| PBE1PBE | 80.3770 | 80.5482 | 80.5994 | 80.7279* | 80.0743 | 79.4220 | 78.7398 | 77.5024 |

Table 3.13: Similar to Table 3.1 for Sm^{3+} .

| method | $-E_2$ | $-E_4$ | $-E_6$ | $-E_8$ | $-E_{10}$ | $-E_{12}$ | $-E_{14}$ |
|-----------|---------|---------|----------|---------|-----------|-----------|-----------|
| B1LYP | 79.5062 | 79.4896 | 79.7154* | 79.1542 | 78.5713 | 77.8438 | 76.4594 |
| B3LYP | 79.6694 | 79.7959 | 79.8556* | 79.3155 | 78.7504 | 78.0243 | 76.6474 |
| B3P86 | 80.0094 | 80.0041 | 80.1560* | 79.6287 | 79.0917 | 78.3780 | 77.0469 |
| B3PW91 | 79.7282 | 79.8262 | 79.9013* | 79.4183 | 78.8393 | 78.1313 | 76.8048 |
| B971 | 79.6395 | 79.6948 | 79.8230* | 79.3282 | 78.7357 | 78.0196 | 76.7085 |
| B972 | 79.6991 | 79.7398 | 79.8988* | 79.4162 | 78.8479 | 78.1309 | 76.8255 |
| B98 | 79.6604 | 79.7225 | 79.8223* | 79.3457 | 78.7546 | 78.0391 | 76.7218 |
| BHandH | 78.8015 | 78.9162 | 78.9809* | 78.5151 | 77.8613 | 77.1606 | 75.8078 |
| BHandHLYP | 79.1654 | 79.1460 | 79.3611* | 78.7405 | 78.0982 | 77.3836 | 76.0113 |
| HFB | 79.5553 | 79.5772 | 79.7442* | 79.3243 | 78.8149 | 78.1475 | 76.9065 |
| MPW1PW91 | 79.6174 | 79.7359 | 79.7952* | 79.3259 | 78.7338 | 78.0293 | 76.7143 |
| O3LYP | 79.8689 | 79.9583 | 80.0482* | 79.5904 | 79.0399 | 78.3173 | 76.9389 |
| PBE1PBE | 79.5811 | 79.6688 | 79.7678* | 79.2758 | 78.6881 | 77.9851 | 76.6729 |

been observed.

Now the order comes to mention about the first, second, and third ionization energy and electron affinity of Sm atom. The process of first ionization energy was given above for the Co atom. Similarly, $IE_1 + \text{Sm} \rightarrow \text{Sm}^{1+} + e^-$ is used for finding the first ionization energy of Sm with the recipe $IE_1 = E_8(\text{Sm}^{1+}) - E_7(\text{Sm})$ and the results demonstrated in Table 3.15. The same procedure was followed for second and third ionization energies. If we start with IE_1 of Sm, we will first call attention to the errors originating from the difference between experimental (5.643 eV [43]) and the calculated results. HFB method is again discriminated from others by a great error of 21 percent. Except HFB, other methods have quite acceptable errors. Minimum errors are given by B3P86 (0 percent) and B98 (3 percent). The next discussion is about IE_2 , which is based on Table 3.16. The error values are remarkably smaller than the IE_2 , in fact half of them give values around zero and 1 percent. The worst result comes from B3P86 with the value 6 percent. The experimental values of second ionization energy is 11.090 eV [43]. For the third ionization energy error values are increase around 11 percent unlikely to Co case which errors have been decreased by increasing the ionization number. Only BHandHLYP and B1LYP indicate smaller error than others, numerically 1 and 7 percent respectively.

The electron affinity of the Sm atom can be demonstrated by $\text{Sm} + e^- \rightarrow \text{Sm}^{1-}$ which is calculated with $EA = E_8(\text{Sm}) - E_7(\text{Sm}^{1-})$. In accordance with Co atom calculations, errors of electron affinity is very large for Sm atom. The reason was explained above by the small experimental value (which is 0.518 eV for Sm atom [43]). The interesting point here is that the energy values are so close to each other, in other words there is a consistency among all methods. Maybe O3LYP can be excluded from this case with slightly smaller energy value 2.7 eV, since the others are changing in the range of 3.0–3.6 eV.

3.2 Dimers

3.2.1 SmCo Dimer Calculations

The SmCo dimer calculations can be explained into two parts and each one consists of approximately 6000 calculations. The first part of the calculations aim to determine the interaction between Sm and Co atoms, if it is Lennard-Jones type or not. So it includes three dimensions;

Table 3.14: Similar to Table 3.1 for Sm^{1-} .

| method | $-E_2$ | $-E_4$ | $-E_6$ | $-E_8$ | $-E_{10}$ | $-E_{12}$ | $-E_{14}$ | $-E_{16}$ | $-E_{18}$ |
|-----------|---------|---------|----------|----------|-----------|-----------|-----------|-----------|-----------|
| BILYP | 80.8742 | 81.0447 | 81.1149 | 81.1327* | 70.3971 | 80.3891 | 79.7224 | 79.1246 | 77.8979 |
| B3LYP | 81.0792 | 81.2035 | 81.2968 | 81.3123* | 70.5189 | 80.5715 | 79.9258 | 79.3328 | 78.1167 |
| B3P86 | 77.2028 | 81.5399 | 81.6916* | 81.6847 | 70.8295 | 80.9810 | 80.3704 | 79.8004 | 78.6390 |
| B3PW91 | 76.8817 | 81.2061 | 81.3580* | 81.3460 | 70.5195 | 80.6494 | 80.0406 | 79.4747 | 78.3123 |
| B971 | 80.9460 | 81.1005 | 81.2486 | 81.2631* | 70.3525 | 80.5210 | 79.8899 | 79.3234 | 78.1932 |
| B972 | 81.0153 | 81.2409 | 81.3377 | 81.3675* | 81.2716 | 80.5881 | 80.0156 | 79.4289 | 78.3015 |
| B98 | 80.9631 | 81.1689 | 81.2806 | 81.2835* | 70.3537 | 80.5473 | 79.9198 | 79.3526 | 78.2165 |
| BHandH | 80.0259 | 80.2363 | 80.4198 | 80.4272* | 80.3274 | 79.7053 | 79.0217 | 78.4478 | 77.2619 |
| BHandHLYP | 80.4732 | 80.6328 | 80.6992 | 80.7132* | 80.6076 | 79.9831 | 79.2616 | 78.6722 | 77.4640 |
| HFB | 72.5404 | 80.9615 | 81.1416 | 81.1554* | 69.9344 | 80.3339 | nc | 79.4142 | 78.3421 |
| MPWIPW91 | 77.1460 | 81.0956 | 81.2708* | 81.2500 | 70.5101 | 80.5571 | 79.9357 | 79.3719 | 78.2186 |
| O3LYP | 81.2048 | 81.4355 | 81.5311 | 81.5415* | 70.5887 | 80.5800 | 80.2025 | 79.6193 | 78.4072 |
| PBEIPBE | 77.4614 | 81.0321 | 81.2131* | 81.2024 | 70.5060 | 80.5026 | 79.8858 | 79.3227 | 79.3227 |

Table 3.15: The first ionization energy IE_1 of Sm atom for the process $IE_1 + \text{Sm} \rightarrow \text{Sm}^{1+} + e^-$, calculated as $IE_1 = E_8(\text{Sm}^{1+}) - E_7(\text{Sm})$. The experimental value is 5.643 eV [43]. Δ in the second column gives the error between the experimental and the calculated results; the last column is for the corresponding percentage error.

| method | IE_1 (eV) | Δ (eV) | % error |
|-----------|-------------|---------------|---------|
| B1LYP | 5.059 | 0.585 | 10 |
| B3LYP | 5.214 | 0.430 | 7 |
| B3P86 | 5.685 | 0.042 | 0 |
| B3PW91 | 4.863 | 0.780 | 13 |
| B971 | 5.292 | 0.351 | 6 |
| B972 | 5.321 | 0.322 | 5 |
| B98 | 5.472 | 0.171 | 3 |
| BHandH | 4.971 | 0.673 | 11 |
| BHandHLYP | 4.879 | 0.764 | 13 |
| HFB | 4.449 | 1.194 | 21 |
| MPW1PW91 | 5.055 | 0.589 | 10 |
| O3LYP | 5.039 | 0.604 | 10 |
| PBE1PBE | 4.964 | 0.680 | 12 |

methods, multiplicity values, and interatomic separation. This part of the study is performed for all 13 DFT methods, to be sure if they are appropriate as predicted from previous calculations. The second dimension is the multiplicity for which each method is scanned for seven discrete values; from $m = 2$ to $m = 14$ since there are odd number of unpaired electrons and so multiplicity value is even. The last dimension is interatomic separation, so that the initial interatomic distance is varied from $r = 1.0 \text{ \AA}$ to 7.0 \AA , 0.1 \AA added to r for each calculation (61 calculations for each method and each multiplicity value). By this means of calculation we can determine the multiplicity which gives the minimum total energy, the spectroscopic constants and some electronic properties for each method. These spectroscopic constants are binding energy D_e , equilibrium interatomic separation r_e , and fundamental frequency w_e and the electronic properties are the highest occupied molecular orbit (HOMO), the lowest unoccupied molecular orbit (LUMO), HOMO-LUMO gap energy, dipole moment, and excess charges on the atoms.

The first set of calculations includes the self-consistent energy values of SmCo dimer with respect to multiplicity values and results are listed in Table 3.19. It can be clearly seen that all functionals give the minimum energy value for the $m = 10$ condition. This distinctive determination means that both Sm and Co atoms do not lose their own electronic structure and keep their original multiplicity values four and seven. It is an expected situation since

Table3.16: The second ionization energy IE_2 of Sm atom for the process $IE_2 + \text{Sm}^{1+} \rightarrow \text{Sm}^{2+} + e^-$, calculated as $IE_2 = E_7(\text{Sm}^{2+}) - E_8(\text{Sm}^{1+})$. The experimental value is 11.090 eV [43]. Δ in the second column gives the error between the experimental and the calculated results; the last column is for the corresponding percentage error.

| method | $IE_2(\text{eV})$ | Δ (eV) | % error |
|-----------|-------------------|---------------|---------|
| B1LYP | 11.095 | 0.005 | 0 |
| B3LYP | 11.232 | 0.142 | 1 |
| B3P86 | 11.757 | 0.667 | 6 |
| B3PW91 | 10.963 | 0.127 | 1 |
| B971 | 10.666 | 0.424 | 3 |
| B972 | 10.859 | 0.231 | 2 |
| B98 | 10.683 | 0.407 | 3 |
| BHandH | 10.713 | 0.377 | 3 |
| BHandHLYP | 11.062 | 0.028 | 0 |
| HFB | 10.817 | 0.273 | 2 |
| MPW1PW91 | 10.920 | 0.170 | 1 |
| O3LYP | 11.027 | 0.063 | 0 |
| PBE1PBE | 11.071 | 0.019 | 0 |

the unpaired electrons of the Co atom are in the 3d orbitals and the Sm atom are in the 4f orbitals. By their nature, they are at different energy levels however by six 4f-electrons and seven 3d-electrons the interaction between the atoms can be defined as very strong. In this case we expect to determine interaction between Sm and Co atoms as the Lennard Jones type. If it is the case we can conclude that the values for binding energy D_e and the equilibrium separation distance r_e are in plausible range. We will turn to this point while discussing these variables.

If energy values are arranged in order, it is seen that the case $E_{10} < E_6 < E_4 < E_8 < E_{12} < E_2 < E_{14}$ is common for most of the methods. The methods B1LYP, B3LYP, HFB, and O3LYP has the same order with the interchange of E_{14} and E_2 . Only B98 gives a different pattern, that is $E_{10} < E_4 < E_8 < E_6 < E_{12} < E_{14} < E_2$. There is only one not-completed calculation, E_2 of the method BHandH.

One of the important part of the study summarized on Table 3.20 by exhibiting the spectroscopic and electronic properties of each method according to multiplicity value that gives the minimum total energy. This part is important because there is no experimental data found in the literature about SmCo dimer. As mentioned before, these spectroscopic constants are binding energy D_e , equilibrium interatomic separation r_e , and fundamental frequency ω_e .

Table3.17: The third ionization energy IE_3 of Sm atom for the process $IE_3 + \text{Sm}^{2+} \rightarrow \text{Sm}^{3+} + e^-$, calculated as $IE_3 = E_6(\text{Sm}^{3+}) - E_7(\text{Sm}^{2+})$. The experimental value is 23.423 eV [43]. Δ in the second column gives the error between the experimental and the calculated results; the last column is for the corresponding percentage error.

| method | IE_3 (eV) | Δ (eV) | % error |
|-----------|-------------|---------------|---------|
| B1LYP | 25.285 | 1.862 | 7 |
| B3LYP | 25.958 | 2.535 | 10 |
| B3P86 | 26.901 | 3.478 | 14 |
| B3PW91 | 26.585 | 3.162 | 13 |
| B971 | 25.777 | 2.354 | 10 |
| B972 | 26.391 | 2.968 | 12 |
| B98 | 26.256 | 2.833 | 12 |
| BHandH | 26.761 | 3.338 | 14 |
| BHandHLYP | 23.809 | 0.386 | 1 |
| HFB | 26.225 | 2.802 | 11 |
| MPW1PW91 | 26.714 | 3.291 | 14 |
| O3LYP | 26.798 | 3.375 | 14 |
| PBE1PBE | 26.123 | 2.700 | 11 |

The binding energy D_e can be defined as the energy required to decompose a molecule into its constituents. As a calculation example of binding energy, HFB can be shown as; $D_e = -C(E_{10}^{SmCo} - E_7^{Sm} - E_4^{Co})$, where C is the conversion constant of Hartrees to electronvolt, $C = 27.211383$ eV/Hartree. The energy values at the right hand side of the equation are obtained from tables of Co, Sm and SmCo calculations, Table 3.1, Table 3.10, Table 3.19 respectively. In the same way, to calculate binding energy of B3PW91, B972, BHandH, or MPW1PW91, $D_e = -C(E_{10}^{SmCo} - E_7^{Sm} - E_2^{Co})$ has to be used, since the minimum energy values are at $m = 2$ case for them.

The binding energy values are not so successful since the range is wide and values are spread between 0.9092 eV to 1.8315 eV for hybrid functionals. Unfortunately, even similar methods do not give close values for binding energy, i.e. B971 has 1.2402 eV where B972 has 1.6230 eV. (One more: BHandH has 1.5669 eV and BHandHLYP has 1.0493 eV). Although the D_e range is wide, the binding energy values of the $m = 10$ case are actually small.

The equilibrium interatomic separation r_e is the distance between the atoms where the possible energy is minimum, so the most stable state. Unlike D_e , r_e values are proper and the range is 2.95-3.09 Å for the $m = 10$ cases. This range can be defined as $r_e = 2.975 \pm 0.035$ Å for the $m = 10$ case of the SmCo bond length. In contrast to D_e , similar methods gives similar re-

Table3.18: The electron affinity EA of Sm atom for the process $\text{Sm} + e^- \rightarrow \text{Sm}^{1-}$, calculated as $EA = E_8(\text{Sm}) - E_7(\text{Sm}^{1-})$. The experimental value is 0.518 eV [43]. Δ in the second column gives the error between the experimental and the calculated results; the last column is for the corresponding percentage error.

| method | EA (eV) | Δ (eV) | % error |
|-----------|-----------|---------------|---------|
| B1LYP | -2.872 | 3.390 | 654 |
| B3LYP | -2.765 | 3.283 | 633 |
| B3P86 | -2.745 | 3.263 | 629 |
| B3PW91 | -3.100 | 3.618 | 698 |
| B971 | -2.550 | 3.068 | 592 |
| B972 | -2.607 | 3.125 | 603 |
| B98 | -2.651 | 3.169 | 611 |
| BHandH | -3.087 | 3.605 | 695 |
| BHandHLYP | -2.957 | 3.475 | 670 |
| HFB | -3.089 | 3.607 | 696 |
| MPW1PW91 | -3.100 | 3.618 | 698 |
| O3LYP | -2.231 | 2.749 | 530 |
| PBE1PBE | -3.121 | 3.639 | 702 |

sults for r_e . For example, B3LYP gives 2.9669 Å where B1LYP gives 3.0111 Å and another acceptable result is coming from Becke series; B98 gives 3.0077 Å, B971 gives 3.0061 Å, and B972 gives 2.9903 Å.

The calculated excess charge on Sm, $q(\text{Sm})$ and dipole moment μ for SmCo also demonstrated in Table 3.20. Excess charge is written only for Sm, since it is known that $q(\text{Co}) = -q(\text{Sm})$, for SmCo dimer. Again for the $m = 10$ case $q(\text{Sm})$ and μ gives acceptable results. $q(\text{Sm})$ values can be placed in the interval of $0.58|e|$ to $0.63|e|$, also represent as $q(\text{Sm}) = 0.60 \pm 0.03|e|$. Similarly, dipole moment change between 3.7 D and 4.5 D and can be represented as $\mu = 4.1 \pm 0.4$ D which has greater error value than $q(\text{Sm})$.

The charge separation and dipole moment values are based on unpaired electrons of the Sm and Co atoms. It can be claimed that the structure of the unpaired electrons in atoms are not degrade while composing the SmCo dimer. Also for $q(\text{Sm})$ and μ values, similar methods give similar results; such as B3LYP ($0.6252|e|$ and 4.4947 D) and B1LYP ($0.6291|e|$ and 4.4694 D); and B98 ($0.5870|e|$ and 3.8195 D), B971($0.5846|e|$ and 3.7881 D), and B972 ($0.5752|e|$ and 3.7224 D).

In Table 3.21, HOMO and LUMO energy values and energy gap between HOMO-LUMO for SmCo dimer are represented for both alpha and beta energy terms. The energy gap corre-

Table 3. 19: Total energies, E_m , in Hartrees, for SmCo dimer for different multiplicities, m ($2S + 1$). The starred ones show the lowest energy.

| method | $-E_2$ | $-E_4$ | $-E_6$ | $-E_8$ | $-E_{10}$ | $-E_{12}$ | $-E_{14}$ | $-E_{16}$ |
|-----------|----------|----------|----------|----------|-----------|-----------|-----------|-----------|
| BLYP | 226.1846 | 226.2942 | 226.2969 | 226.2898 | 226.2989* | 226.2367 | 226.1454 | 225.8855 |
| B3LYP | 226.4338 | 226.5832 | 226.5862 | 226.5789 | 226.5888* | 226.5234 | 226.4287 | 226.1652 |
| B3P86 | 227.1681 | 227.3348 | 227.3371 | 227.3296 | 227.3398* | 227.2785 | 227.1938 | 226.9362 |
| B3PW91 | 226.4880 | 226.6633 | 226.6653 | 226.6580 | 226.6681* | 226.6060 | 226.5304 | 226.2783 |
| B971 | 226.2444 | 226.4631 | 226.4655 | 226.4592 | 226.4689* | 226.3970 | 226.2952 | 226.0283 |
| B972 | 226.5168 | 226.7612 | 226.7642 | 226.7570 | 226.7672* | 226.6815 | 226.5826 | 226.3181 |
| B98 | 226.2968 | 226.5220 | 226.5180 | 226.5183 | 226.5283* | 226.4578 | 226.3594 | 226.0932 |
| BHandH | nc | 225.1359 | 225.1378 | 225.1303 | 225.1415* | 225.0941 | 225.0073 | 224.7866 |
| BHandHLYP | 225.6693 | 225.7897 | 225.8099 | 225.7795 | 225.8129* | 225.7688 | 225.6883 | 225.4487 |
| HFB | 225.6727 | 225.7303 | 225.7326 | 225.7234 | 225.7354* | 225.6781 | 225.6162 | 225.3877 |
| MPW1PW91 | 226.3690 | 226.5399 | 226.5414 | 226.5343 | 226.5445* | 226.4897 | 226.4148 | 226.1667 |
| O3LYP | 226.8260 | 226.9734 | 226.9750 | 226.9677 | 226.9779* | 226.9098 | 226.8165 | 226.5527 |
| PBE1PBE | 226.2321 | 226.4188 | 226.4205 | 226.4132 | 226.4236* | 226.3686 | 226.2913 | 226.0441 |

Table3.20: Spectroscopic constants of the SmCo dimer calculated for the multiplicity, m ($2S + 1$), at which the total energy is minimum. Binding energy D_e is in eV, equilibrium interatomic separation r_e is in Å, and the fundamental frequency ω_e is in cm^{-1} . Also given are the calculated excess charge $q(\text{Sm})$ on the Sm atom (in units of electron charge $|e|$) and the dipole moment μ (in Debyes). Note that for the excess charge on the Co atom, we have $q(\text{Co}) = -q(\text{Sm})$.

| method | m | D_e | r_e | ω_e | q | μ |
|-----------|-----|--------|--------|------------|----------|--------|
| B1LYP | 10 | 1.2900 | 3.0111 | 120.7479 | 0.625214 | 4.4947 |
| B3LYP | 10 | 1.3725 | 2.9669 | 126.2534 | 0.629150 | 4.4694 |
| B3P86 | 10 | 1.2799 | 2.9465 | 129.7313 | 0.622319 | 4.2417 |
| B3PW91 | 10 | 1.8315 | 2.9686 | 126.8396 | 0.618716 | 4.2142 |
| B971 | 10 | 1.2402 | 3.0061 | 117.7587 | 0.584616 | 3.7881 |
| B972 | 10 | 1.6230 | 2.9903 | 120.5058 | 0.575191 | 3.7224 |
| B98 | 10 | 1.1059 | 3.0077 | 117.5993 | 0.586995 | 3.8195 |
| BHandH | 10 | 1.5669 | 2.9705 | 122.0213 | 0.628273 | 4.2536 |
| BHandHLYP | 10 | 1.0493 | 3.0870 | 111.2646 | 0.609532 | 4.4178 |
| HFB | 10 | 0.9092 | 3.0718 | 118.5861 | 0.630904 | 4.7738 |
| MPW1PW91 | 10 | 1.7757 | 2.9817 | 124.5935 | 0.619642 | 4.1843 |
| O3LYP | 10 | 1.5760 | 3.0097 | 120.2384 | 0.630045 | 4.0206 |
| PBE1PBE | 10 | 1.3294 | 2.9819 | 124.1326 | 0.619590 | 4.1239 |

sponds to an evaluation of the stability of the dimer. If the gap is large, means excitation probability is greater, in other words dimer is more stable and vice versa. The HOMO-LUMO gap also shows the interaction probability of the SmCo dimer with other atoms or species. For this situation, it gives an opportunity to make a comment about the structure of the higher order compound of Sm and Co atoms, such as industrially important, highly magnetized SmCo_5 and $\text{Sm}_2\text{Co}_{17}$. These will be the scope of future studies.

The main discussion in the scope of previous study is the validity and reliability of the methods. In this sense, it is easily pointed that HBF gives significantly lower value than the other methods for the $m = 10$ case. As known, HBF is an only-exchange method, so the reason of the result may be the cause of lack of correlation energy. Another exception is about half-and-half functionals; BHandH and BHandHLYP. These two functionals give much larger values than the other methods, that are $E_g(\alpha) = 3.7914$ eV and $E_g(\beta) = 4.1685$ eV for BHandH and $E_g(\alpha) = 3.9312$ eV and $E_g(\beta) = 4.0017$ eV for BHandHLYP. The other methods for the $m = 10$ case give similar results which spread out to an interval from 2.25 eV to 2.85 eV for $E_g(\alpha)$ values, in other representation; $E_g(\alpha) = 2.55 \pm 0.3$ eV. For $E_g(\beta)$ the situation includes a bit more uncertainty that the interval lays between 1.85 eV to 3.25 eV, can be written as $E_g(\beta) = 2.55 \pm 0.70$ eV.

Table3.21: HOMO and LUMO energies (in Hartrees), and HOMO-LUMO gap (E_g) energies (in eV) of the SmCo dimer, calculated for the multiplicity, m ($2S + 1$), at which the total energy is minimum.

| method | m | HOMO(α) | LUMO(α) | $E_g(\alpha)$ | HOMO(β) | LUMO(β) | $E_g(\beta)$ |
|-----------|-----|------------------|------------------|---------------|-----------------|-----------------|--------------|
| B1LYP | 10 | -0.11965 | -0.01584 | 2.82481 | -0.16135 | -0.05294 | 2.94999 |
| B3LYP | 10 | -0.12080 | -0.02676 | 2.55896 | -0.15661 | -0.06062 | 2.61202 |
| B3P86 | 10 | -0.14301 | -0.04713 | 2.60903 | -0.17962 | -0.07479 | 2.85257 |
| B3PW91 | 10 | -0.12384 | -0.02705 | 2.63379 | -0.15684 | -0.05225 | 2.84604 |
| B971 | 10 | -0.11558 | -0.02309 | 2.51678 | -0.16070 | -0.07328 | 2.37882 |
| B972 | 10 | -0.11442 | -0.02238 | 2.50454 | -0.15647 | -0.07189 | 2.30154 |
| B98 | 10 | -0.11860 | -0.02351 | 2.58753 | -0.16484 | -0.07175 | 2.53311 |
| BHandH | 10 | -0.13529 | 0.00404 | 3.79136 | -0.18174 | -0.02855 | 4.16851 |
| BHandHLYP | 10 | -0.13847 | 0.00600 | 3.93123 | -0.17917 | -0.03211 | 4.00171 |
| HFB | 10 | -0.09223 | -0.05521 | 1.00737 | -0.07084 | -0.04017 | 0.83457 |
| MPW1PW91 | 10 | -0.12675 | -0.02208 | 2.84822 | -0.16615 | -0.04679 | 3.24795 |
| O3LYP | 10 | -0.10715 | -0.02436 | 2.25283 | -0.12544 | -0.05759 | 1.84629 |
| PBE1PBE | 10 | -0.12529 | -0.02224 | 2.80413 | -0.16639 | -0.04982 | 3.17203 |

3.2.2 Co₂ Dimer Calculations

The Co₂ discussion constitutes the second part of the dimer calculations. There are a few experimental and theoretical studies about electronic and structural properties of Co₂ dimer in the literature, however there are still inconsistencies in the results [40]. The number of studies are not sufficient for solving these inconsistencies. The results that are gathered from several studies in the literature, are demonstrated in the Table 3.22 [40]. The range of binding energy is wide enough to point out the inconsistency. The results for the bond length are better than binding energy, they are close to each other, change from 1.95 Å to 2.41 Å .

Table3.22: Results for Co₂ from previous works in literature.

| method | D_e (eV) | r_e (Å) | ω_e (cm ⁻¹) |
|----------------|------------|-----------|--------------------------------|
| Ref. [44] | 2.85 | 2.04 | – |
| Ref. [45] | 2.35 | 1.99 | 373 |
| Ref. [46] | 1.50 | 2.41 | 230 |
| Ref. [47] | 0.87 | 1.96 | – |
| Ref. [48] | 2.90 | 1.96 | – |
| Ref. [49] | 5.08 | 2.14 | – |
| Ref. [50] | 2.26 | 1.95 | 421 |
| Ref. [51] | 2.26 | 2.01 | 342 |
| Ref. [40]-BLYP | 1.71 | 2.13 | 329 |
| Ref. [40]-PBE | 2.03 | 2.10 | 271 |
| Ref. [40]-exp | 1.69 | 2.31 | – |

As mentioned before, Co atom has three unpaired electrons in the 3d orbitals. For Co₂ dimer, the number of unpaired electrons is 6, so expected multiplicity value is 7. According to Table 3.23, eight of the methods gives minimum potential at $m = 7$. Whereas five of them gives the minimum energy at $m = 5$, that are B3P86, B3PW91, B971, B972, and O3LYP. They can obtain the multiplicity 5 only by sharing the electrons by overlapping of the shells. It is an unexpected result whereas $-E_5$ and $-E_7$ values are close to each other. The five methods which indicate the minimum energy at $m = 5$, have the same sequence of energies; $-E_5 < -E_7 < -E_3 < -E_9 < -E_1 < -E_{11} < -E_{13} < -E_{15}$. Most of the methods that indicate minimum energy for the case $m = 7$ give the sequence as $-E_7 < -E_5 < -E_3 < -E_9 < -E_1 < -E_{11} < -E_{13} < -E_{15}$. Only for B98 and BHandH, the sequence of first three energies changes as $-E_7 < -E_3 < -E_5$.

Since there is not a concurrence about minimum energy values we prefer to give corresponding variables both for $m = 5$ and $m = 7$ in Table 3.24. The binding energy values for $m = 5$ case, have not seen appropriate, since the range is so wide and even BHandH method gives a negative value. It seems much more convenient for $m = 7$. The values change from 0.5316 eV to 1.9743 eV. The interatomic separation can be written as $r_e = 2.306 \pm 0.212 \text{ \AA}$ for $m = 7$ and $r_e = 2.412 \pm 0.075 \text{ \AA}$ for $m = 5$. The corresponding error part is smaller for $m = 7$, but the value when $m = 7$ is closer to the experimental one $r_e = 2.31 \text{ \AA}$ given by Sebetci [40]. The vibrational frequency of Co₂ has been determined distinctively by researchers according to Table 3.22.

The frequency value given by B98 for $m = 5$ is 374.20 cm⁻¹ that is remarkably greater than the others. If it is ignored, error can be decreased and value can be expressed as $\omega_e = 251 \pm 42 \text{ cm}^{-1}$. The circumstance appears more acceptable for $m = 7$ case, given range is $\omega_e = 232 \pm 31 \text{ cm}^{-1}$. The BHandH method gives a negative value for binding energy at $m = 5$ case, that is of course nonsense. The reason for this situation is not clear to comment on it, but we estimate that will be arised from the minimum energy values of Co atom which is obtained at $m = 2$ case instead of the expected $m = 4$ case. Although the reason is not clear, it is obvious that this value is problematic, so it can be neglected.

In Table 3.25, HOMO and LUMO energy values and energy gap between HOMO-LUMO for Co₂ dimer are represented. The HFB method gives significantly smaller values for both multiplicity values and for both energy gap. It is meaningful since HFB is an only ex-

Table 3.23: Total energies, E_m , in Hartrees, for Co_2 dimer for different multiplicities, m ($2S + 1$). The starred ones show the lowest energy.

| method | $-E_1$ | $-E_3$ | $-E_5$ | $-E_7$ | $-E_9$ | $-E_{11}$ | $-E_{13}$ | $-E_{15}$ |
|-----------|----------|----------|-----------|-----------|----------|-----------|-----------|-----------|
| B1LYP | 289.9089 | 290.0088 | 290.0400 | 290.0675* | 289.9906 | 289.8519 | 289.5032 | 289.2835 |
| B3LYP | 290.1572 | 290.2322 | 290.2855 | 290.2915* | 290.1806 | 290.0641 | 289.7323 | 289.4179 |
| B3P86 | 290.9203 | 290.9951 | 291.0649* | 291.0548 | 290.9305 | 290.8402 | 290.5165 | 290.2057 |
| B3PW91 | 290.2076 | 290.2888 | 290.3570* | 290.3496 | 290.2707 | 290.1453 | 289.8255 | 289.5213 |
| B971 | 290.0234 | 290.1342 | 290.1669* | 290.1526 | 290.0646 | 289.8826 | 289.6515 | 289.3360 |
| B972 | 290.4341 | 290.5023 | 290.5778* | 290.5611 | 290.4392 | 290.2615 | 290.0387 | 289.7328 |
| B98 | 290.0974 | 290.2246 | 290.2232 | 290.2320* | 290.1458 | 289.9934 | 289.7323 | 289.4237 |
| BHandH | 288.9592 | 289.0931 | 289.0810 | 289.1573* | 289.0719 | 288.8353 | 288.6190 | 288.4724 |
| BHandHLYP | 289.7437 | 289.8876 | 289.9151 | 289.9393* | 289.8957 | 289.6122 | 289.3627 | 289.0768 |
| HFB | 288.7937 | 288.8510 | 288.8916 | 288.9062* | 288.8208 | 288.7130 | 288.4981 | 288.2112 |
| MPW1PW91 | 290.1317 | 290.2371 | 290.2684 | 290.2977* | 290.2067 | 290.1059 | 289.7716 | 289.4738 |
| O3LYP | 290.5250 | 290.5775 | 290.6404* | 290.6293 | 290.5318 | 290.3918 | 290.1405 | 289.7774 |
| PBE1PBE | 289.9921 | 290.0954 | 290.1489 | 290.1571* | 290.0655 | 289.9613 | 289.7165 | 289.3340 |

Table3.24: Spectroscopic constants of the Co₂ dimer calculated for the multiplicity, m ($2S + 1$), at which the total energy is minimum. For notation used, see Table 3.20.

| method | m | D_e | r_e | ω_e | q | μ |
|-----------|-----|---------|--------|------------|---------|--------|
| B1LYP | 5 | 0.3685 | 2.5182 | 212.78 | 0.00000 | 0.0000 |
| B3LYP | 5 | 0.9957 | 2.4115 | 219.49 | 0.01815 | 0.1283 |
| B3P86 | 5 | 1.3738 | 2.3978 | 236.80 | 0.00000 | 0.0000 |
| B3PW91 | 5 | 2.0494 | 2.4109 | 232.33 | 0.00000 | 0.0000 |
| B971 | 5 | 0.9233 | 2.4301 | 224.14 | 0.00000 | 0.0000 |
| B972 | 5 | 2.4293 | 2.4262 | 225.71 | 0.00000 | 0.0000 |
| B98 | 5 | 0.2612 | 2.0939 | 374.20 | 0.00000 | 0.0000 |
| BHandH | 5 | -0.1486 | 2.4351 | 228.81 | 0.00000 | 0.0000 |
| BHandHLYP | 5 | 0.2753 | 2.5283 | 208.66 | 0.00000 | 0.0000 |
| HFB | 5 | 0.6974 | 2.1864 | 292.63 | 0.00000 | 0.0000 |
| MPW1PW91 | 5 | 1.0276 | 2.4985 | 219.43 | 0.00000 | 0.0000 |
| O3LYP | 5 | 1.2879 | 2.4483 | 217.01 | 0.00000 | 0.0000 |
| PBE1PBE | 5 | 0.9169 | 2.4079 | 223.64 | 0.01815 | 0.1189 |
| B1LYP | 7 | 1.1169 | 2.4340 | 217.38 | 0.00000 | 0.0000 |
| B3LYP | 7 | 1.1590 | 2.4373 | 215.01 | 0.00000 | 0.0000 |
| B3P86 | 7 | 1.1005 | 2.4110 | 224.78 | 0.00000 | 0.0000 |
| B3PW91 | 7 | 1.8480 | 2.4229 | 221.80 | 0.00000 | 0.0000 |
| B971 | 7 | 0.5316 | 2.4471 | 209.90 | 0.00000 | 0.0000 |
| B972 | 7 | 1.9743 | 2.4202 | 213.41 | 0.00000 | 0.0000 |
| B98 | 7 | 0.5012 | 2.4415 | 210.53 | 0.00000 | 0.0000 |
| BHandH | 7 | 1.9271 | 2.3370 | 264.00 | 0.00000 | 0.0000 |
| BHandHLYP | 7 | 0.9356 | 2.3950 | 240.17 | 0.00000 | 0.0000 |
| HFB | 7 | 1.0930 | — | 199.38 | 0.02873 | 0.0792 |
| MPW1PW91 | 7 | 1.8258 | 2.4132 | 226.98 | 0.00000 | 0.0000 |
| O3LYP | 7 | 0.9870 | 2.4874 | 199.93 | 0.00000 | 0.0000 |
| PBE1PBE | 7 | 1.1391 | 2.4150 | 226.83 | 0.00000 | 0.0000 |

change method, no contribution from correlation. Both half and half functions, BHandH and BHandHLYP methods give greater values from other values. One more method, O3LYP disrupts the general consistency of results by smaller values. These results also in accordance with the SmCo dimer results. The results from other methods are close to each other; can be demonstrated as $E_g(\alpha) = 3.10 \pm 0.19$ Hartrees and $E_g(\beta) = 2.10 \pm 0.30$ Hartrees for $m = 5$ and similarly $E_g(\alpha) = 3.32 \pm 0.18$ Hartrees and $E_g(\beta) = 2.63 \pm 0.26$ for $m = 7$.

3.2.3 Sm₂ Dimer Calculations

The third part of the dimer calculations consists of Sm₂ dimer energies and other characteristics. As mentioned before Sm is a massive atom with 62 electrons and this is the most problematic part of the dimer calculations since most of the energy calculations have not gave result. The present results are demonstrated in Table 3.26. According to the table, $m = 1$,

Table 3.25: HOMO and LUMO energies (in Hartrees), and HOMO-LUMO gap (E_g) energies (in eV) of the Co_2 dimer, calculated for the multiplicity, m ($2S + 1$), at which the total energy is minimum.

| method | m | HOMO(α) | LUMO(α) | $E_g(\alpha)$ | HOMO(β) | LUMO(β) | $E_g(\beta)$ |
|-----------|-----|------------------|------------------|---------------|-----------------|-----------------|--------------|
| B1LYP | 5 | -0.20354 | -0.08960 | 3.10046 | -0.15723 | -0.07948 | 2.11569 |
| B3LYP | 5 | -0.20505 | -0.09794 | 2.91461 | -0.15276 | -0.08643 | 1.80493 |
| B3P86 | 5 | -0.22666 | -0.11276 | 3.09938 | -0.18720 | -0.09883 | 2.40467 |
| B3PW91 | 5 | -0.20526 | -0.09175 | 3.08876 | -0.16486 | -0.07751 | 2.37691 |
| B971 | 5 | -0.20031 | -0.08746 | 3.07080 | -0.16641 | -0.07989 | 2.35433 |
| B972 | 5 | -0.19875 | -0.08366 | 3.13176 | -0.16144 | -0.07531 | 2.34372 |
| B98 | 5 | -0.20562 | -0.08584 | 3.25938 | -0.15496 | -0.07571 | 2.15650 |
| BHandH | 5 | -0.28473 | -0.06748 | 5.91167 | -0.17467 | -0.08750 | 2.37202 |
| BHandHLYP | 5 | -0.22139 | -0.06049 | 4.37831 | -0.20691 | -0.05325 | 4.18130 |
| HFB | 5 | -0.17026 | -0.10092 | 1.88684 | -0.10516 | -0.08315 | 0.59892 |
| MPW1PW91 | 5 | -0.20677 | -0.08795 | 3.23326 | -0.15947 | -0.07313 | 2.34943 |
| O3LYP | 5 | -0.18640 | -0.09524 | 2.48059 | -0.13801 | -0.08171 | 1.53200 |
| PBE1PBE | 5 | -0.20676 | -0.08556 | 3.29802 | -0.15954 | -0.07144 | 2.39732 |
| B1LYP | 7 | -0.16814 | -0.04240 | 3.42156 | -0.19708 | -0.09560 | 2.76141 |
| B3LYP | 7 | -0.16941 | -0.05145 | 3.20985 | -0.20288 | -0.11582 | 2.36902 |
| B3P86 | 7 | -0.19148 | -0.07063 | 3.28850 | -0.22738 | -0.13706 | 2.45773 |
| B3PW91 | 7 | -0.17211 | -0.05075 | 3.30237 | -0.20390 | -0.11376 | 2.45283 |
| B971 | 7 | -0.16112 | -0.04564 | 3.14237 | -0.19637 | -0.10809 | 2.40222 |
| B972 | 7 | -0.15618 | -0.04019 | 3.15625 | -0.19708 | -0.10704 | 2.45011 |
| B98 | 7 | -0.16475 | -0.04631 | 3.22292 | -0.19855 | -0.10690 | 2.49392 |
| BHandH | 7 | -0.18785 | -0.02370 | 4.46675 | -0.21208 | -0.05592 | 4.24933 |
| BHandHLYP | 7 | -0.19165 | -0.02335 | 4.57968 | -0.20498 | -0.05968 | 3.95381 |
| HFB | 7 | -0.13592 | -0.05031 | 2.32957 | -0.15880 | -0.11311 | 1.24329 |
| MPW1PW91 | 7 | -0.17563 | -0.04703 | 3.49938 | -0.20391 | -0.09802 | 2.88141 |
| O3LYP | 7 | -0.15448 | -0.04976 | 2.84958 | -0.19382 | -0.13289 | 1.65799 |
| PBE1PBE | 7 | -0.17385 | -0.04711 | 3.44877 | -0.20319 | -0.09783 | 2.86699 |

$m = 13$, and $m = 19$ are most probable multiplicity values, most of the calculation ended with an energy value. In the outermost shell of Sm atom has six unpaired electrons, so the expected multiplicity for Sm_2 dimer is 13. From Table 3.26 all the methods end up with expected value.

According to half-shell stability, $-E_{17}$ is the most probable result greater than the minimum energy, whereas most of the methods do not conclude calculations. Results for $-E_{19}$ are better than the expected $-E_{17}$.

The spectroscopic constants of Sm_2 dimer are summarized in Table 3.27. The binding energies alter in a wide range, from 0.0215 Hartrees to 0.9465 Hartrees. Table 3.24 which was

Table3.26: Total energies, E_m , in Hartrees, for a Sm_2 dimer for different multiplicities, m ($2S + 1$). The starred ones show the lowest energy. 'nc' indicates a 'not completed' calculation due to a non-convergent- or confused-SCF process.

| method | $-E_1$ | $-E_{11}$ | $-E_{13}$ | $-E_{15}$ | $-E_{17}$ | $-E_{19}$ |
|-----------|----------|-----------|-----------|-----------|-----------|-----------|
| B1LYP | 162.0049 | nc | 162.4809* | nc | 162.3261 | 161.7638 |
| B3LYP | 162.3152 | nc | 162.8333* | nc | nc | nc |
| B3P86 | 162.9753 | nc | 163.5781* | nc | nc | 162.8820 |
| B3PW91 | 162.3071 | nc | 162.9440* | nc | nc | 162.2511 |
| B971 | 162.2467 | nc | 162.7483* | 162.6940 | nc | 161.9666 |
| B972 | 162.3565 | 162.8510 | 162.9345* | nc | nc | 162.1602 |
| B98 | 162.2568 | 162.7206 | 162.7860* | nc | nc | 162.0122 |
| BHandH | 160.0575 | nc | 161.0975* | nc | nc | 160.3717 |
| BHandHLYP | 160.7964 | nc | 161.6445* | nc | 161.4819 | 160.8953 |
| HFB | nc | 162.4818 | 162.5401* | nc | nc | nc |
| MPW1PW91 | 162.0955 | 162.6234 | 162.7453* | nc | nc | 162.0657 |
| O3LYP | 162.5760 | nc | 163.2803* | nc | 163.1469 | 162.5705 |
| PBE1PBE | 161.9428 | nc | 162.6501* | nc | nc | 161.9049 |

arranged for Co_2 , HFB method gives the minimum vibrational frequency and the maximum intermolecular distance remarkably different than all other methods. Except HFB, all other methods conclude the calculations with closer values for r_e and ω_e , which can be presented as $4.780 \pm 0.108 \text{ \AA}$ $35.6 \pm 3.3 \text{ cm}^{-1}$ respectively. If HFB is included, the expression turns to $r_e = 4.88 \pm 0.203 \text{ \AA}$, where error duplicates.

Table 3.28 has been arranged for HOMO–LUMO energies and $E_g(\alpha)$ and $E_g(\beta)$ energy gaps of Sm_2 . It is clearly seen that again HFB gives the minimum result. Similar to the Co_2 calculations, half and half functional methods BHandH and BHandHLYP methods give significantly greater values than the other methods. Additionally, O3LYP also gives smaller values for $E_g(\alpha)$ and $E_g(\beta)$. The results of the other methods can be indicated as $E_g(\alpha) = 2.79 \pm 0.15$ Hartrees and $E_g(\beta) = 2.68 \pm 0.35$ Hartrees.

3.2.4 SCF Calculations

In the second part of dimer calculations we performed "single-point" (sp) self-consistent field calculations (SCF). In a sp calculation, GAUSSIAN 03 compels the dimer under question to converge as it is specified at the very beginning of the simulation, without changing the interatomic separation r . We carried out sp calculations for Co_2 dimer with multiplicity $m =$

Table 3.27: Spectroscopic constants of the Sm_2 dimer calculated for the multiplicity, m ($2S + 1$), at which the total energy is minimum. For notation used, see Table 3.20.

| method | m | D_e | r_e | ω_e | q | μ |
|-----------|-----|--------|--------|------------|---------|--------|
| B1LYP | 13 | 0.1204 | 4.8416 | 33.4884 | 0.00000 | 0.0000 |
| B3LYP | 13 | 0.1460 | 4.8009 | 34.1305 | 0.00000 | 0.0000 |
| B3P86 | 13 | 0.1905 | 4.6724 | 37.0425 | 0.00000 | 0.0000 |
| B3PW91 | 13 | 0.6584 | 4.7043 | 37.3122 | 0.00000 | 0.0000 |
| B971 | 13 | 0.9465 | 4.7183 | 37.7456 | 0.00000 | 0.0000 |
| B972 | 13 | 0.2173 | 4.7396 | 36.8318 | 0.00000 | 0.0000 |
| B98 | 13 | 0.6600 | 4.7398 | 36.7767 | 0.00000 | 0.0000 |
| BHandH | 13 | 0.4405 | 4.6959 | 36.8246 | 0.00189 | 0.0817 |
| BHandHLYP | 13 | 0.0215 | 4.8883 | 32.3220 | 0.00000 | 0.0000 |
| HFB | 13 | 0.0617 | 5.0780 | 27.6654 | 0.00000 | 0.0000 |
| MPW1PW91 | 13 | 0.4742 | 4.6798 | 38.4687 | 0.00068 | 0.0278 |
| O3LYP | 13 | 0.9084 | 4.8032 | 36.9029 | 0.00245 | 0.0983 |
| PBE1PBE | 13 | 0.4327 | 4.6807 | 38.8403 | 0.00000 | 0.0000 |

5 and 7, for Sm_2 with $m = 13$, and for SmCo with $m = 10$; the multiplicity values here are the ones for which the energy minima are spotted.

To do so, we scanned the distance r between the two atoms of a dimer from 1.0 to 5.0 Å for Co_2 and SmCo , and from 2.0 to 7.0 Å for Sm_2 . We carried out a total of 300 sp calculations for each cases considered. Figures 3.1–3.8 present the resulting outcomes for the most clear-looking r -intervals. The formation energy E_f of SmCo is calculated for B1LYP, say, as $E_f = -27.211 (E_{10}^{\text{SmCo}} - E_7^{\text{Sm}} - E_4^{\text{Co}})$ (eV) where E_7^{Sm} and E_4^{Co} values are from Tables 3.1 and 3.10, respectively, and E_{10}^{SmCo} values are the results of present sp-calculations.

Let us start with the SmCo scan results which shown in Figures 3.1 and 3.2, where we omitted the graph of HFB because it does not contain the electron correlation energy in its formulation. We see that all the results have some common features: most of the data points from the 300 sp calculations are organized in a plainly noticed order, leading to not-so-smooth and frequently broken plots. Nonetheless, we can safely say that all the graphs in these two figures are of the Lennard-Jones nature. Obviously, we do not speak, for any given method, of a consummate, faultless Lennard-Jones plot, since there happen to be many data points which are just out of the main plot.

It follows from Figures 3.1 and 3.2 that all the twelve methods resulted in almost the same equilibrium interatomic distance r_e around 3.0 Å. Noting that this value is just the aforesaid

Table 3.28: HOMO and LUMO energies (in Hartrees), and HOMO-LUMO gap (E_g) energies (in eV) of the Sm₂ dimer, calculated for the multiplicity, m ($2S + 1$), at which the total energy is minimum.

| method | m | HOMO(α) | LUMO(α) | $E_g(\alpha)$ | HOMO(β) | LUMO(β) | $E_g(\beta)$ |
|-----------|-----|------------------|------------------|---------------|-----------------|-----------------|--------------|
| B1LYP | 13 | -0.10947 | -0.00114 | 2.94781 | -0.10027 | 0.01094 | 3.02618 |
| B3LYP | 13 | -0.11148 | -0.01194 | 2.70862 | -0.10195 | 0.00055 | 2.78917 |
| B3P86 | 13 | -0.13263 | -0.03559 | 2.64059 | -0.12263 | -0.02288 | 2.71434 |
| B3PW91 | 13 | -0.11404 | -0.01658 | 2.65202 | -0.10428 | -0.00404 | 2.72767 |
| B971 | 13 | -0.10863 | -0.00923 | 2.70481 | -0.09866 | 0.00400 | 2.79352 |
| B972 | 13 | -0.10909 | -0.00957 | 2.70808 | -0.09935 | 0.00276 | 2.77855 |
| B98 | 13 | -0.11097 | -0.00976 | 2.75406 | -0.10112 | 0.00356 | 2.84849 |
| BHandH | 13 | -0.12267 | 0.01919 | 3.86021 | -0.11378 | 0.03194 | 3.96524 |
| BHandHLYP | 13 | -0.12613 | 0.02056 | 3.99164 | -0.11758 | 0.03338 | 4.10783 |
| HFB | 13 | -0.07595 | -0.04280 | 0.90206 | -0.06459 | 0.01514 | 2.16956 |
| MPW1PW91 | 13 | -0.11559 | -0.01237 | 2.80876 | -0.10608 | 0.00060 | 2.90291 |
| O3LYP | 13 | -0.09664 | -0.01508 | 2.21936 | -0.08795 | -0.00248 | 2.32576 |
| PBE1PBE | 13 | -0.11452 | -0.01053 | 2.82971 | -0.10478 | 0.00216 | 2.90999 |

one in Table 3.20, the features seen in these graphs are impressively beautiful. As to the corresponding formation energies E_f , except B98 and B971, they are in agreement to a great degree to the binding energy D_e values listed in Table 3.20.

We note before passing that two Becke functionals B98 and B971 have given rise almost to the same curve, for they both have the same D_e and r_e values for SmCo dimer. Their another peculiarity is that their curves cross the $E_f = 0$ line; if we are to speak of a proper Lennard-Jones curve for SmCo, this crossing should not have occurred.

A final point about the graphs in Figures 3.1 and 3.2 is that the plot of O3LYP contains actually more than one curve; if we had increased the data points in the sp calculations from 300 to 3000, say, we would clearly distinguish at least three distinct curves, all of them sharing the same equilibrium interatomic distance, r_e , value about 3.0 Å. The only difference among them would be their different D_e values. Actually this situation is common in all the curves seen in these two figures: although they are barely discernable, a careful eye can readily recognize the remnants of more than one curve in each of them.

We show in Figures 3.3 and 3.4 the curves which are the outcomes of sp-scan results for Co₂ dimer for multiplicity $m = 5$. Again we see that the data points are ordered in a noticeable order, resulting in occasionally broken curves. Obviously, the curves in these tables cannot be said to be of the Lennard-Jones nature. To compound the situation further, we see the

features exhibited in these graphs are not at all in agreement with those in Table 3.24 which are the results from optimization calculations. As we see in Table 3.24, the equilibrium interatomic distances were mostly about 2.40-2.50 Å. But in these curves, it is usually around 1.90-2.20 Å. Even worse, except B3P86, B3PW91, B972, MPW1PW91, and O3LYP, all the remaining seven functionals, the equilibrium point is above the $E_f = 0$ line, which is of course unacceptable, for it leads to a negative binding energy D_e ! For the last, but not least, all the curves have parts again $E_f = 0$ line.

We see one more time that in the graphs of Co_2 , which are the results of sp calculations; all the curves are composed of the remnants of several different curves. Take the B3LYP case in Figure 3.3 as an example. Its curve starts from right, say, continues to the left a while, then abruptly brakes and jumps to another part of curve, continues again a little, and again brakes suddenly jumping to the next one, and so on. Here the natural question is this: which features should be correct? Those seen in the curves of Figures 3.3 and 3.4 or those listed in Table 3.24. We believe that the results in Table 3.24 are the more acceptable ones because the r_e values there are somehow close to the experimental and the other theoretical literature values and, for the most, they are the results of optimization calculations.

Figures 3.5 and 3.6 present the sp-scan calculations results for again Co_2 , but for $m = 7$ this time. All the comments we have made about the $m = 5$ case are seen to valid also here. Again we observe curves composed of several broken parts, with their minima above the $E_f = 0$ line (for B98, B971, and BHandHLYP). Again all of them have some part of their tails above the $E_f = 0$ line. More importantly, all the curves make their minimum around $r_e = 2$ Å, not at all in agreement with those listed in Table 3.24, which are around 2.3–2.5 Å. Nevertheless, the curves shown in Figures 3.5 and 3.6 are seem to have a better appearance, for they have better-ordered data points. Notice how B98 and B971 functionals have produced nearly flawless Lennard-Jones-like curves, though they have completely unacceptable D_e and r_e values.

All the curves exhibited in Figures 3.1–3.4 portend somehow the unceasing debate about the ground-state of Co_2 dimer: should its multiplicity be $m = 5$ or $m = 7$? Its correct answer seems still evasive. Each DFT functional produces its own result which is usually very different than that resulted from another functional. Only the r_e values are exempt from this fact for the time being. Finally in this section, in Figures 3.7 and 3.8 are the sp calculation results

for Sm_2 dimer. Curves bear features which are the reminiscent of a general Lennard-Jones curve. Although we see an overall order in these curves, we cannot speak of any smoothness. Nonetheless, the features observed here are much better than those for the Co_2 cases discussed above. In Sm_2 curves, at least the equilibrium interatomic distance r_e values are hinted to be close to those tabulated in Table 3.27. Even the situation for the binding energy D_e values are not bad at all; only the B3P86 and B972 (and maybe including O3LYP and BHandHLYP), cases in which the minima are above $E_f = 0$ line are unsatisfactory.

3.3 Trimers

The third part of the study consists of possible trimers of Co and Sm atoms. These are Co_3 , Sm_3 , SmCo_2 , and Sm_3Co clusters. In accordance with dimer calculations, we can determine the calculate the minimum total energy with respect to multiplicity, the spectroscopic constants that are; binding energy D_e , equilibrium interatomic separation r_e , and fundamental frequency w_e , HOMO, LUMO, and HOMO-LUMO gap energy, dipole moment and excess charges on the atoms.

3.3.1 Co_3 Trimer Calculations

Before looking into the energy results for the Co_3 trimer, we should first note that two different multiplicity m values we may see. In the first case, if the multiplicity of the Co_2 dimer is really 5, this means that the Co_2 dimer has four unpaired electrons, then another three unpaired electrons will come from the third cobalt elements; this configuration gives us a total of seven unpaired electrons. As a result, we might expect a multiplicity value $m = 8$ for the Co_3 trimer. In the second case in which we may have a total of nine unpaired electrons in Co_3 , three for each Co elements, then it is possible that the multiplicity of Co_3 would be $m = 10$. It is apparent from Table 3.29 that these expectations have materialized: Except for B3PW91, BHandHLYP, MPW1PW91, PBE1PBE, all the other nine methods have given the somewhat expected multiplicity value $m = 8$. The former four methods have resulted in $m = 10$ value. Are the minimum energy values E_8 and E_{10} so different from each other? As we see clearly from this table, the mentioned difference is so small, meaning that it is so difficult in reality to discern the real minimum configuration between them. Before passing, we might notice

that there is no distinct order or pattern among the energy values E_2 to E_{10} ; after them they monotonically increase. Actually, the same situation can be seen in all the other atom, dimer, and trimer energy tables. What we want to say that it might be quite difficult to detect the real minimum energy configuration by looking only the first minimum, for this first minimum might only be a local minimum. Consequently, we humbly recommend a diligent researcher to scan all the possible multiplicity values, of course if he or she has no difficulty in allocating the time required.

Since it was not possible to determine absolutely the real multiplicity value for the Co_3 trimer, it seems appropriate to give all the geometric details, spectroscopic constants, charges, dipoles, and HOMO-LUMO energies for the Co_3 trimer separately for the $m = 8$ and 10 values. Table 3.30 tabulates the bond lengths, bond angles, and vibrational frequencies of the Co_3 trimer obtained for the 13 different DFT methods we employed.

For $m = 8$ in Table 3.30 (for the notation employed there, refer to Fig. 3.9), the first thing to note that all the methods have led to a linear geometric configuration (D_∞). Although the exact angle values are never exactly 180° , we can safely accept them to be so; the very small differences, including the MPW1PW91 case in which the discrepancy is a little bit larger, can be attributed to the initial random atomic configurations, to the accuracy of GAUSSIAN03 package, and to the performance of the computer we made use of. It is clear from the same table that there is a definite C_2 symmetry in the linear Co_3 trimers; that is, the R_{12} values are (nearly) equal to the R_{23} values. This is expected, because we are dealing with three identical and indistinguishable Co atoms, and there should be no way to label them. This, in turn, gives rise to the conclusion that the distance between the first and second atoms and that between the second and third atoms must be equal to each other, for a linear Co_3 trimer. It is seen from the same table that all the bond length R_{12} and R_{23} values for $m = 8$ are in a range of 2.28–2.44 Å. This consistency among the different 13 methods in giving nearly the same results is especially notable, hinting at the reliability of the methods, which are all the culmination of many researchers' unceasing quests for the ultimate perfect method.

As to the vibrational frequencies of the Co_3 dimer with $m = 8$, we see that the three fundamental frequencies are distinct from each other. We mean these values are not at all close to each other and that in a real spectroscopy measurement experiment, it is very likely to see three well-separated peaks for each of the fundamental frequencies listed in Table 3.30. Nu-

Table3.29: Total energies, E_m , in Hartrees, for Co_3 trimer for different multiplicities, m ($2S + 1$).

| method | $-E_2$ | $-E_4$ | $-E_6$ | $-E_8$ | $-E_{10}$ | $-E_{12}$ | $-E_{14}$ | $-E_{16}$ | $-E_{18}$ | $-E_{20}$ |
|-----------|----------|----------|----------|-----------|-----------|-----------|-----------|-----------|-----------|-----------|
| B1LYP | 435.1196 | 435.0915 | 435.1257 | 435.1451* | 435.1357 | 435.0579 | 434.9495 | 434.7862 | 434.5371 | 434.2429 |
| B3LYP | 435.4596 | 435.4332 | 435.4669 | 435.4848* | 435.4746 | 435.3863 | 435.2762 | 435.1070 | 434.8597 | 434.5579 |
| B3P86 | 436.6143 | 436.5396 | 436.6197 | 436.6328* | 436.6327 | 436.5465 | 436.4376 | 436.2773 | 436.0272 | 435.7453 |
| B3PW91 | 435.5515 | 435.5233 | 435.5568 | 435.5704 | 435.5729* | 435.4912 | 435.3880 | 435.2332 | 434.9882 | 434.7123 |
| B971 | 435.2110 | 435.2543 | 435.2670 | 435.2831* | 435.2701 | 435.1670 | 435.0578 | 434.8792 | 434.6062 | 434.3244 |
| B972 | 435.8247 | 435.8147 | 435.8847 | 435.8980* | 435.8820 | 435.7768 | 435.6474 | 435.4793 | 435.2081 | 434.9253 |
| B98 | 435.3438 | 435.3415 | 435.3832 | 435.4003* | 435.3882 | 435.2871 | 435.1962 | 435.0062 | 434.7339 | 434.4550 |
| BHandH | 433.7472 | 433.7257 | 433.7616 | 433.7849* | 433.7837 | 433.7073 | 433.6367 | 433.4232 | 433.2363 | 432.9933 |
| BHandHLYP | 434.7492 | 434.8915 | 434.9262 | 434.9537 | 434.9565* | 434.9048 | 434.8032 | nc | 434.4003 | 434.1592 |
| HFB | 433.3568 | 433.3578 | 433.3486 | 433.3815* | 433.3814 | 433.3085 | 433.2067 | 433.0915 | 432.8984 | 432.6275 |
| MPW1PW91 | 435.4724 | 435.4425 | 435.4765 | 435.4900 | 435.4944* | 435.4196 | 435.3224 | 435.1232 | 434.9353 | 434.6537 |
| O3LYP | 435.9738 | 435.9123 | 435.9841 | 435.9972* | 435.9868 | 435.8934 | 435.7569 | 435.6035 | 435.3816 | 435.0761 |
| PBE1PBE | 435.2616 | 435.2271 | 435.2665 | 435.2810 | 435.2841* | 435.2086 | 435.0997 | 434.9579 | 434.7239 | 434.4430 |

Table 3.30: Bond lengths R_{12} and R_{23} (Å), bond angle θ_{123} (deg), and vibrational frequencies ω_n (cm^{-1}) of Co_3 trimer. For the notation used, see Fig. 3.9.

| method | m | R_{12} | R_{23} | θ_{123} | ω_1 | ω_2 | ω_3 |
|-----------|-----|----------|----------|----------------|------------|------------|------------|
| B1LYP | 8 | 2.3383 | 2.3383 | 179.9977 | 57.9769 | 165.2187 | 273.1134 |
| B3LYP | 8 | 2.3054 | 2.3054 | 179.9875 | 40.3645 | 168.1510 | 282.4238 |
| B3P86 | 8 | 2.2804 | 2.2803 | 179.9540 | 36.6931 | 170.6370 | 287.0438 |
| B3PW91 | 8 | 2.3013 | 2.2930 | 179.5183 | 68.0735 | 171.4295 | 288.1704 |
| B971 | 8 | 2.3291 | 2.3284 | 179.9959 | 67.8216 | 164.7834 | 277.5973 |
| B972 | 8 | 2.2958 | 2.2958 | 179.9965 | 47.7114 | 166.3232 | 276.8408 |
| B98 | 8 | 2.3307 | 2.3305 | 179.9822 | 77.3060 | 168.5791 | 284.1932 |
| BHandH | 8 | 2.3346 | 2.3346 | 179.9963 | 76.4149 | 159.2871 | 273.1480 |
| BHandHLYP | 8 | 2.4423 | 2.4428 | 179.9971 | 66.3563 | 142.6938 | 245.1946 |
| HFB | 8 | 2.3170 | 2.3167 | 179.9897 | 63.2225 | 157.6999 | 232.7209 |
| MPW1PW91 | 8 | 2.3164 | 2.3235 | 179.1373 | 68.4773 | 166.5265 | 281.8294 |
| O3LYP | 8 | 2.2769 | 2.2769 | 179.8262 | 52.9335 | 164.3737 | 263.5213 |
| PBE1PBE | 8 | 2.3211 | 2.3214 | 179.9848 | 58.7694 | 169.3582 | 280.1786 |
| B1LYP | 10 | 2.4931 | 2.4931 | 60.2067 | 161.6978 | 163.3248 | 217.0806 |
| B3LYP | 10 | 2.4701 | 2.4701 | 60.4498 | 161.8123 | 162.8664 | 218.8316 |
| B3P86 | 10 | 2.4008 | 2.4961 | 58.6009 | 166.5900 | 182.7480 | 233.8198 |
| B3PW91 | 10 | 2.4150 | 2.5096 | 58.6799 | 166.0688 | 179.6791 | 229.8943 |
| B971 | 10 | 2.5424 | 2.4762 | 59.1337 | 162.6439 | 171.0763 | 213.8466 |
| B972 | 10 | 2.5201 | 2.4335 | 58.8170 | 161.4558 | 173.0234 | 216.3178 |
| B98 | 10 | 2.4858 | 2.4858 | 60.8054 | 158.7981 | 167.4695 | 211.4643 |
| BHandH | 10 | 2.5399 | 2.5399 | 60.3833 | 141.6028 | 167.9064 | 175.9585 |
| BHandHLYP | 10 | 2.9937 | 2.9994 | 59.7120 | 69.0480 | 92.2697 | 95.1655 |
| HFB | 10 | 2.6259 | 2.4800 | 58.0495 | 134.6271 | 146.6539 | 187.9772 |
| MPW1PW91 | 10 | 2.4276 | 2.5127 | 58.8097 | 165.9933 | 179.6142 | 229.2789 |
| O3LYP | 10 | 2.3551 | 2.5231 | 57.6225 | 156.5483 | 171.2290 | 219.1099 |
| PBE1PBE | 10 | 2.4258 | 2.5109 | 58.8808 | 167.9620 | 180.6394 | 229.9148 |

merically, these three frequency values are roughly centered around 65, 165, and 280 cm^{-1} . Now we have come to the $m = 10$ case. It follows from the second part of Table 3.30 that, the minimum energy configuration for this case are all equilateral triangles, though nearly all of them are distorted. This distortion is the biggest in O3LYP and the smallest B1LYP and these are the reasons why the R_{12} and R_{23} values are so apart for O3LYP and equal to each other for B1LYP. Except for BHandHLYP, the bond lengths of the equilateral structures are in the range of 2.36–2.63 Å. The corresponding value for BHandHLYP is about 3.00 Å, which we believe is not reliable. We remember from Table 3.24 that BHandHLYP method gave us a 2.395-Å the bond length for the Co_2 dimer. It seems unrealistic that in forming a Co_3 trimer from a Co_2 dimer by adding a third Co atom would increase this 2.395-Å value to 3.00-Å, for this would be a huge leap in the atomic scale. A close look at the corresponding vibrational frequency values reveals the same oddness for BHandHLYP method; its results are remarkably smaller than those of other methods. By the way, a similar situation in concerning these

frequency values are noticed for BHandH and HFB methods; for the latter this should be seen normal if we remember that HFB does not include the crucially important electron correlation phenomenology in its formulation. (Note that the frequency values of HFB are not drastically different from others.) We do not manage to ascribe *properly* the strangeness witnessed in BHandH case to a logical reason for the time being, for this requires a profound analysis into the internal details of the BHandH method's formulation, which is out of scope of this master thesis. Apart from the mentioned three methods, the numerical frequency values of the other ten methods are centered around 160, 170, and 220 cm^{-1} , with the former two being somehow close to each other.

We give in Table 3.31 the calculated excess charge on the atoms of the Co_3 trimer and the closely related dipole moment values for again the $m = 8$ and 10 cases. It is seen a net charge separation for all the results listed in this table. In the geometrically linear $m = 8$ case, the symmetry dictates a zero net dipole moment, as is clearly seen in the last column: we have two dipoles, opposite to each other, one say, to the left and the other to the right, possessing nearly the same magnitude, leading to a zero dipole moment. Again the non-zero but very small μ values are acceptable within the accuracy of the results. Referring to Table 3.30, we see that all the non-zero μ values belong to the non-perfect linear geometries. It is plain from the same table that $2|q_1| = 2|q_3| = q_2$, of course, this is unsurprising. Numerically, the charge values are in a wide range such that $0.14|e| < q_2 < 0.29|e|$.

In the $m = 10$ cases, which are geometrically equilateral triangles, we observe *symmetric* charge separations in all the cases considered, but not so much clearly as in the case of the linear $m = 8$ geometries mentioned above. We note that the magnitudes of these charge values are so small if we compare them with those for the $m = 8$ cases. There might be two explanations here. Firstly, we may suppose that there is no charge separation at all in the ingredients Co atoms of the trimer, so that there is no net resulting dipole moment. This also explains the feature seen in the $m = 10$ portion of Table 3.31: the more distorted triangle, the bigger total dipole moment value it has. Secondly, there *is* really a charge separation among Co atoms, which are listed in the same table, so that we have some amount of total dipole moments, though they are very small. Therefore, the numeric μ values are distributed in a broad range: 0.0051 D for B98 and 0.1728 D for HFB. Not surprisingly, here again HFB determines, probably incidentally, the extremum value for the μ value.

Table3.31: Calculated excess charge (in units of electron charge) on atoms and dipole moments (in Debye) of Co₃ trimer.

| method | m | q_1 | q_2 | q_3 | μ |
|-----------|-----|-----------|-----------|-----------|--------|
| B1LYP | 8 | -0.144537 | 0.289072 | -0.144534 | 0.0001 |
| B3LYP | 8 | -0.121604 | 0.243213 | -0.121609 | 0.0001 |
| B3P86 | 8 | -0.119827 | 0.239652 | -0.119826 | 0.0003 |
| B3PW91 | 8 | -0.094048 | 0.187872 | -0.093824 | 0.0137 |
| B971 | 8 | -0.120109 | 0.240230 | -0.120121 | 0.0016 |
| B972 | 8 | -0.091263 | 0.182526 | -0.091263 | 0.0000 |
| B98 | 8 | -0.114555 | 0.229116 | -0.114561 | 0.0004 |
| BHandH | 8 | -0.135364 | 0.270729 | -0.135364 | 0.0000 |
| BHandHLYP | 8 | -0.135942 | 0.271805 | -0.135863 | 0.0010 |
| HFB | 8 | -0.068695 | 0.137315 | -0.068619 | 0.0005 |
| MPW1PW91 | 8 | -0.079160 | 0.158003 | -0.078843 | 0.0145 |
| O3LYP | 8 | -0.099895 | 0.199796 | -0.099901 | 0.0009 |
| PBE1PBE | 8 | -0.116921 | 0.233828 | -0.116907 | 0.0007 |
| B1LYP | 10 | 0.013894 | -0.027789 | 0.013895 | 0.0788 |
| B3LYP | 10 | 0.010801 | -0.021603 | 0.010801 | 0.0525 |
| B3P86 | 10 | 0.009223 | -0.017803 | 0.008580 | 0.1361 |
| B3PW91 | 10 | 0.008662 | -0.017616 | 0.008954 | 0.1328 |
| B971 | 10 | 0.002091 | -0.003327 | 0.001236 | 0.0839 |
| B972 | 10 | 0.000675 | -0.001468 | 0.000793 | 0.1134 |
| B98 | 10 | 0.009839 | -0.019678 | 0.009839 | 0.0051 |
| BHandH | 10 | -0.001741 | 0.003482 | -0.001741 | 0.0143 |
| BHandHLYP | 10 | -0.002614 | 0.005284 | -0.002670 | 0.0519 |
| HFB | 10 | 0.013931 | -0.027650 | 0.013719 | 0.1728 |
| MPW1PW91 | 10 | 0.004903 | -0.009380 | 0.004477 | 0.1152 |
| O3LYP | 10 | 0.022138 | -0.044295 | 0.022157 | 0.1101 |
| PBE1PBE | 10 | 0.005352 | -0.011242 | 0.005890 | 0.1140 |

The HOMO and LUMO energies and HOMO-LUMO energy gaps E_g for Co₃ dimer are tabulated in Table 3.32. It can be easily noticed that the trend in other HOMO-LUMO tables does not change in this table; meaning that HFB and O3LYP again give the minimum values among all results, additionally BHandH and BHandHLYP give notably greater values than others. Except these methods, the results of other nine methods can be described as in a good manner. For $m = 8$ case, the results of latter group can be expressed as $E_g(\alpha) = 3.22 \pm 0.12$ Hartrees and $E_g(\beta) = 2.72 \pm 0.23$ Hartrees. These ranges are a bit larger for $m = 10$; $E_g(\alpha) = 2.91 \pm 0.13$ Hartrees and $E_g(\beta) = 3.24 \pm 0.33$ Hartrees. At the end of Co₃ trimer calculations, we can conclude that the results of $m = 8$ case seem more acceptable than the results of $m = 10$. The unexpected or doubtful situations that are mentioned above are generally about the multiplicity value 10, especially for values exhibited in Table 3.30.

Table3.32: HOMO and LUMO energies (in Hartrees), and HOMO-LUMO gap (E_g) energies (in eV) of the Co_3 trimer, calculated for the multiplicity, m ($2S + 1$), at which the total energy is minimum.

| method | m | HOMO(α) | LUMO(α) | $E_g(\alpha)$ | HOMO(β) | LUMO(β) | $E_g(\beta)$ |
|-----------|-----|------------------|------------------|---------------|-----------------|-----------------|--------------|
| B1LYP | 8 | -0.19403 | -0.07465 | 3.24849 | -0.18281 | -0.08683 | 2.61175 |
| B3LYP | 8 | -0.19695 | -0.08307 | 3.09883 | -0.18662 | -0.09491 | 2.49556 |
| B3P86 | 8 | -0.21808 | -0.10037 | 3.20305 | -0.20541 | -0.11420 | 2.48195 |
| B3PW91 | 8 | -0.19681 | -0.08015 | 3.17448 | -0.18388 | -0.09092 | 2.52957 |
| B971 | 8 | -0.19014 | -0.07569 | 3.11434 | -0.18223 | -0.08994 | 2.51134 |
| B972 | 8 | -0.18888 | -0.07189 | 3.18346 | -0.18294 | -0.09016 | 2.52467 |
| B98 | 8 | -0.19232 | -0.07613 | 3.16169 | -0.18384 | -0.08596 | 2.66345 |
| BHandH | 8 | -0.20682 | -0.04572 | 4.38375 | -0.19754 | -0.03962 | 4.29722 |
| BHandHLYP | 8 | -0.20295 | -0.04950 | 4.17559 | -0.19371 | -0.04293 | 4.10293 |
| HFB | 8 | -0.16259 | -0.08170 | 2.20113 | -0.13958 | -0.09685 | 1.16274 |
| MPW1PW91 | 8 | -0.19740 | -0.07466 | 3.33993 | -0.18488 | -0.07642 | 2.95135 |
| O3LYP | 8 | -0.18043 | -0.07800 | 2.78726 | -0.17037 | -0.10302 | 1.83269 |
| PBE1PBE | 8 | -0.19759 | -0.07512 | 3.33258 | -0.18444 | -0.08792 | 2.62644 |
| B1LYP | 10 | -0.17084 | -0.05896 | 3.04441 | -0.21324 | -0.09033 | 3.34455 |
| B3LYP | 10 | -0.17257 | -0.06886 | 2.82209 | -0.21865 | -0.10809 | 3.00849 |
| B3P86 | 10 | -0.19342 | -0.09114 | 2.78318 | -0.24005 | -0.12377 | 3.16414 |
| B3PW91 | 10 | -0.17392 | -0.07094 | 2.80223 | -0.21628 | -0.10050 | 3.15053 |
| B971 | 10 | -0.16570 | -0.06300 | 2.79461 | -0.21104 | -0.10395 | 2.91407 |
| B972 | 10 | -0.16259 | -0.05983 | 2.79624 | -0.21726 | -0.10560 | 3.03842 |
| B98 | 10 | -0.17050 | -0.06436 | 2.88822 | -0.21449 | -0.10226 | 3.05393 |
| BHandH | 10 | -0.20163 | -0.04480 | 4.26756 | -0.21568 | -0.04341 | 4.68770 |
| BHandHLYP | 10 | -0.22233 | -0.04411 | 4.84961 | -0.20843 | -0.04138 | 4.54566 |
| HFB | 10 | -0.13907 | -0.06770 | 1.94208 | -0.14890 | -0.10631 | 1.15893 |
| MPW1PW91 | 10 | -0.17780 | -0.06633 | 3.03325 | -0.21766 | -0.08626 | 3.57558 |
| O3LYP | 10 | -0.15564 | -0.06754 | 2.39732 | -0.19639 | -0.11801 | 2.13283 |
| PBE1PBE | 10 | -0.17642 | -0.06643 | 2.99298 | -0.21711 | -0.08574 | 3.57476 |

3.3.2 Sm_3 Trimer Calculations

Only $m = 19$ and $m = 21$ calculations give results, even no results for MPW1PW91, BHandH, and BHandHLYP methods. In spite of too few data there is not an accuracy about minimum energy multiplicity. HFB and O3LYP indicate the minimum energy at $m = 19$, other seven methods at $m = 21$. Since Sm atom has six unpaired electrons, the expected multiplicity value is 19, whereas most of the methods failed to conclude the calculation at this multiplicity. Table 3.33 demonstrates the all attained results of minimum energy values of Sm_3 . The starred values in the energy tables indicate the minimum energy values through this study, however in the previous table except O3LYP, all methods give only one result, so

these minimum values are not reliable to accept them exact minimum points. By comparing to the previous total energy tables, it is clearly seen that Sm_3 trimer calculations are the most difficult and challenging ones, since even Sm atom is an extensive one with 62 electrons, three Sm atoms not easy to handle.

Table3.33: Total energies, E_m , in Hartrees, for Sm_3 trimer for different multiplicities, m ($2S + 1$). The starred ones show the lowest energy. ‘nc’ indicates a ‘not completed’ calculation due to a non-convergent- or confused-SCF process.

| method | $-E_{19}$ | $-E_{21}$ |
|-----------|-----------|-----------|
| B1LYP | nc | 243.7079* |
| B3LYP | nc | 244.2362* |
| B3P86 | nc | 245.3442* |
| B3PW91 | nc | 244.3930* |
| B971 | nc | 244.0959* |
| B972 | nc | 244.3823* |
| B98 | nc | 244.1446* |
| BHandH | nc | nc |
| BHandHLYP | nc | nc |
| HFB | 243.8163* | nc |
| MPW1PW91 | nc | nc |
| O3LYP | 244.9254* | 244.8975 |
| PBE1PBE | nc | 243.9542* |

The spectroscopic constants of Sm_3 trimer are demonstrated in Table 3.34, which are optimized interatomic separations, bond angle, and vibrational frequencies. Because of the lack of information about Sm_3 trimer, we prefer to give all attained results. The corresponding calculations of expected multiplicity value for Sm_3 conclude only for HFB and O3LYP methods. Although their bond lengths are very close each other around 4.7 Å, bond angles are 60.1 and 126.7 °, different from each other. The vibrational frequencies of this trimer are given nearly the same by HFB method, but no significant relation for O3LYP. The information about $m = 19$ case for Sm_3 is not enough to discuss on it. If we continue from the second part of the same table, where $m = 21$ cases are demonstrated, we can see that only method that breaks the general tendency is B972. Except B972, other methods give separation values R_{12} and R_{23} are in the range of 4.19 - 4.30 Å. The bond angle changes from 111 ° to 118 ° and we cannot talk about symmetry for the geometrical structure of Sm_3 trimers. The only thing, remarkable about frequencies is that at least two of them are comparatively close two each other and the remaining one is smaller than these two. These three frequency values are

roughly centered around 12, 53, and 57 cm^{-1} .

Table3.34: Bond lengths R_{12} and R_{23} (\AA), bond angle θ_{123} (deg), and vibrational frequencies ω_n (cm^{-1}) of Sm_3 trimer. For the notation used, see Fig. 3.9.

| method | m | R_{12} | R_{23} | θ_{123} | ω_1 | ω_2 | ω_3 |
|-----------|-----|----------|----------|----------------|------------|------------|------------|
| HFB | 19 | 4.7886 | 4.7956 | 60.0690 | 33.1440 | 33.6374 | 34.4114 |
| O3LYP | 19 | 4.7378 | 4.7272 | 126.7256 | 5.7828 | 32.3123 | 45.3594 |
| B1LYP | 21 | 4.2668 | 4.2696 | 113.7498 | 11.4360 | 49.9752 | 57.3797 |
| B3LYP | 21 | 4.2477 | 4.2490 | 111.8027 | 15.3370 | 51.9261 | 57.9838 |
| B3P86 | 21 | 4.2110 | 4.1936 | 113.6510 | 9.3339 | 54.7454 | 59.5442 |
| B3PW91 | 21 | 4.2336 | 4.2522 | 117.6514 | 12.5195 | 53.5626 | 57.8730 |
| B971 | 21 | 4.2662 | 4.2396 | 117.7272 | 13.9140 | 55.8347 | 59.1260 |
| B972 | 21 | 3.8016 | 3.9382 | 69.9648 | 31.4646 | 44.3272 | 70.8001 |
| B98 | 21 | 4.2689 | 4.2319 | 118.4543 | 12.3124 | 54.1845 | 57.7793 |
| BHandH | 21 | – | – | – | – | – | – |
| BHandHLYP | 21 | – | – | – | – | – | – |
| HFB | 21 | – | – | – | – | – | – |
| MPW1PW91 | 21 | – | – | – | – | – | – |
| O3LYP | 21 | 4.2917 | 4.3024 | 115.4995 | 14.1583 | 49.7005 | 56.4101 |
| PBE1PBE | 21 | 4.2255 | 4.2512 | 117.9038 | 14.3396 | 53.7545 | 59.2637 |

According to Table 3.35, there is no symmetry between the charges of the Sm_3 trimer. The dipole moment values for $m = 19$ are not notable, however for $m = 21$ they seem accurate and close to the 1.6 Debye with the exception of B972 methods which gives 1.3 Debye approximately.

It is interesting to note in HOMO–LUMO table of Sm_3 (Table 3.36) that for $m = 19$ case only methods HFB and O3LYP give results which method were gain a fame by generating exceptional situations. It can be more meaningful to talk about only $m = 21$ case for this table. The methods BHandH, BHandHLYP, HFB, and MPW1PW91 have not been completed the calculations as seen in table. O3LYP gives the minimum value for $E_g(\alpha)$ as 0.90 Hartrees where the others are averaged around 1.30 Hartrees. There is an exceptional case for B972 also, for the first time in HOMO–LUMO tables, it gives $E_g(\beta)$ value minimum as 0.84 Hartrees where the other values are around 1.50 Hartrees.

Table3.35: Calculated excess charge (in units of electron charge) on atoms and dipole moments (in Debye) of Sm₃ trimer.

| method | m | q_1 | q_2 | q_3 | μ |
|-----------|-----|-----------|----------|-----------|--------|
| HFB | 19 | -0.000199 | 0.000331 | -0.000132 | 0.0015 |
| O3LYP | 19 | -0.004715 | 0.005272 | -0.000558 | 0.1981 |
| B1LYP | 21 | -0.039669 | 0.077510 | -0.037841 | 1.6431 |
| B3LYP | 21 | -0.037984 | 0.077902 | -0.039918 | 1.5683 |
| B3P86 | 21 | -0.040334 | 0.086364 | -0.046030 | 1.6384 |
| B3PW91 | 21 | -0.046829 | 0.087904 | -0.041075 | 1.6758 |
| B971 | 21 | -0.024885 | 0.057284 | -0.032400 | 1.6228 |
| B972 | 21 | -0.041501 | 0.144653 | -0.103152 | 1.3033 |
| B98 | 21 | -0.027456 | 0.063010 | -0.035554 | 1.5795 |
| BHandH | 21 | – | – | – | – |
| BHandHLYP | 21 | – | – | – | – |
| HFB | 21 | – | – | – | – |
| MPW1PW91 | 21 | – | – | – | – |
| O3LYP | 21 | -0.039062 | 0.077230 | -0.038168 | 1.6493 |
| PBE1PBE | 21 | -0.044694 | 0.081461 | -0.036767 | 1.7668 |

3.3.3 SmCo₂ Trimer Calculations

The total energy and corresponding multiplicity values of SmCo₂ are demonstrated in Table 3.37. By a short glimpse, an interesting situation take attention, that is the discrimination of the corresponding multiplicity values for minimum energy. There are two values, $m = 3$ and $m = 11$ and for the first time given multiplicities are not consecutive values. As mentioned before, Sm atom has 6 unpaired electrons and Co atom has 3, so to experience the $m = 3$ case three of these atom has to be tied as remaining only two unpaired electrons, this situation seems not so feasible. Unfortunately, nearly half of our methods give this nonsense value for multiplicity, which are B3LYP, B3P86, B3PW91, B972, BHandH, HFB, and O3LYP. Besides, the results of $m = 11$ case are plausible as will be discussed in a short time. Another interesting thing is that the difference between energies are very small for all possible multiplicity values. For example, all energy values from $-E_1$ to $-E_{19}$ fluctuate between the values 370.9404-371.3720 Hartrees for B1LYP, the difference is 0.4316 Hartrees and another example PBE1PBE values from 371.0343 to 371.5420 Hartrees, the difference is 0.5077 Hartrees. If we closely look to Table 3.37 to catch any pattern among energy values, the only thing we will obtain is a clutter.

In Table 3.38 and Table 3.39, the spectroscopic constants of SmCo₂ are displayed for both

Table3.36: HOMO and LUMO energies (in Hartrees), and HOMO-LUMO gap (E_g) energies (in eV) of the Sm_3 trimer, calculated for the multiplicity, m ($2S+1$), at which the total energy is minimum.

| method | m | HOMO(α) | LUMO(α) | $E_g(\alpha)$ | HOMO(β) | LUMO(β) | $E_g(\beta)$ |
|-----------|-----|------------------|------------------|---------------|-----------------|-----------------|--------------|
| HFB | 19 | -0.07445 | -0.03798 | 0.99240 | -0.06394 | 0.00297 | 1.82071 |
| O3LYP | 19 | -0.08784 | -0.02207 | 1.78969 | -0.07916 | -0.01133 | 1.84575 |
| B1LYP | 21 | -0.04760 | 0.00447 | 1.41690 | -0.09871 | -0.04145 | 1.55812 |
| B3LYP | 21 | -0.04947 | -0.00501 | 1.20982 | -0.10075 | -0.04911 | 1.40520 |
| B3P86 | 21 | -0.07490 | -0.03013 | 1.21825 | -0.12144 | -0.06662 | 1.49173 |
| B3PW91 | 21 | -0.05624 | -0.01152 | 1.21689 | -0.10319 | -0.04778 | 1.50778 |
| B971 | 21 | -0.05095 | -0.00279 | 1.31050 | -0.10044 | -0.05010 | 1.36982 |
| B972 | 21 | -0.06333 | -0.01399 | 1.34261 | -0.08840 | -0.05746 | 0.84192 |
| B98 | 21 | -0.05260 | -0.00322 | 1.34370 | -0.10164 | -0.04920 | 1.42696 |
| BHandH | 21 | - | - | - | - | - | - |
| BHandHLYP | 21 | - | - | - | - | - | - |
| HFB | 21 | - | - | - | - | - | - |
| MPW1PW91 | 21 | - | - | - | - | - | - |
| O3LYP | 21 | -0.04128 | -0.00819 | 0.90042 | -0.08514 | -0.04290 | 1.14941 |
| PBE1PBE | 21 | -0.05806 | -0.00559 | 1.42778 | -0.10415 | -0.04371 | 1.64466 |

$m = 3$ and $m = 11$ cases. The $m = 3$ case, only the seven methods are take into account, which gives the minimum energies at this value for the reasons mentioned above. Despite all disalignments, bond lengths R_{12} and R_{23} are in accordance with each other. The two values are already equal to each other for all methods and varies in a range 2.93-3.04 Å can be regarded as close to each other among all methods. Except BHandH and B3LYP methods, they show nearly linear geometric configurations, even B3P86 and B3PW91 gives 180°. O3LYP method disturbs the general accuracy of vibrational frequency by giving three frequency values around 109, 119, and 146 cm^{-1} . Other methods seen as coherent with the frequency values around 23, 116, and 150 cm^{-1} . The charge separation and dipole moment values, which can be checked from Table 3.39, are compatible with the results of Table 3.38. It has to be point out at that the unfeasible situation about $m = 3$ multiplicity value of SmCo_2 is making compact bonds with this linearly geometric structure.

The results of more acceptable multiplicity $m = 11$ from the same tables indicates two different structure, one is very close to linear geometric configurations and the other gives bond angle around 163°. The latter group consists of B1LYP, B3LYP, B3P86, B3PW91, B971, and B98. Although there is a significant discrimination about bond angle among the methods, other all constants, bond lengths, vibrational frequencies, and excess charges are in almost perfect agreement. The bond lengths might be described as $R_i = 2.98 \pm 0.06$ Å and vibrational frequencies are very close to average values 23, 113, and 147 cm^{-1} . In addition

Table 3.37: Total energies, E_m , in Hartrees, for SmCo₂ trimer for different multiplicities, m ($2S + 1$).

| method | $-E_1$ | $-E_3$ | $-E_5$ | $-E_7$ | $-E_9$ | $-E_{11}$ | $-E_{13}$ | $-E_{15}$ | $-E_{17}$ | $-E_{19}$ |
|-----------|----------|-----------|----------|----------|----------|-----------|-----------|-----------|-----------|-----------|
| BILYP | 370.9404 | 371.3683 | 371.2813 | 371.3110 | 371.3404 | 371.3720* | 371.3630 | 371.3094 | 371.2319 | 371.0836 |
| B3LYP | 371.3499 | 371.7761* | 371.7239 | 371.7503 | 371.7435 | 371.7748 | 371.7667 | 371.7103 | 371.6241 | 371.4695 |
| B3P86 | 372.4809 | 372.9115* | 372.8918 | 372.8843 | 372.8536 | 372.9094 | 372.9061 | 372.8507 | 372.7723 | 372.6373 |
| B3PW91 | 371.4313 | 371.8854* | 371.8652 | 371.8076 | 371.8325 | 371.8832 | 371.8802 | 371.8279 | 371.7552 | 371.6144 |
| B971 | 371.1997 | 371.5868 | 371.5587 | 371.5740 | 371.5557 | 371.5934* | 371.5784 | 371.5089 | 371.4350 | 371.2719 |
| B972 | 371.6799 | 372.0979* | 372.0664 | 372.0777 | 372.0660 | 372.0976 | 372.0812 | 372.0187 | 371.8881 | 371.7558 |
| B98 | 371.2790 | 371.6831 | 371.6630 | 371.6715 | 371.6438 | 371.6913* | 371.6762 | 371.6087 | 371.5373 | 371.3780 |
| BHandH | 369.0493 | 369.7590* | 369.7386 | 369.6944 | 369.6715 | 369.7573 | 369.7536 | 369.7200 | 369.6666 | 369.5323 |
| BHandHLYP | 370.4053 | 370.8037 | 370.6520 | 370.7347 | 370.7585 | 370.8192* | 370.8075 | 370.7501 | 370.6895 | 370.5791 |
| HFB | nc | 370.2119* | 370.1849 | 370.2081 | 370.1715 | 370.2064 | 370.2085 | 370.1714 | 370.0983 | 369.9873 |
| MPW1PW91 | 371.2493 | 371.7319 | 371.6793 | 371.7115 | 371.7013 | 371.7332* | 371.7309 | 371.6512 | 371.6176 | 371.4784 |
| O3LYP | 371.8877 | 372.3369* | 372.3126 | 372.2690 | 372.2878 | 372.3338 | 372.3273 | 372.2664 | 372.1758 | 372.0207 |
| PBE1PBE | 371.0343 | 371.5413 | 371.4987 | 371.5193 | 371.5081 | 371.5420* | 371.5399 | 371.3687 | 371.4264 | 371.2839 |

charges match the equality $2|q_1| = 2|q_3| = q_2$ perfectly, even their numerical values are so close to each other, might be averaged at $0.6|e|$ for $|q_1|$ and so $|q_3|$. The discrimination is also observed in dipole moment values, as expected; the structures close to linear geometry give μ nearly zero and the others give approximately $1.5|e|$. Only PBE1PBE is an exception here, with the value $0.6|e|$.

Table3.38: Bond lengths R_{12} and R_{23} (Å), bond angle θ_{123} (deg), and vibrational frequencies ω_n (cm^{-1}) of SmCo_2 trimer. For the notation used, see Fig. 3.9.

| method | m | R_{12} | R_{23} | θ_{123} | ω_1 | ω_2 | ω_3 |
|-----------|-----|----------|----------|----------------|------------|------------|------------|
| B3LYP | 3 | 2.9331 | 2.9331 | 161.1631 | 17.5528 | 116.3024 | 149.7179 |
| B3P86 | 3 | 2.9266 | 2.9266 | 180.0000 | 20.4975 | 118.8106 | 155.7995 |
| B3PW91 | 3 | 2.9452 | 2.9452 | 180.0000 | 23.0975 | 116.8782 | 153.0267 |
| B972 | 3 | 2.9434 | 2.9434 | 179.9705 | 16.7771 | 112.6143 | 147.2985 |
| BHandH | 3 | 2.9317 | 2.9317 | 148.4707 | 31.3149 | 118.1967 | 147.4468 |
| HFB | 3 | 3.0368 | 3.0382 | 179.8909 | 32.3718 | 107.4464 | 139.8954 |
| O3LYP | 3 | 2.9686 | 2.9670 | 174.2533 | 108.7929 | 118.5958 | 146.2946 |
| B1LYP | 11 | 2.9752 | 2.9752 | 162.9116 | 18.4599 | 113.6248 | 146.5105 |
| B3LYP | 11 | 2.9542 | 2.9542 | 162.1995 | 18.9965 | 115.8427 | 149.5719 |
| B3P86 | 11 | 2.9186 | 2.9186 | 163.5896 | 20.4025 | 118.6954 | 154.0548 |
| B3PW91 | 11 | 2.9392 | 2.9392 | 165.4604 | 17.6081 | 116.3699 | 151.2471 |
| B971 | 11 | 2.9653 | 2.9653 | 163.0069 | 24.5386 | 113.9750 | 147.7167 |
| B972 | 11 | 2.9645 | 2.9646 | 179.9848 | 32.7519 | 112.9972 | 147.8264 |
| B98 | 11 | 2.9660 | 2.9660 | 163.2708 | 24.4891 | 113.5142 | 147.0553 |
| BHandH | 11 | 2.9454 | 2.9454 | 180.0000 | 13.8876 | 111.8542 | 147.2085 |
| BHandHLYP | 11 | 3.0413 | 3.0413 | 179.9766 | 19.4891 | 106.3679 | 138.8708 |
| HFB | 11 | 3.0283 | 3.0324 | 179.9553 | 17.3908 | 108.9150 | 141.1502 |
| MPW1PW91 | 11 | 2.9515 | 2.9516 | 179.9731 | 31.4940 | 114.1198 | 149.7423 |
| O3LYP | 11 | 2.9779 | 2.9779 | 179.9968 | 28.9573 | 110.6921 | 144.6396 |
| PBE1PBE | 11 | 2.9521 | 2.9521 | 180.0000 | 35.5184 | 113.7510 | 149.1385 |

The general tendency about HOMO–LUMO tables has not been broken for SmCo_2 trimer which tabulated in Table 3.40. That means HFB and O3LYP give smaller values for $E_g(\alpha)$ and $E_g(\beta)$ and half and half methods BHandH and BHandHLYP methods give greater values in comparison to other methods. To exemplify this, we can notify the results for $m = 11$ case of HFB method as $E_g(\alpha) = 1.69$ Hartrees and $E_g(\beta) = 0.91$ Hartrees and for BHandH method as $E_g(\alpha) = 3.98$ Hartrees and $E_g(\beta) = 3.83$ Hartrees. Other methods are average around $E_g(\alpha) = 2.90$ Hartrees and $E_g(\beta) = 2.75$ Hartrees.

Table3.39: Calculated excess charge (in units of electron charge) on atoms and dipole moments (in Debye) of SmCo₂ trimer.

| method | m | q_1 | q_2 | q_3 | μ |
|-----------|-----|-----------|----------|-----------|--------|
| B3LYP | 3 | -0.589815 | 1.179631 | -0.589815 | 1.8171 |
| B3P86 | 3 | -0.595703 | 1.191407 | -0.595703 | 0.0000 |
| B3PW91 | 3 | -0.598929 | 1.197858 | -0.598929 | 0.0000 |
| B972 | 3 | -0.599011 | 1.198022 | -0.599011 | 0.0029 |
| BHandH | 3 | -0.594011 | 1.188022 | -0.594011 | 2.8019 |
| HFB | 3 | -0.570854 | 1.141626 | -0.570772 | 0.0111 |
| O3LYP | 3 | -0.594475 | 1.187688 | -0.593214 | 0.5286 |
| B1LYP | 11 | -0.601043 | 1.202085 | -0.601042 | 1.6473 |
| B3LYP | 11 | -0.598515 | 1.197035 | -0.598519 | 1.7165 |
| B3P86 | 11 | -0.602447 | 1.204895 | -0.602448 | 1.5750 |
| B3PW91 | 11 | -0.606147 | 1.212293 | -0.606147 | 1.3890 |
| B971 | 11 | -0.598255 | 1.196510 | -0.598255 | 1.5898 |
| B972 | 11 | -0.611554 | 1.223105 | -0.611551 | 0.0015 |
| B98 | 11 | -0.602870 | 1.205739 | -0.602870 | 1.5761 |
| BHandH | 11 | -0.600931 | 1.201863 | -0.600931 | 0.0000 |
| BHandHLYP | 11 | -0.611686 | 1.223373 | -0.611686 | 0.0023 |
| HFB | 11 | -0.592752 | 1.185177 | -0.592425 | 0.0116 |
| MPW1PW91 | 11 | -0.608873 | 1.217731 | -0.608859 | 0.0027 |
| O3LYP | 11 | -0.608725 | 1.217449 | -0.608724 | 0.0003 |
| PBE1PBE | 11 | -0.603623 | 1.207247 | -0.603623 | 0.5558 |

3.3.4 Sm₂Co Trimer Calculations

The last part of this study is allocated to the Sm₂Co trimer calculations. In Table 3.41, total energy values are given and seen that minimum energies are given at two different multiplicity values $m = 12$ and $m = 16$, intensively at latter one. B3P86, B3PW91, O3LYP, and PBE1PBE give minimum at $m = 12$, however the values are very close to each other, even the difference are about 0.0024 Hartrees of the first three and 0.0003 Hartrees for the last one. There cannot be caught any pattern, energy values are fluctuated for all possible multiplicity values, and additionally too many missing data which make evaluation harder. The missing results are not surprising for us since this trimer includes two Sm atoms. Even the dimer of Sm atom failed to give energy values completely, can be seen in Table 3.26.

Because of two values of multiplicity, we arrange the following tables as including the both of them. As we start from $m = 12$ case, all results seen in accordance with each other. All the bond angles are around 74° and the vibrational frequency values can be averaged around 56, 77, and 112cm^{-1} . For $m = 16$, situation is not that simple, even three groups of angle, means that of geometrical structure. The first group consist of B3P86, B3PW91, B971, O3LYP, and

Table3.40: HOMO and LUMO energies (in Hartrees), and HOMO-LUMO gap (E_g) energies (in eV) of the SmCo₂ trimer, calculated for the multiplicity, m ($2S + 1$), at which the total energy is minimum.

| method | m | HOMO(α) | LUMO(α) | $E_g(\alpha)$ | HOMO(β) | LUMO(β) | $E_g(\beta)$ |
|-----------|-----|------------------|------------------|---------------|-----------------|-----------------|--------------|
| B3LYP | 3 | -0.15811 | -0.06810 | 2.44930 | -0.16732 | -0.06344 | 2.82672 |
| B3P86 | 3 | -0.17819 | -0.08053 | 2.65746 | -0.18914 | -0.07622 | 3.07271 |
| B3PW91 | 3 | -0.15750 | -0.05796 | 2.70862 | -0.16859 | -0.05425 | 3.11135 |
| B972 | 3 | -0.15508 | -0.05484 | 2.72767 | -0.15999 | -0.05246 | 2.92604 |
| BHandH | 3 | -0.17482 | -0.03257 | 3.87082 | -0.18101 | -0.03165 | 4.06429 |
| HFB | 3 | -0.09318 | -0.06240 | 0.83757 | -0.13313 | -0.05303 | 2.17963 |
| O3LYP | 3 | -0.14157 | -0.06182 | 2.17011 | -0.15096 | -0.05884 | 2.50671 |
| B1LYP | 11 | -0.16764 | -0.06195 | 2.87597 | -0.15470 | -0.05368 | 2.74889 |
| B3LYP | 11 | -0.17009 | -0.07061 | 2.70699 | -0.15669 | -0.06231 | 2.56821 |
| B3P86 | 11 | -0.19115 | -0.08261 | 2.95352 | -0.17504 | -0.07499 | 2.72250 |
| B3PW91 | 11 | -0.17049 | -0.06064 | 2.98917 | -0.15427 | -0.05290 | 2.75842 |
| B971 | 11 | -0.16556 | -0.06471 | 2.74427 | -0.15318 | -0.05454 | 2.68413 |
| B972 | 11 | -0.16363 | -0.05861 | 2.85774 | -0.15215 | -0.04852 | 2.81992 |
| B98 | 11 | -0.16801 | -0.06453 | 2.81583 | -0.15462 | -0.05405 | 2.73665 |
| BHandH | 11 | -0.18413 | -0.03791 | 3.97885 | -0.17098 | -0.03033 | 3.82728 |
| BHandHLYP | 11 | -0.18326 | -0.03974 | 3.90538 | -0.17066 | -0.03244 | 3.76116 |
| HFB | 11 | -0.13255 | -0.07053 | 1.68765 | -0.08983 | -0.05650 | 0.90696 |
| MPW1PW91 | 11 | -0.17268 | -0.05603 | 3.17421 | -0.15648 | -0.04783 | 2.95652 |
| O3LYP | 11 | -0.15313 | -0.06524 | 2.39161 | -0.13865 | -0.05657 | 2.23351 |
| PBE1PBE | 11 | -0.17191 | -0.05858 | 3.08387 | -0.15638 | -0.04978 | 2.90073 |

PBE1PBE methods corresponding angles are approximately 74° , reflects isosceles triangle geometric structure with equal R_{12} and R_{23} values. The corresponding frequency values are averaged around 62, 73, and 104 cm^{-1} . BHandH and MPW1PW91 constitute the second group that the corresponding angles are around 94 and 92° and the bond lengths are equal to each other for each method. The geometric structure seems to be close to isosceles right triangle. There is not a similarity between the frequency values ω_n for these two methods. The last group consists of six methods, B1LYP, B3LYP, B972, B98, BHandHLYP, and HFB, whose angle can be average around 177° seems close the linear structure but can not be acceptable as so. The bond lengths are equal to each other similar to the other groups. the values of HFB is a bit smaller than others, so except it frequency values of other methods are around 27, 56, and 100 cm^{-1} .

There is no need to say much about excess charge and dipole moments of Sm₂Co trimer. All charge values seems symmetric for $m = 12$, so they can fulfill the mentioned equality $2|q_1| = 2|q_3| = q_2$. Although this is not the case for $m = 12$, their dipole moments are in accordance with each other. There are two groups for dipole moments at multiplicity value 16. One of them average about 3.80 Hartrees and the other group is about 0.17 Hartrees. This

Table 3.41: Total energies, E_m , in Hartrees, for Sm_2Co trimer for different multiplicities, m ($2S + 1$).

| method | $-E_2$ | $-E_4$ | $-E_6$ | $-E_8$ | $-E_{10}$ | $-E_{12}$ | $-E_{14}$ | $-E_{16}$ | $-E_{18}$ | $-E_{20}$ | $-E_{22}$ | $-E_{24}$ |
|-----------|----------|----------|----------|----------|-----------|-----------|-----------|-----------|-----------|-----------|-----------|-----------|
| BILYP | nc | nc | 307.3820 | 307.3734 | 307.5552 | 307.5601 | 307.5523 | 307.5624* | 307.5323 | 307.4605 | 307.3784 | 307.0865 |
| B3LYP | nc | 307.7121 | 307.9101 | 307.9813 | 308.0214 | 308.0275 | 308.0043 | 308.0281* | 307.9994 | 307.9300 | 307.8385 | 307.5513 |
| B3P86 | 308.8220 | 309.1482 | 309.0449 | nc | nc | 309.1517* | 309.1374 | 309.1493 | 309.0756 | 309.0660 | 308.9809 | 308.7021 |
| B3PW91 | 307.7418 | 307.9437 | nc | 308.1239 | nc | 308.1614* | 308.1476 | 308.1590 | 308.1380 | 308.0806 | nc | 307.7271 |
| B971 | nc | 307.4331 | 307.7423 | 307.8121 | 307.8582 | 307.8624 | 307.8394 | 307.8648* | nc | 307.7706 | 307.6494 | 307.3577 |
| B972 | 308.0024 | 307.8218 | nc | 308.2037 | 308.2475 | 308.2530 | 308.2433 | 308.2547* | 308.2249 | 308.1544 | 308.0260 | 307.7352 |
| B98 | nc | nc | 307.8209 | 307.8919 | 307.9350 | 307.9401 | 307.9176 | 307.9420* | 307.9149 | 307.8336 | 307.7259 | 307.4439 |
| BHandH | nc | nc | nc | 305.4312 | 305.6189 | 305.7035 | 305.6746 | 305.7107* | 305.6688 | 305.6405 | 305.5412 | 305.3087 |
| BHandHLYP | nc | nc | 306.4881 | 306.4552 | 306.6448 | 306.6041 | 306.6453 | 306.6562* | 306.5205 | 306.5799 | 306.4869 | 306.2436 |
| HFB | 307.0138 | 306.8543 | 306.9288 | 306.9803 | 307.0095 | 307.0157 | 307.0051 | 307.0163* | 306.9895 | nc | nc | nc |
| MPW1PW91 | nc | 307.7370 | 307.8477 | nc | 307.9257 | nc | 307.9279 | 307.9381* | nc | 307.8640 | 307.7892 | 307.5190 |
| O3LYP | 308.6259 | 308.3850 | 308.5235 | 308.5933 | 308.6275 | 308.6350* | 308.6196 | 308.6327 | 308.6116 | 308.5434 | 308.4483 | 308.1325 |
| PBE1PBE | nc | 307.4739 | 307.6745 | 307.7317 | 307.7556 | 307.7695* | 307.7558 | 307.7692 | 307.7286 | 307.6919 | 307.6012 | 307.3458 |

Table 3.42: Bond lengths R_{12} and R_{23} (Å), bond angle θ_{123} (deg), and vibrational frequencies ω_n (cm^{-1}) of Sm_2Co trimer. For the notation used, see Fig. 3.9.

| method | m | R_{12} | R_{23} | θ_{123} | ω_1 | ω_2 | ω_3 |
|-----------|-----|----------|----------|----------------|------------|------------|------------|
| B3P86 | 12 | 3.0963 | 3.0994 | 74.5181 | 60.1835 | 78.8503 | 117.1174 |
| B3PW91 | 12 | 3.1245 | 3.1245 | 74.3311 | 52.9945 | 77.9446 | 113.8776 |
| O3LYP | 12 | 3.1705 | 3.1696 | 74.3520 | 59.0937 | 74.5383 | 106.2918 |
| PBE1PBE | 12 | 3.1119 | 3.2255 | 74.4213 | 54.6425 | 78.5844 | 111.8161 |
| B1LYP | 16 | 3.2014 | 3.2014 | 178.4943 | 27.4209 | 56.1642 | 100.9899 |
| B3LYP | 16 | 3.1809 | 3.1808 | 178.4454 | 28.0331 | 57.5204 | 102.3097 |
| B3P86 | 16 | 3.1634 | 3.1634 | 74.2914 | 62.1771 | 75.4311 | 111.4082 |
| B3PW91 | 16 | 3.1844 | 3.1844 | 74.4633 | 59.3317 | 74.1704 | 106.6047 |
| B971 | 16 | 3.2368 | 3.2368 | 73.6098 | 67.9045 | 73.6846 | 103.9630 |
| B972 | 16 | 3.1973 | 3.1973 | 177.1633 | 26.0410 | 56.4952 | 100.9982 |
| B98 | 16 | 3.1957 | 3.1957 | 174.3087 | 26.7266 | 58.2751 | 106.2278 |
| BHandH | 16 | 3.0301 | 3.0301 | 94.0566 | 34.7092 | 69.8729 | 110.8845 |
| BHandHLYP | 16 | 3.2544 | 3.2544 | 179.0175 | 24.9222 | 52.3997 | 98.5364 |
| HFB | 16 | 3.3108 | 3.3108 | 175.1862 | 20.9194 | 52.1416 | 81.7126 |
| MPW1PW91 | 16 | 3.0778 | 3.0778 | 92.0486 | 27.1021 | 39.5214 | 112.6796 |
| O3LYP | 16 | 3.2529 | 3.2529 | 73.9851 | 66.4491 | 71.6462 | 98.0373 |
| PBE1PBE | 16 | 3.1925 | 3.1925 | 73.8788 | 58.8473 | 75.3725 | 106.0738 |

discrimination is about the geometry of the trimers, can be observed clearly when the methods are compared with the angle discrimination of Table 3.42.

From Table 3.44 we can investigate the HOMO–LUMO energies and energy gaps of Sm_2Co trimer for multiplicity values 12 and 16. There are four methods given for $m = 12$ case which are B3P86, B3PW91, O3LYP, and PBE1PBE. The O3LYP known by giving smaller energy gap values from previous similar discussions, here is the same situation however the difference is not so remarkable. For $m = 16$ case BHandH and BHandHLYP give greater values and HFB again gives the smaller values as expected, however for the time being O3LYP does not show significant difference from other methods. B3LYP, B972, and B98 also give smaller values, close to O3LYP, can be defined as around 1.85 Hartrees for $E_g(\alpha)$, where the average of the other methods is 2.18 Hartrees. A similar incident exist for $E_g(\beta)$, HFB significantly small, O3LYP and B971 also smaller but the difference is not so exact. BHandH and BHandHLYP demonstrate greater values as usual. The average of the remaining methods is 1.56 Hartrees.

Table3.43: Calculated excess charge (in units of electron charge) on atoms and dipole moments (in Debye) of Sm₂Co trimer.

| method | m | q_1 | q_2 | q_3 | μ |
|-----------|-----|----------|-----------|----------|--------|
| B3P86 | 12 | 0.403150 | -0.804128 | 0.400978 | 3.7349 |
| B3PW91 | 12 | 0.393664 | -0.787327 | 0.393664 | 3.7048 |
| O3LYP | 12 | 0.406509 | -0.805947 | 0.399437 | 3.8616 |
| PBE1PBE | 12 | 0.429600 | -0.786355 | 0.356755 | 3.8478 |
| B1LYP | 16 | 0.446890 | -0.893781 | 0.446891 | 0.0870 |
| B3LYP | 16 | 0.448514 | -0.897070 | 0.448556 | 0.0885 |
| B3P86 | 16 | 0.390296 | -0.780592 | 0.390296 | 3.8876 |
| B3PW91 | 16 | 0.384138 | -0.768275 | 0.384138 | 3.8481 |
| B971 | 16 | 0.384868 | -0.769736 | 0.384868 | 3.8910 |
| B972 | 16 | 0.427848 | -0.855696 | 0.427848 | 0.1795 |
| B98 | 16 | 0.439240 | -0.878480 | 0.439240 | 0.3130 |
| BHandH | 16 | 0.455413 | -0.910825 | 0.455413 | 3.5345 |
| BHandHLYP | 16 | 0.441154 | -0.882307 | 0.441154 | 0.0636 |
| HFB | 16 | 0.429272 | -0.858540 | 0.429268 | 0.2944 |
| MPW1PW91 | 16 | 0.422975 | -0.845954 | 0.422979 | 3.4561 |
| O3LYP | 16 | 0.382235 | -0.764471 | 0.382236 | 3.8888 |
| PBE1PBE | 16 | 0.389958 | -0.779916 | 0.389957 | 3.9040 |

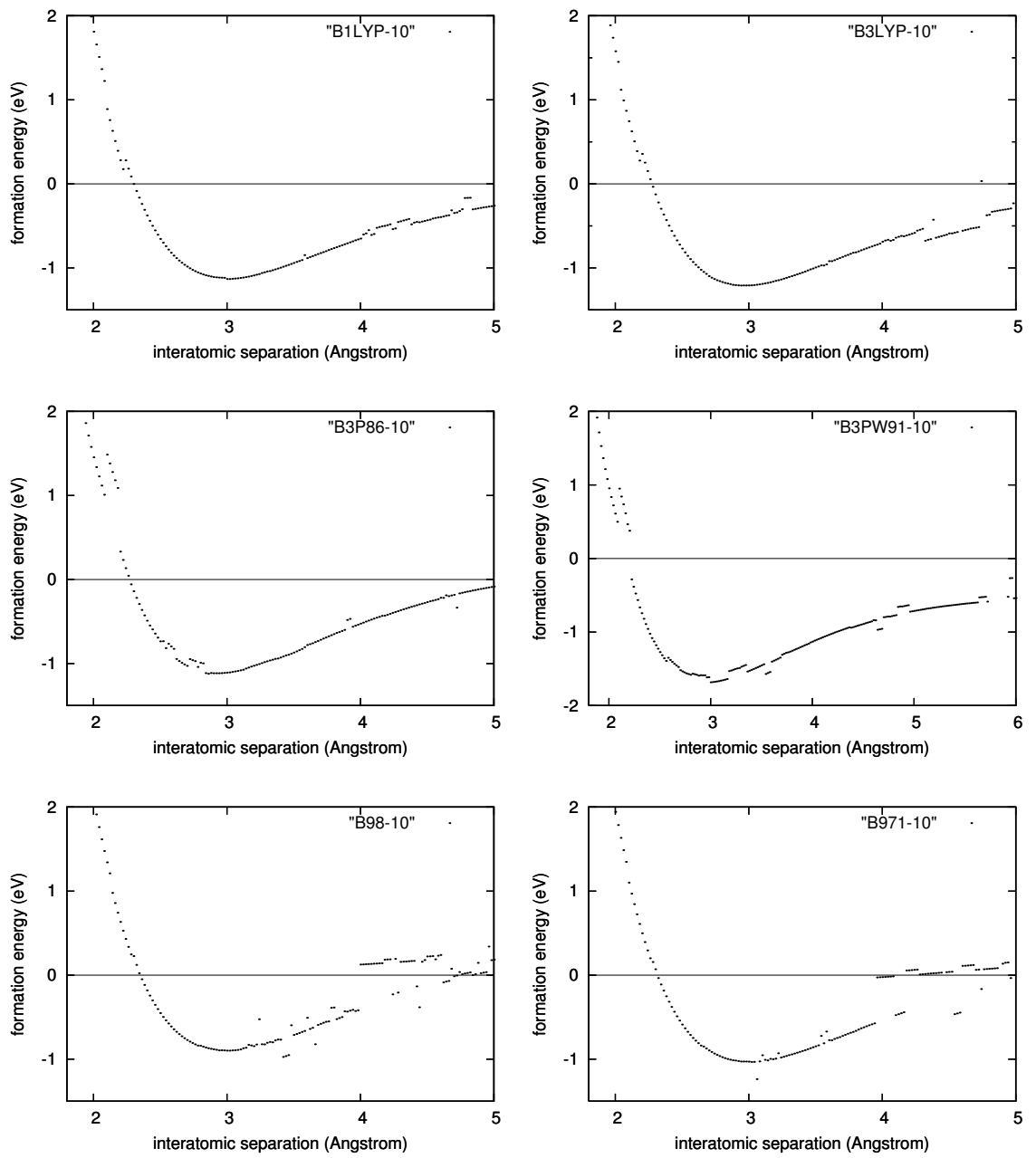


Figure 3.1: Nominal Lennard-Jones curves, describing the nature of the interaction between Sm and Co atoms, for the 12 methods in Tables or in which the total energy values are minimum for the multiplicity $m = 10$.

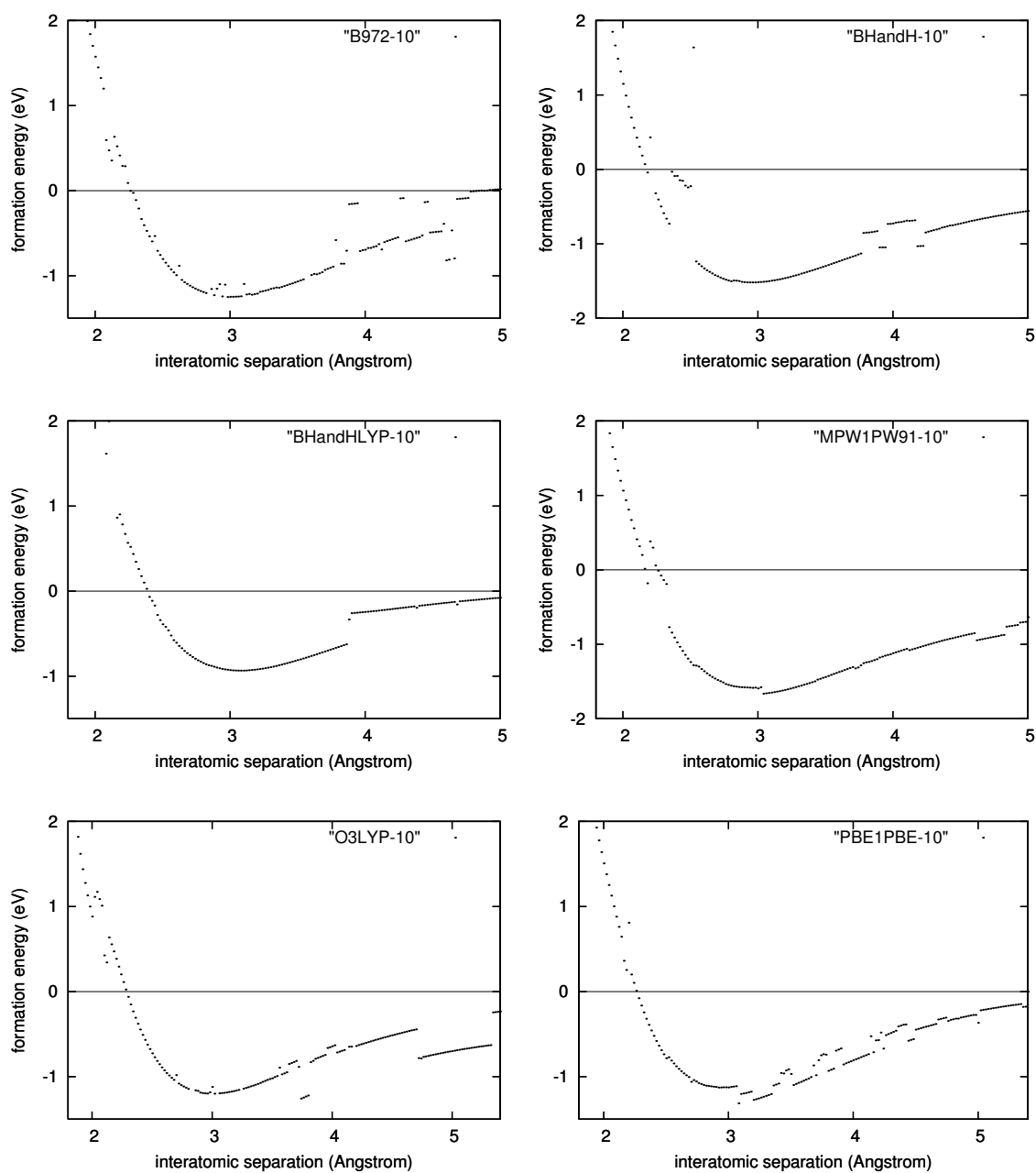


Figure 3.2: Nominal Lennard-Jones curves, describing the nature of the interaction between Sm and Co atoms, for the 12 methods in Tables or in which the total energy values are minimum for the multiplicity $m = 10$ (Cont).

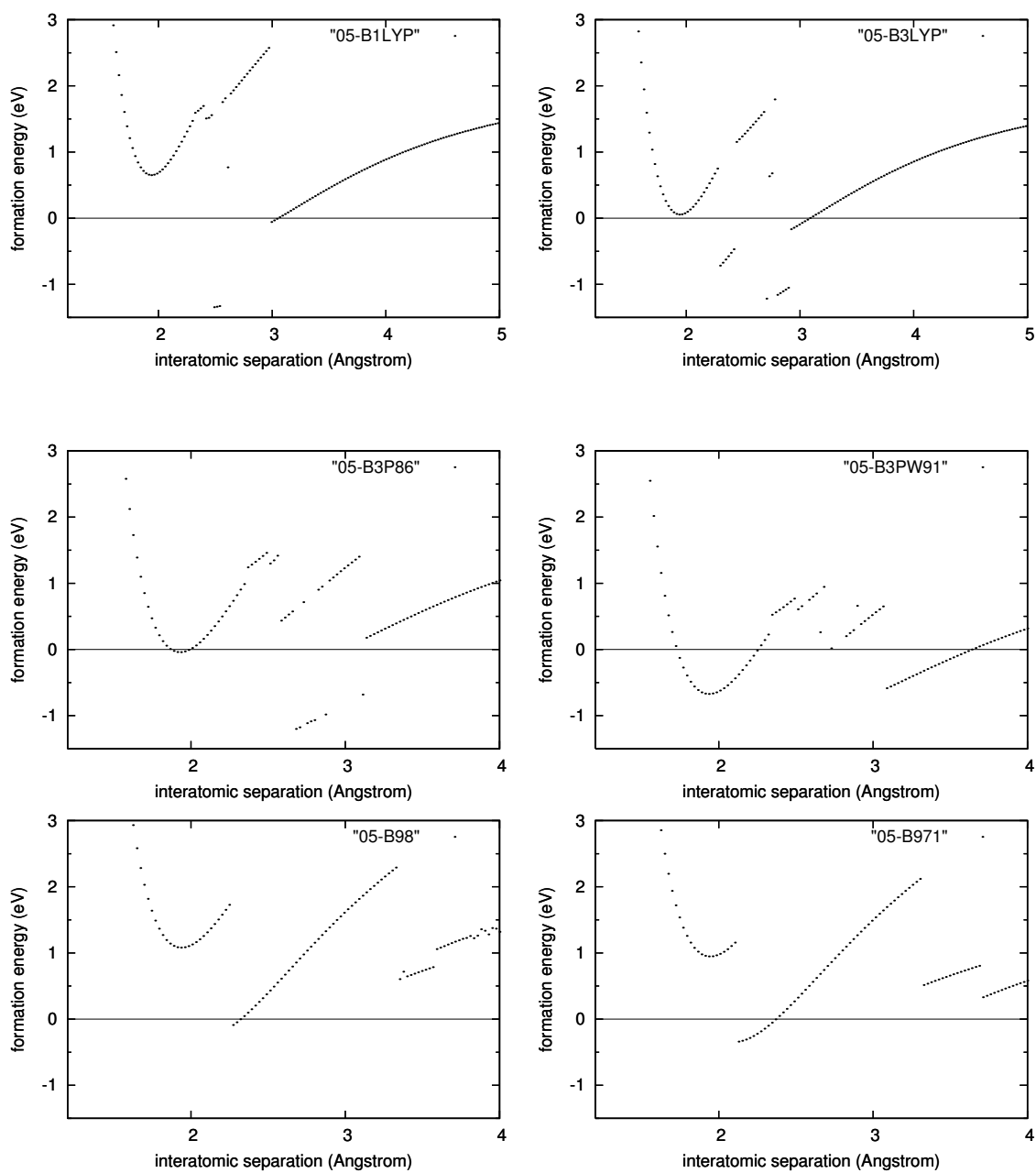


Figure 3.3: Nominal Lennard-Jones curves for Co_2 dimer with respect to DFT methods for $m = 7$.

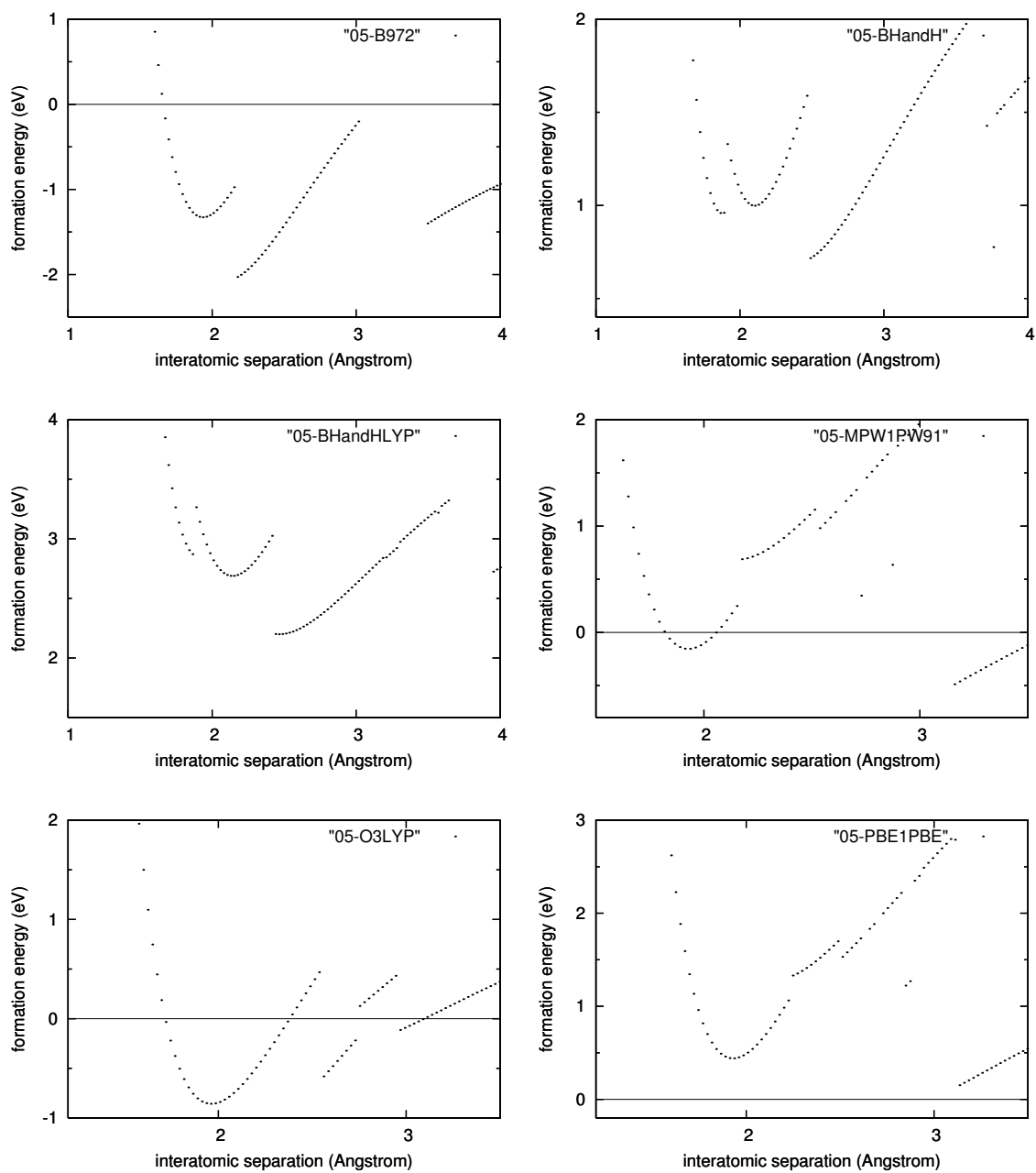


Figure 3.4: Nominal Lennard-Jones curves for CO_2 dimer with respect to DFT methods for $m = 7$.(Cont.)

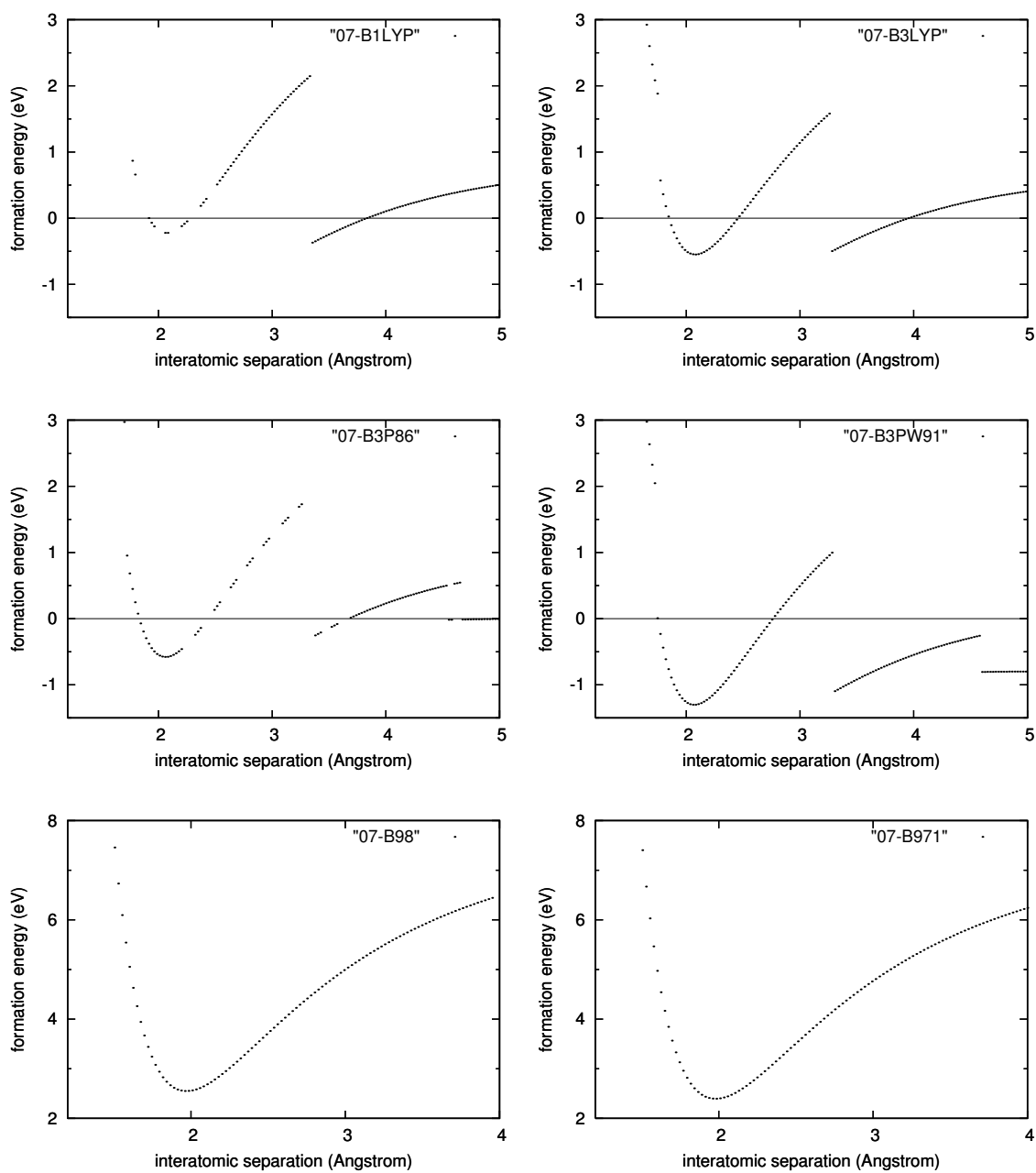


Figure 3.5: Nominal Lennard-Jones curves for Co₂ dimer with respect to DFT methods for $m = 7$.

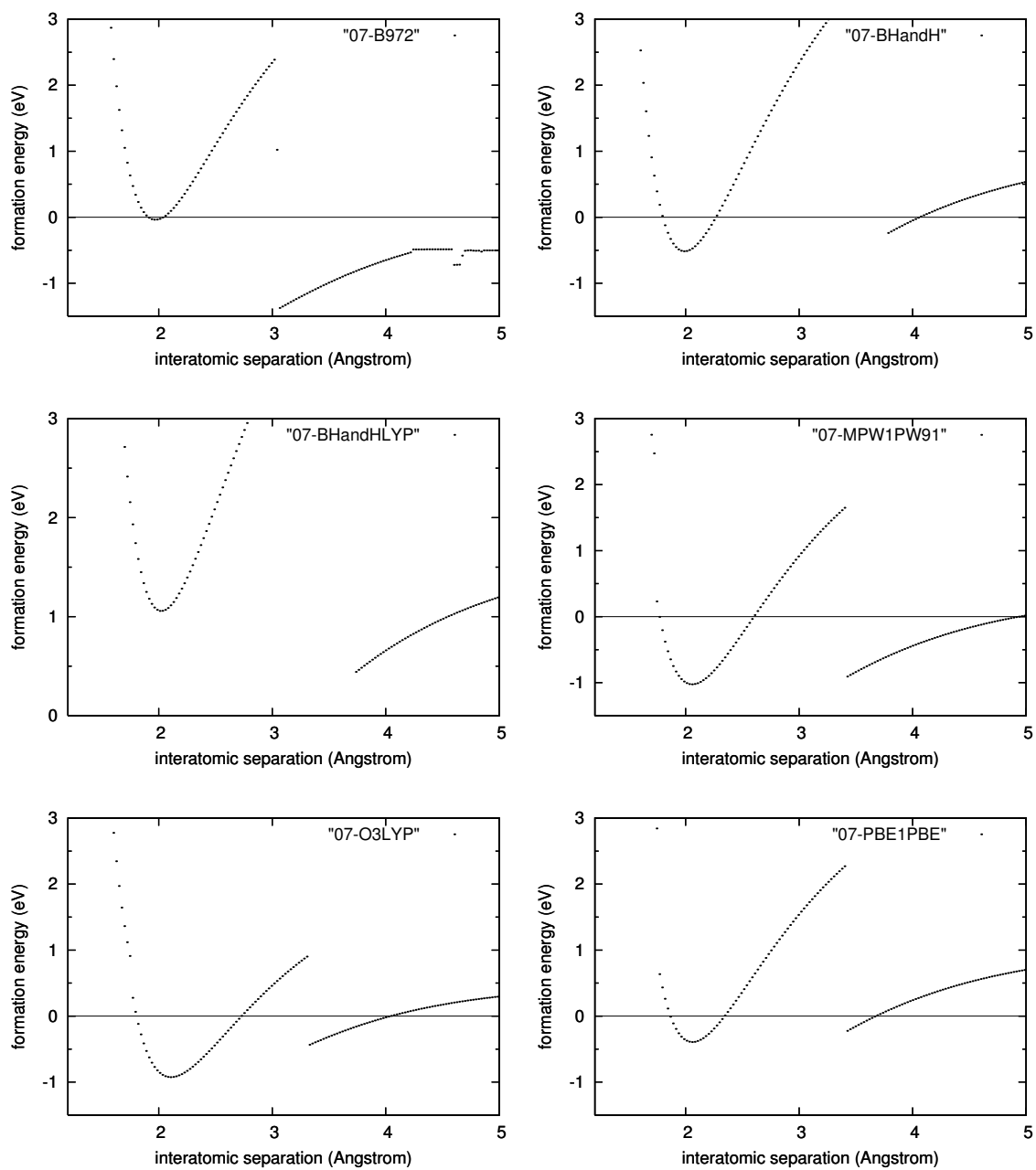


Figure 3.6: Nominal Lennard-Jones curves for Co_2 dimer with respect to DFT methods for $m = 7$.(Cont.)

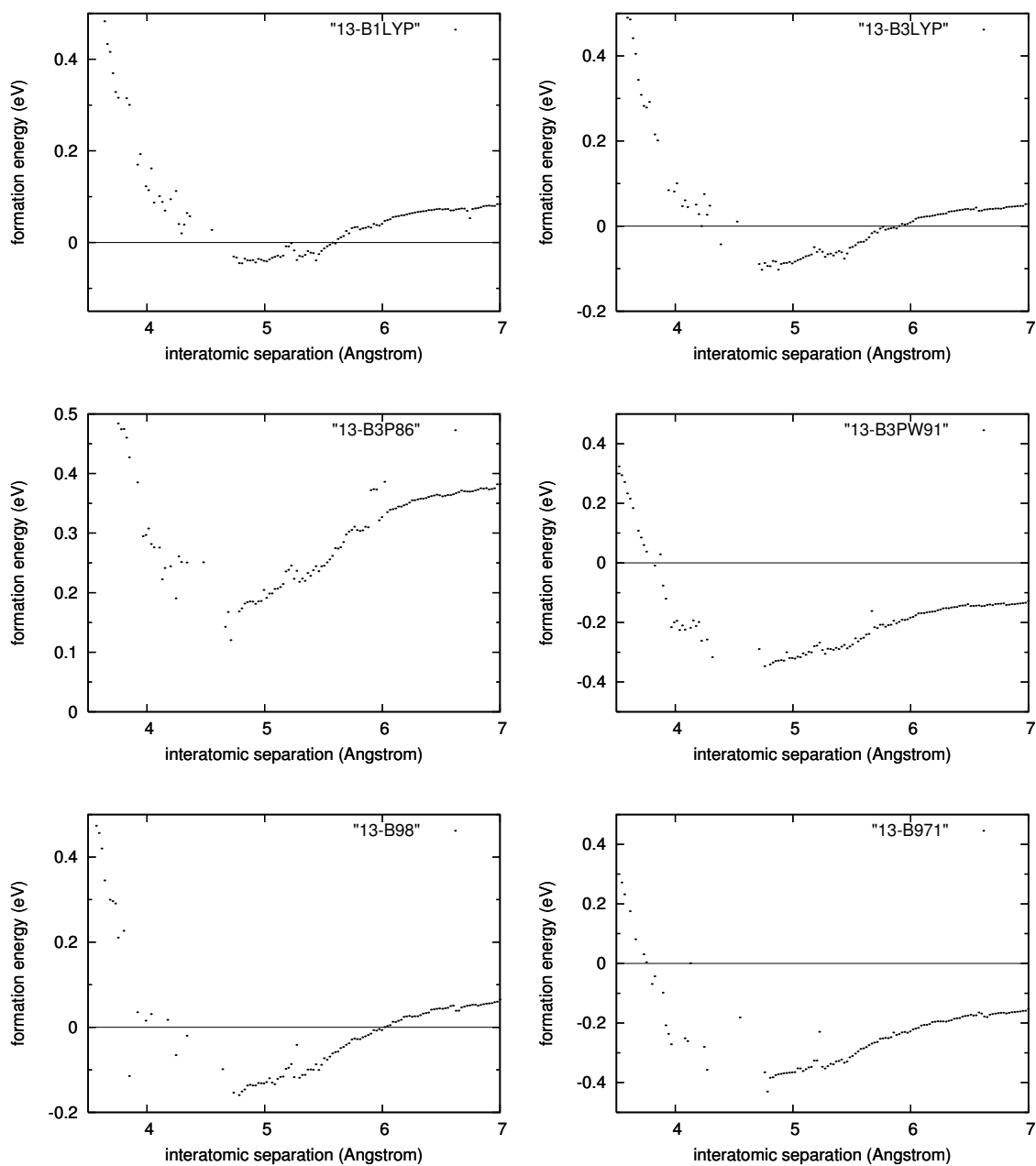


Figure 3.7: Nominal Lennard-Jones curves for Sm₂ dimer with respect to DFT methods.

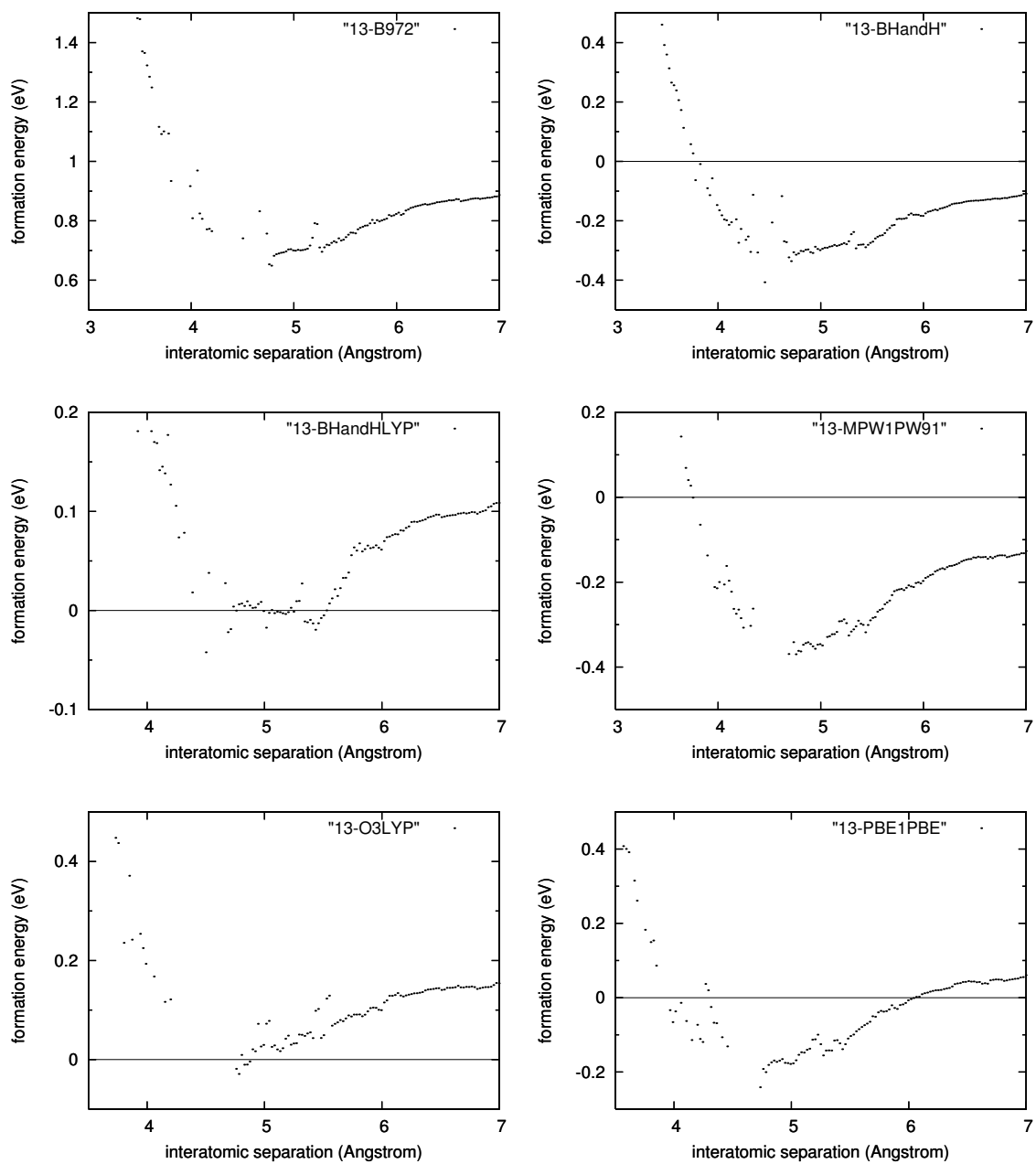


Figure 3.8: Nominal Lennard-Jones curves for Sm₂ dimer with respect to DFT methods.(Cont.)

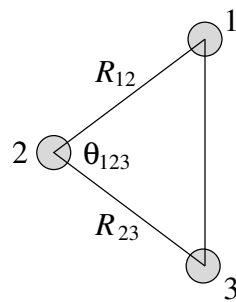


Figure 3.9: Trimer Angle

Table 3.44: HOMO and LUMO energies (in Hartrees), and HOMO-LUMO gap (E_g) energies (in eV) of the Sm_2Co trimer, calculated for the multiplicity, m ($2S + 1$), at which the total energy is minimum.

| method | m | HOMO(α) | LUMO(α) | $E_g(\alpha)$ | HOMO(β) | LUMO(β) | $E_g(\beta)$ |
|-----------|-----|------------------|------------------|---------------|-----------------|-----------------|--------------|
| B3P86 | 12 | -0.13578 | -0.05568 | 2.17963 | -0.12802 | -0.07806 | 1.35948 |
| B3PW91 | 12 | -0.11612 | -0.03589 | 2.18317 | -0.10857 | -0.05753 | 1.38887 |
| O3LYP | 12 | -0.09799 | -0.03146 | 1.81037 | -0.09176 | -0.05411 | 1.02451 |
| PBE1PBE | 12 | -0.11804 | -0.03480 | 2.26508 | -0.11043 | -0.05564 | 1.49091 |
| B1LYP | 16 | -0.09642 | -0.01973 | 2.08684 | -0.10866 | -0.04019 | 1.86316 |
| B3LYP | 16 | -0.09837 | -0.03002 | 1.85990 | -0.11056 | -0.04886 | 1.67894 |
| B3P86 | 16 | -0.13590 | -0.05779 | 2.12548 | -0.12584 | -0.07777 | 1.30805 |
| B3PW91 | 16 | -0.11669 | -0.03745 | 2.15623 | -0.10624 | -0.05702 | 1.33934 |
| B971 | 16 | -0.10942 | -0.03317 | 2.07487 | -0.10576 | -0.06681 | 1.05988 |
| B972 | 16 | -0.09557 | -0.02716 | 1.86153 | -0.11128 | -0.04953 | 1.68030 |
| B98 | 16 | -0.09843 | -0.02881 | 1.89446 | -0.11260 | -0.04939 | 1.72003 |
| BHandH | 16 | -0.13011 | -0.00969 | 3.27679 | -0.11506 | -0.03015 | 2.31052 |
| BHandHLYP | 16 | -0.11381 | -0.00180 | 3.14591 | -0.12582 | -0.02118 | 2.84740 |
| HFB | 16 | -0.06861 | -0.04180 | 0.72954 | -0.06281 | -0.03200 | 0.83838 |
| MPW1PW91 | 16 | -0.12123 | -0.03623 | 2.31297 | -0.10574 | -0.05338 | 1.42479 |
| O3LYP | 16 | -0.09969 | -0.03198 | 1.84248 | -0.09120 | -0.05468 | 0.99376 |
| PBE1PBE | 16 | -0.11789 | -0.03247 | 2.32440 | -0.10807 | -0.05373 | 1.47867 |

CHAPTER 4

CONCLUSION

In the present study, structural and electronic properties of Sm-Co cluster systems are studied theoretically. We deal with the microclusters of samarium and cobalt in all combinations Sm_mCo_n up to $(m+n=3)$. We performed the density functional theory (DFT) calculations.

This work consists of three main parts. In the first part of our study, we investigated structural and electronic properties of Sm and Co atoms and their ions, by indicating self consistent energies for all possible values of the multiplicity. Also their ionization energies and electron affinities are searched for possible ions. In the second part SmCo , Co_2 , and Sm_2 dimers are investigated according to self consistent energy. In addition, we presented binding energy D_e , bond lengths, r_e , the fundamental frequency w_e , charge q , dipole moment μ , the calculated HOMO (highest occupied molecular orbital), LUMO (lowest unoccupied molecular orbital), and HOMO–LUMO gap energies of dimers. The third part of the calculations cover the structural and electronic properties of Co_3 , Sm_3 , SmCo_2 , and Sm_2Co trimers. We investigated the minimum energy configurations of the trimers (bond lengths and bond angle, as well as their fundamental frequencies w_n). For all the microclusters considered, we presented the possible dissociation channels and the corresponding dissociation energies, the calculated HOMO, LUMO, and HOMO–LUMO gap energies. We also gave the calculated dipole moments and excess charges on the atoms of the trimers.

Within the scope of this study, we met in the literature of microclusters there are limited experimental and theoretical studies focused on Sm_mCo_n alloys. To our best knowledge, there is no study other than Co_2 for the rest of the clusters mentioned above. Therefore, exploring the uncertain geometrical and electronic properties of the remaining microclusters has been constituted the aim of present study.

In this study we presented our theoretical computational outcomes on the structural and energetic features Sm_mCo_n microclusters via DFT techniques. We believe that the structural features obtained in this treatise are reasonable and reliable. The present study can be seen a preliminary work for higher order microcluster of transition metal–rare earth alloys.

REFERENCES

- [1] P. Larson and I.I. Mazin, *J. Appl. Phys.* **93**, 6888 (2003).
- [2] P. Larson, I.I. Mazin, and D.A. Papaconstantopoulos, *Phys. Rev. B* **67**, 214405 (2003).
- [3] C.N. Chinnasamy, J.Y. Huang, L.H. Lewis, B. Latha, C. Vittoria, and V.G. Harris, *Appl. Phys. Lett.* **93**, 032505 (2008).
- [4] J. Sayama, T. Asahi, K. Mizutani, and T. Osaka, *J. Phys. D: Appl. Phys.* **37**, L1 (2004).
- [5] H. Oymak and Ş. Erkoç, *J. Phys. Chem. A* **37**, 1897 (2010).
- [6] K.J. Strnat, *Ferromagnetic Materials*, edited by E.P. Wohlfarth (North-Holland, Amsterdam, 1980), Vol. 4, p. 131.
- [7] J. Zhang, Y.K. Takahashi, R. Gopalan, and K. Hono, *J. Magn. Magn. Mater.* **310**, 1 (2007).
- [8] Y. Hou, Z. Xu, S. Peng, C. Rong, J.P. Liu, and S. Sun, *Adv. Mater.* **19**, 3349 (2007).
- [9] E. Danieli, J. Perlo, B. Blümich, and F. Casanova, *Angewandte Chemie* **24**, 49 (2010).
- [10] R. Chang, *Chemistry*; Tenth Edition, McGraw Hill, New York, 2010.
- [11] D.D. Ebbing and S.D. Gammon, *General Chemistry*; Sixth Edition, Houghton Mifflin, USA, 1999.
- [12] M. Gerloch and E.C. Constable, *Transition Metal Chemistry: The Valence Shell in d-Block Chemistry*; VCH, Weinheim, 1994.
- [13] S. Cotton, *Lanthanide and Actinide Chemistry*; Wiley, Chichester, 2006.
- [14] Ş. Erkoç and T. Uzer, *Lecture Notes on Atomic and Molecular Physics*, World Scientific, Singapore, 1996.
- [15] D.S. Sholl and J.A. Steckel, *Density Functional Theory: A Practical Introduction*, Wiley, New Jersey, 2009.
- [16] R.G. Parr and W. Yang, *Density-Functional Theory of Atoms and Molecules*, Oxford University Press, New York, 1989.
- [17] J. K. Labanowski, J. W. Andzelm, *Density Functional Methods in Chemistry*, Springer, New York, 1991.
- [18] B. G. Johnson, in *Modern Density Functional Theory: A Tool for Chemistry*, Theoretical and Computational Chemistry, Vol. 2, Eds. J. M. Seminario and P. Politzer, Elsevier Science B. V., 1995.
- [19] J. C. Slater, *Phys. Rev.* **81** 385 (1951).

- [20] J. C. Slater, *The Self-Consistent Field for Molecules and Solids: Quantum Theory of Molecules and Solids*, Vol. 4, McGraw-Hill, New York, 1974.
- [21] J. M. Seminario, in *Modern Density Functional Theory: A Tool for Chemistry*, Theoretical and Computational Chemistry, Vol. 2, Eds. J. M. Seminario and P. Politzer, Elsevier Science B. V., 1995.
- [22] P. Hohenberg and W. Kohn, *Phys. Rev.* **136**, B864 (1964).
- [23] W. Koch and M.C. Holthausen, *A Chemist's Guide to Density Functional Theory*; Second Edition, Wiley-VCH, Weinheim, 2001.
- [24] W. Kohn and L. J. Sham, *Phys. Rev.* **140**, A1133 (1965).
- [25] A. D. Becke, *Phys. Rev. A* **33**, 3098 (1988).
- [26] J. P. Perdew, in *Electronic Structure of Solids*, edited by P. Ziesche and H. Eschrig (Akademie Verlag, Berlin, 1991).
- [27] J. P. Perdew, K. Burke, and M. Ernzerhof, *Phys. Rev. Lett.* **77** 3865 (1996) .
- [28] C. Lee, W. Yang, and R. G. Parr, *Phys. Rev. B* **37**, 785 (1988).
- [29] A. D. Becke, *J Chem. Phys.* **104**, 1040 (1996).
- [30] M. D. Liptak, G. C. Shields, *Int. J. Quantum Chem.* **105**, 580 (2005).
- [31] J. P. Perdew, *Phys. Rev. B* **33**, 8822 (1986).
- [32] J. P. Perdew, Y. Wang, *Phys. Rev. B* **45**, 13244 (1992).
- [33] A. D. Becke, *J. Chem. Phys.* **107**, 8554 (1997).
- [34] H. L. Schmider and A. D. Becke, *J. Chem. Phys.* **108**,9624 (1998).
- [35] F. A. Hamprecht, A. Cohen, D. J. Tozer, and N. C. Handy, *J. Chem. Phys.* **109** 6264 (1998).
- [36] P. J. Wilson, T. J. Bradley, and D. J. Tozer, *J. Chem. Phys.* **115** 9233 (2001).
- [37] C. Adamo and V. Barone, *J. Chem. Phys.* **110** 6158 (1999).
- [38] C. Adamo and V. Barone, *J. Chem. Phys.* **108** 664 (1998).
- [39] A. J. Cohen and N. C. Handy, *Mol. Phys.* **99** 607 (2001).
- [40] A. Sebetci, *Chem. Phys.* **354**, 196-201 (2008).
- [41] S. Yang, M.B. Knickelbein, *J. Chem. Phys.* **93**, 1533 (1990).
- [42] M.J. Frisch *et al.*, Gaussian 03, Revision D.01, Gaussian, Inc., Wallingford, CT, 2004.
- [43] D.R. Lide (Ed.), *CRC Handbook of Chemistry and Physics*, 90th Edition
- [44] H.J. Fan, C.W. Liu, M.S. Liao, *Chem. Phys. Lett.* **273**, 353 (1997).
- [45] M. Pereiro, D. Baldomir, M. Iglesias, C. Rosales, M. Castro, *Int. J. Quantum Chem.* **81**, 422 (2001).

- [46] C.J. Barden, J.C. Rienstra-Kiracofe, H.F. Schaefer III, *J. Chem. Phys.* **113**, 690 (2000).
- [47] M. Pereiro, S. Mankovsky, D. Baldomir, M. Iglesias, P. Mlynarski, M. Valladares, D. Suarez, M. Castro, J.E. Arias, *Comput. Mater. Sci* **22**, 118 (2001).
- [48] S. Datta, M. Kabir, S. Ganguly, B. Sanyal, T. Saha-Dasgupta, A. Mookerjee, *Phys. Rev. B* **76**, 014429 (2007).
- [49] Q.M. Ma, Z. Xie, J. Wang, Y. Liu, Y.C. Li, *Phys. Lett. A* **385**, 289 (2006).
- [50] M. Castro, C. Jamorski, D.R. Salahub, *Chem. Phys. Lett.* **271**, 133 (1997).
- [51] C. Jamorski, A. Martinez, M. Castro, D.R. Salahub, *Phys. Rev. B* **55**, 10905 (1997).